From the Department of Medical Biochemistry and Biophysics
Karolinska Institutet, Stockholm
Sweden

Bioactive peptides and proteins in disease

Essam Refai

Doctoral thesis
Karolinska Institutet
Sweden

Printed by Karolinska University Press
Box 200, SE-171 77 Stockholm, Sweden

ISBN 91-7349-914-5

Surah 20. Ta Ha

"O my Lord! Advance me in knowledge."

To
my Mother, the first school of life,
my Father who planted the seeds
of knowledge & scientific research
within me, & the joy of my life:
Sara, Josef & Mariam

Abstract

Regulatory peptides and marker proteins are important to study in order to understand disease mechanisms. This applies of course also to our common diseases where all relationships are not yet known. Cancer and diabetes are two such complex diseases that affect hundreds of millions of people worldwide. This thesis addresses particular aspects of these two diseases, regarding one regulatory peptide (VIP, vasoactive intestinal polypeptide) that may be useful for tumor tracing and two proteins (apoCIII, apolipoprotein CIII, and TTR, transthyretin) that are altered in type 1 diabetes.

VIP and functional VIP receptors are expressed in neuroblastomas, suggesting that the growth of these cells may be mediated in part by an autocrine action of VIP. VIP receptors are present in many epithelial cancers including breast, colon, non-small cell lung cancer, and pancreatic and prostate cancers. Due to the high density of VIP receptors on cancer cells, radiolabelled VIP may be used to image these tumours. It was therefore important for us to study in vivo distribution of the radiolabelled VIP prior to its usage as tumour tracer. We also studied the biological effects of VIP on tumours in an animal model, as there may be differences with respect to receptor expression between cultured tumour cells and tumour cells grown in vivo. Our studies could provide new insight into tumour imaging with respect to radiolabelled VIP.

Type 1 diabetes serum was shown to increase intracellular Ca^{2+} and cause cell death. ApoCIII and TTR were isolated from sera of newly diagnosed type 1 diabetic patients based on a biological assay of increases of intracellular Ca^{2+}. The exposure of the pancreatic β-cell to apoCIII not only increases intracellular Ca^{2+}, but also causes programmed cell death. Furthermore, the activity of apoCIII and type 1 diabetes serum was totally blocked when a polyclonal antibody against human apoCIII was added. TTR did not have any effect on cell death. When applying the patch clamp technique, both cells treated with apoCIII and those treated with TTR displayed larger Ca^{2+}-channel currents than control cells. Research over the last 30 years has established that type 1 diabetes is an autoimmune disease, but the triggers of the initiation and progression of the disease are still not identified. Genetic, immunological and environmental factors are involved in the pathogenesis of type 1 diabetes and it is most likely that the events involved can differ between different patients. Further investigations are needed to elucidate all pathways and how they are related to the underlying autoimmunity, but our results show that there is at least a group of type 1 diabetes patients where apoCIII and TTR play a role.

LIST OF PUBLICATIONS

This thesis is based on the following papers, which will be referred to by their Roman numerals:

I. Hassan M, **Refai E**, Andersson M, Schnell PO, Jacobsson H.

In vivo dynamical distribution of ^{131}I-VIP in the rat studied by gamma-camera.
Nucl Med Biol. 1994; 21: 865-872.

II. **Refai E**, Jonsson C, Andersson M, Jacobsson H, Larsson S, Kogner P, Hassan M.

Biodistribution of liposomal ^{131}I-VIP in rat using gamma camera.
Nucl Med Biol. 1999; 26: 931-936.

III. Kogner P, Borgstrom P, Bjellerup P, Schilling FH, **Refai E**, Jonsson C, Dominici C, Wassberg E, Bihl H, Jacobsson H, Theodorsson E, Hassan M.

Somatostatin in neuroblastoma and ganglioneuroma.
Eur J Cancer. 1997; 33: 2084-2089.

IV. Lisa Juntti-Berggren†, **Essam Refai**†, Ioulia Appelskog, Mats Andersson, Gabriela Imreh, Nancy Dekki, Sabine Uhles, Lina Yu, William J Griffiths, Sergei Zaitsev, Ingo Leibiger, Shao-Nian Yang, Gunilla Olivecrona, Hans Jörnvall and Per-Olof Berggren.
† These authors contributed equally to this work.

Apolipoprotein CIII promotes Ca^{2+} dependent β-cell death in type 1 diabetes.
Submitted.

V. **Essam Refai**, Nancy Dekki, Shao-Nian Yang, Lina Yu, Svante Norgren, Claude Marcus, Mats Andersson, Hans Jörnvall, Per-Olof Berggren and Lisa Juntti-Berggren.

Transthyretin increases activity of voltage-gated L-type Ca^{2+}-channels and affects insulin release in pancreatic β-cells.
Manuscript.

PUBLICATIONS NOT INCLUDED IN THE THESIS

- Borgström P, Hassan M, Wassberg E, **Refai E,** Jonsson C, Larsson SA, Jacobsson H, Kogner P.

The somatostatin analogue octreotide inhibits neuroblastoma growth in vivo.
Pediatr Res. 1999; 46:328-332.

- Hassan M, Eskilsson A, Nilsson C, Jonsson C, Jacobsson H, **Refai E**, Larsson S, Efendic S.

In vivo dynamic distribution of ^{131}I-glucagon-like peptide-1 (7-36) amide in the rat studied by gamma camera.
Nucl Med Biol. 1999; 26:413-420.

- Linde CM, Hoffner SE, **Refai E,** Andersson M.

In vitro activity of PR-39, a proline-arginine-rich peptide, against susceptible and multi-drug-resistant Mycobacterium tuberculosis.
J Antimicrob Chemother. 2001; 47:575-580.

CONTENTS

ABBREVIATIONS

VIP	Vasoactive intestinal peptide
PACAP	Pituitary adenylate cyclase activiating peptide
VPAC	Vasoactive intestinal peptide/pituitary adenylatecyclase-activating polypeptide
ApoCIII	Apolipoprotein CIII
TTR	Transthyretin
TFA	Triflouroacetic acid
HPLC	High performance liquid chromatography
T1D	Type 1 diabetes
ESMS	Electrospray mass spectrometry

1 INTRODUCTION

Proteins and peptides are central to life, as they play crucial roles in all biological processes in executing cell functions. They are synthesized as linear polypeptide chains, which fold into 3-D structures constituting their functional units. The identification and characterization of peptides and proteins involved in diseases can be of importance in diagnosis and treatment.

During the last half century there has been much progress in our knowledge on bioactive peptides. Nevertheless, the initial observations of their biological activities were carried through long ago. As an example, the presence of a vasodepressor principle in intestinal extracts had been noted by Bayliss and Starling over a century ago [1]. They coined the substance responsible for that activity secretin. Viktor Mutt isolated and characterized secretin almost 60 years later [2]. The amino acid sequence of secretin was determined by Mutt et al. in 1970 [3]. Bayliss and Starling noticed that the intestinal extracts also caused a low blood pressure and suggested that this effect was not due to secretin. In 1969, Said and Mutt found a similar vasodilatory effect in extracts of the lung [4]. A year later, a highly active substance was isolated from porcine intestinal extracts. It was named vasoactive intestinal polypeptide (VIP), based on its activity and origin of isolation [5]. Both secretin and VIP are members of the secretin/glucagon family of related peptides [6] which includes nine hormones in humans that are related in structure, distribution, function and receptors [7]. Those hormones are: secretin, glucagon, glucagon-like peptide (GLP-1) and (GLP-2), gastric inhibitory polypeptide (GIP), vasoactive intestinal polypeptide VIP, pituitary adenylate cyclase activating polypeptide (PACAP), growth hormone-releasing hormone (GRF) and peptide histidine-methionine (PHM).

The mode in which proteins have been characterized follows a classic pattern: collection of material, biological assay, purification, determination of purity, and amino acid sequence analysis. Today, the availability of high performance liquid chromatography (HPLC), masspectrometry, gel electrophoresis and the entire human genome allows identification and detailed studies of the proteins in an ever increasing detail.

Biosynthesis of bioactive peptides has been shown to proceed via precursor proteins [8, 9]. The peptides may either be continuously secreted or stored into specific granules which are released upon cell stimulation. Once released, peptides in plasma and interstitial tissue are normally found at concentrations in the range of 10^{-7} M to 10^{-10} M. Because of these very low physiological concentrations, high affinity receptors have evolved, located on the target cell

plasma membrane. Activation of these receptors leads to signalling, responsible for initiating intracellular biological responses. These responses may include complex events and may end with protein synthesis or cell differentiation. On the other hand, responses may also include regulatory proteins found at milligram concentrations in plasma, and most of those proteins are synthesized by the liver. These proteins have a long half-lives (days) contrary to bioactive peptides that usually have short half-life (min) in the blood stream.

In this thesis the following peptide and proteins are studied with respect to tumour imaging (1) and intracellular calcium ($[Ca^{2+}]_i$) changes in pancreatic β-cells (2,3) :

1) VIP
2) Apolipoprotein CIII (ApoCIII)
3) Transthyretin (TTR)

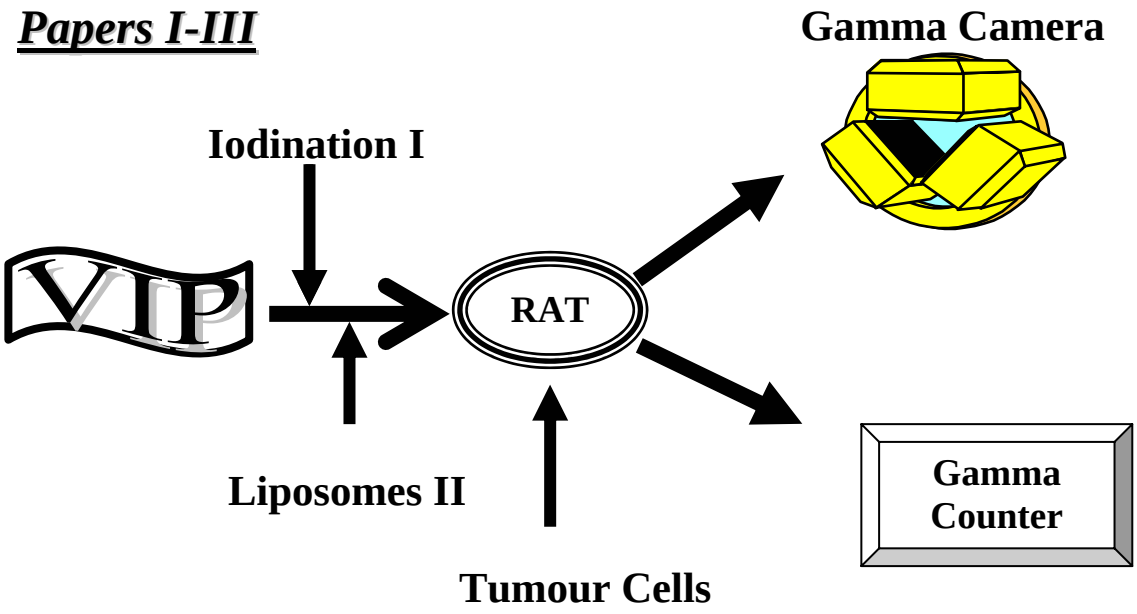

1.1 VIP

VIP is a 28-residue peptide isolated in 1970 [5]. It is a prominent neuropeptide involved in a broad spectrum of biological activities [10-13]. It functions as a neurotransmitter and neuroendocrine hormone. VIP has two structurally related transmembrane receptors $VPAC_1$ and $VPAC_2$ (VPAC = VIP/PACAP). These receptors are G protein-coupled and exert their actions on cells through activation of adenylate cyclase, and by increase of intracellular calcium [14]. VIP receptors were first described in the mid 70´s [15-17]. PACAP is also a potent agonist of $VPAC_1$ and $VPAC_2$ receptors as well as of a third, PACAP-specific receptor (PAC_1) [18-20].

VIP receptors are widely distributed in most normal tissues such as those of the gastrointestinal tract, liver, lung and brain. Interestingly certain human cancer cells have high expression of VIP receptors [21]. The use of radiolabelled VIP, binding to VIP receptors, could thus be a potentially useful agent to identify tumours and their localisation with in vivo imaging. In many cases early diagnosis greatly improves the outcome of cancer diseases. Thus, early detection of cancer cells by the means of radiolabelled peptides could be an important tool for survival of patients.

Deficiency of VIP has been linked to several diseases, including bronchial asthma, cystic fibrosis, and the acquired immunodeficiency syndrome (AIDS) [22]. VIP has important pharmacological actions on the respiratory tract, including relaxation of the airway smooth muscle membranes and attenuation of acute lung inflammation [23].

1.1.1 Tumour imaging

It has been a challenge in medicine to identify a method that has the potential to localize and target tumours at an early stage of development. About 25 years ago, radiolabelled monoclonal antibodies became popular as a potential diagnostic/targeting method in cancer [24]. As antibodies have a molecular weight of approximately 150 kDa, and thus large molecular size which hinders rapid pharmacokinetics, this method turned out to be difficult to realize [25-27]. An alternative to radiolabelled antibodies appeared, almost 15 years ago, in the form of a radiolabelled peptide, somatostatin analogue (1.5 kDa), which led to a major breakthrough. This was due to the fact that neuroendocrine tumours were found to express high levels of somatostatin receptors [28]. Investigations have also characterised and localised VIP receptors on the cells of breast carcinomas and their metastases, ovarian adeno-carcinomas, endometrial carcinomas, prostate cancer metastases, bladder carcinomas, colonic adeno-carcinomas, pancreatic adeno-carcinomas, gastrointestinal squamous cell carcinomas, lymphomas, small-cell lung cancers, inactive pituitary adenomas and neuroblastomas. [29-31]. Today radiolabelled VIP [32] has been shown to visualize the majority of gastrointestinal adeno-carcinomas, as well as some neuroendocrine tumours, including insulinomas which are often missed by somatostatin receptor scintigraphy [33].

Radioisotopes have found extensive use in diagnosis and therapy. They have proven particularly effective as tracers in certain diagnostic procedures. As radioisotopes are chemically identical with stable isotopes of the same element, they can take the place of the latter in physiological processes. Moreover, because of their radioactivity, they can be readily traced even in minute quantities using detection devices like gamma-ray spectrometers and

proportional counters. Although many radioisotopes maybe used as tracers, iodine-123, iodine-131, indium-111, phosphorus-32, and technetium-99 are among the most important.

1.1.2 Neuroblastoma

Neuroblastoma is a malignant tumour that develops from embryonic neural tissue, with the tumour appearing in infancy or childhood. It is most commonly diagnosed in children before the age of five [34]. Most patients have widespread disease at diagnosis. The disorder occurs in approximately 1 out of 100.000 individuals and there is a strong association between early detection of tumours and good prognosis. Neuroblastoma can occur in many areas of the body. It develops from the tissues that form the sympathetic nervous system. Neuroblastoma most commonly begins abdominally, in the tissues of the adrenal gland but may occur in other areas [30]. It usually spreads rapidly to the lymph nodes, liver, lungs, bones, and bone marrow. The cause of the tumour is unknown and it may be linked to hereditary tendencies [35]. Gene abnormalities are seen in patients with the tumour [36, 37].

The SH-SY5Y neuroblastoma cell line has been reported to express VIP receptors [38] and is regulated by VIP in an autoendocrine manner [39]. VIP synthesis is increased in neuroblastoma cells through differentiation which is induced by retinoic acid as well as by VIP. Data show that VIP-induced differentiation of neuroblastoma cells markedly increase VIP receptor expression [40].

1.1.3 Receptor regulation and retinoic acid

Vitamin A and its analogues, including retinoic acid, play important roles in normal cellular differentiation and programmed cell death [41]. Pre-treatment of SH-SY5Y cells with 13-*cis*-retinoic acid dramatically increased VIP receptor numbers (sites per cell) and the VIP immunoreactive content in the cells increased 2-3 fold [42]. Clinical effects of 13-*cis*-retinoic acid have been reported in certain patients with advanced neuroblastoma tumours [43, 44].

1.1.4 Liposomes

Liposomes are microscopic structures consisting of one or more concentric lipid bilayers surrounding an aqueous compartment. The liposomes are non-toxic drug carriers where both hydrophilic and hydrophobic molecules can be entrapped. The properties of liposomes depend on their size, chemical composition and charge. Liposomes target primarily in the liver and spleen and offer sustained release in the blood when administered intravenously.

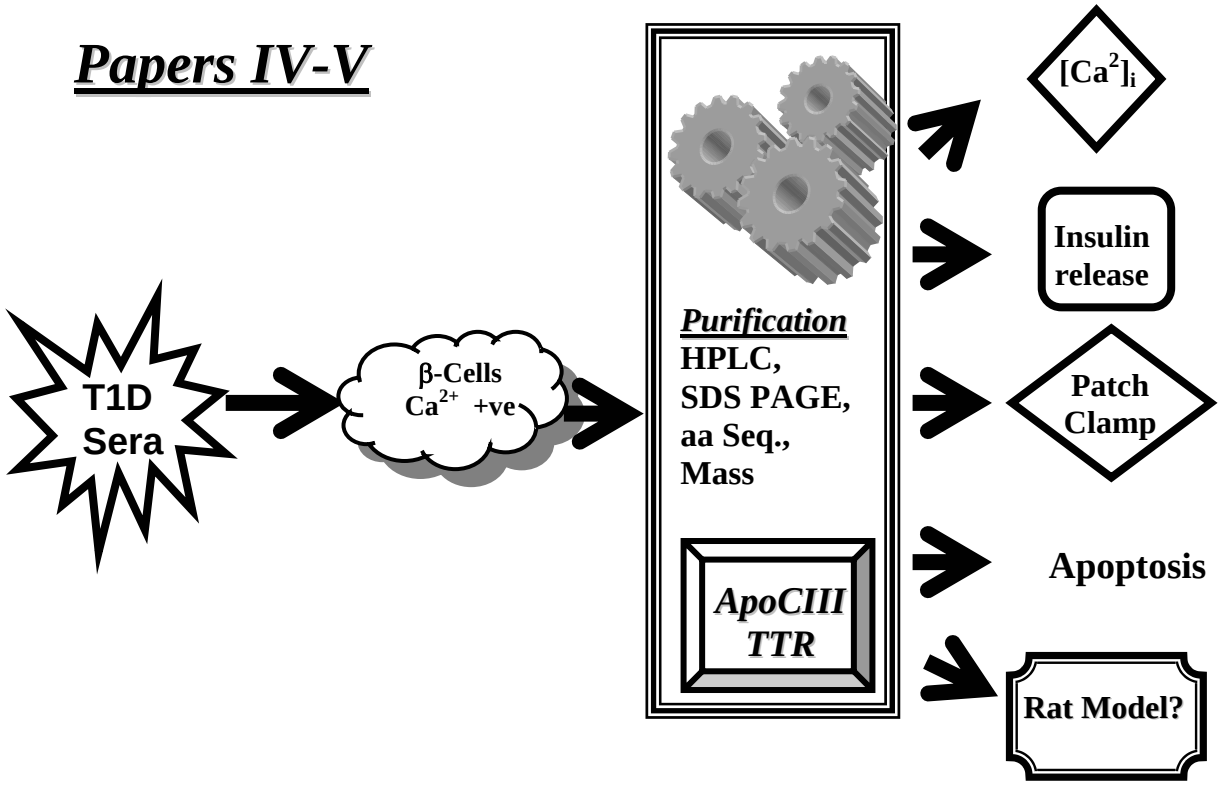

1.2 Apolipoprotein CIII and transthyretin

Apolipoprotein CIII (apoCIII) is a 79-residue, 8.8 kDa polypeptide [45] with three known isoforms that differ in extent of glycosylation, $CIII_0$ (no sialic acid), $CIII_1$ (one sialic acid molecule), $CIII_2$ (two sialic acid molecules), contributing approximately 10%, 55% and 35%, respectively, to the total plasma apoCIII [46]. The human apoC´s (apoCI, apoCII, and apoCIII) have similar distributions among lipoprotein classes, and are often purified together. ApoC´s are protein constituents of chylomicrons, VLDL, and HDL.

ApoCIII is distributed mainly into VLDL and HDL, and into LDL and chylomicrons to a lesser degree. A number of clinical and experimental studies have demonstrated that apoCIII inhibits the action of lipoprotein lipase, a key enzyme in triglyceride (TG) hydrolysis, metabolizing TG in VLDL and facilitating their clearance from plasma [47, 48]. Plasma lipid abnormalities in diabetic patients are elevation of plasma TG´s and reduction in high-density lipoprotein (HDL) cholesterol, which is believed to be associated with the high incidence of coronary heart disease in the diabetic population [49]. Bar-On et al. first reported that apoCIII was increased and apo E decreased in very-low-density lipoprotein (VLDL) obtained from streptozotocin-induced diabetic rats [50], and they suggested that these changes of lipoprotein particles were associated with delayed clearance from the plasma [51, 52]. Takahashi et al [53]

has reported that apoCIII deficiency prevents the development of hypertriglyceridemia associated with diabetes in streptozotocin-induced diabetic mice.

Transthyretin (TTR, formerly called prealbumin) circulates in plasma as a homotetramer. Each subunit is composed of 127 amino acid residues. It is predominantly synthesized in the liver. However, the choroid plexus and the eye are also sites of production. TTR is a β-sheet-rich homotetramer that binds to and transports the hormone thyroxine as well as the retinol-binding protein/vitamin A complex.

The turnover rate of this protein has a half-life of 2-3 days. Protein malnutrition reduces the levels of TTR and refeeding restores its levels. The normal range for serum TTR is 16-33 mg/dL. Although TTR is responsive to nutritional changes, it, too, is a protein that is influenced by a number of disease related factors.

Interestingly it was shown that HNF-4 (hepatocyte nuclear factor 4), a member of the steroid/thyroid hormone receptor superfamily, binds to sites required for the transcription of the genes for both TTR, and apoCIII [54].

1.2.1 Diabetes mellitus

Diabetes mellitus afflicts 120 million people worldwide, and the World Health Organization (WHO) estimates this number will increase dramatically to about 300 million by the year 2025 [55, 56]. Diabetes mellitus is an old disorder; descriptions of it appear in ancient Egyptian and Greek writings. Diabetes comes from the Greek word for siphon, which describes the excessive thirst and polyuria of this condition, and mellitus is the Latin word for honey, because the smell of diabetic urine is sweet.

Diabetes mellitus is a complex disorder which can be divided into several subgroups, the two main forms are:

1. Type 1 diabetes “T1D” (also known as insulin-dependent diabetes mellitus-IDDM – or juvenile onset diabetes).
2. Type 2 diabetes “T2D” (also known as non-insulin-dependent diabetes mellitus-NIDDM – or maturity onset diabetes).

T1D is an autoimmune disease resulting in the destruction of the insulin-producing pancreatic β-cells. The development of TID can be divided into different stages. There is a genetic predisposition and precipitating event(s), starting with the immunological abnormalities leading to a progressive loss of β-cells. The difficulty to identify the factor(s) that trigger the

autoimmune attack against the β-cells depends on the usually long delay time between the start of the autoimmune process and the onset of the disease.

1.2.2 Voltage-gated L-type Ca^{2+}-channels and $[Ca^{2+}]_i$

The pancreatic β-cell stimulus-secretion coupling, leading to release of insulin, is a complex process, where changes in cytoplasmic free Ca^{2+}-concentration, $[Ca^{2+}]_i$, have a key regulatory role [57]. Subsequent to stimulation of the pancreatic β-cell with for example glucose, it has been shown that $[Ca^{2+}]_i$ increases and decreases in an oscillatory pattern. The molecular mechanisms that regulate the oscillations in $[Ca^{2+}]_i$ are not completely understood, but they are likely to represent an interplay between Ca^{2+} influx through voltage-gated L-type Ca^{2+}-channels and Ca^{2+} mobilization from intracellular stores [57], where Ca^{2+} coming from the extracellular space, through the voltage-gated L-type Ca^{2+}-channel, is more important for insulin release. It is important for the β-cell not to be exposed for a prolonged period of time to high $[Ca^{2+}]_i$ as this is toxic for the cell. Unphysiological increases in $[Ca^{2+}]_i$ have been linked to cell death in a number of experimental systems [58-61].

AIMS OF THE INVESTIGATION

- To study the *in vivo* distribution and pharmacokinetics of VIP in animal models.
- To study the *in vivo* distribution and pharmacokinetics of a liposomally encapsulated form of VIP and to evaluate if it prolongs the VIP half-life in blood.
- To evaluate the use of labeled VIP in imaging of neuroblastoma with or without treatment with VIP, synthetic somatostatin, and 13-*cis*-retinoic acid.
- To isolate and identify proteins from Type 1 diabetes serum that increase cytoplasmic free ($[Ca^{2+}]_i$) in pancreatic β-cells.
- To characterize the subforms of two proteins found to be altered in diabetic serum, apolipoprotein CIII and transthyretin.

2 METHODS

2.1 VIP

VIP was isolated from pig intestine [5]. The activity of VIP was tested in vivo by the method described by Mutt and Söderberg [62].

2.2 Iodination

VIP was mixed with carrier-free $Na^{131}I$, the reaction was started by addition of chloramine-T (Sigma, St. Louis, USA) and was terminated after 20-30 s with metabisulfite. Iodinated VIP was passed over a C_{18} Sep-Pak (Waters, MA) and further purified by HPLC using a Vydac C_{18} column. The radioactive fractions corresponding to the labelled VIP were collected, evaporated under N_2, and kept at -20°C until further use.

2.3 Liposomes

L-α-phosphatidylcholine, 1,2-dioleolyl-sn-glycero-3-phosphate and cholesterol in the molar ratio 9.45:1:9.45 were dissolved in dichloromethane, and ^{131}I-VIP was added. The dichloromethane was evaporated, and the mixture of lipids and ^{131}I-VIP formed a thin film coating the inside of a spherical glass vessel. Any trace of solvent was removed under a gentle stream of nitrogen. The mixture was then hydrated with 25 mL glucose solution (50 mg/mL, pH 4.0, Pharmacia-Upjohn, Uppsala, Sweden). Multilamellar vesicles were formed by vortexing the lipid-aqueous mixture. The suspension was transferred to an Extruder (LiposoFast 50, Avestin, Ottawa, Canada) and extruded under nitrogen pressure, through two stacked polycarbonate filters with a pore size of 600 nm (5 times). The average diameter of each liposomal preparation was determined by dynamic light scattering.

2.4 Extraction of VIP from rat organs

Rats were injected intravenously in the tail with ^{131}I-VIP or liposomal ^{131}I-VIP and sacrificed at various time points (2.5, 5, 10, 15, 20, 40 and 60 min). Different organs (lung, blood, kidney, spleen and liver) were removed immediately, washed with saline to remove blood, and placed in tubes (0.5 g/organ) to determine the radioactivity in a gamma-counter.

Another part of the organs was removed, carefully washed with saline and kept at

-20°C. These organs were thawed, homogenized with an Ultra-turrax and then extracted in 0.2 M acetic acid 10 mL/g for 90 min. The supernatant was collected after centrifugation and passed through a preconditioned Sep-Pak C_{18} (Waters, MA). The Sep-Pak was washed with 5 mL 10 % acetonitrile in 0.1 % triflouroacetic acid (TFA), the bound radioactivity was eluted with 2 mL 60 % acetonitrile in 0.1 % TFA. The procedure was repeated twice. The two fractions were pooled and the volume was reduced by lyophilization. The samples were dissolved in 150 µL 0.1 % TFA, centrifuged and submitted to HPLC with a Vydac C_{18} (0.46 x 25 cm) column (Grace Vydac, Hesperia, CA). The analysis was carried out using a linear gradient of 20-40 % acetonitrile in 0.1 % TFA for 30 min. The radioactive peak that eluted at the same retention time as that of iodinated VIP was used for quantification.

2.5 Pharmacokinetic and statistical analysis

Pharmacokinetic modelling and parameter estimates were performed using WinNonlin (Statistical Consultants, Lexington, KY, USA).

Statistical analysis was performed using Wilcoxon´s test (non-parametric, paired, two tailed) and Mann-Whitney´s test (non-parametric, unpaired, two tailed). The mean, median and standard deviations were calculated using Graph Pad In Stat (version 3.0). All values are presented as mean ± SD. A p-value <0.05 was considered significant.

Data analysis was done using the program Sigma Plot for Windows (version 4, Jandel Corp., San Rafael).

2.6 Purification of serum proteins

Sera from T1D patients and control subjects were collected, sterile-processed and stored frozen at –20°C until used. The immunoglobulins of the sera were heat-inactivated by incubation at 56°C for 30 min. Thereafter, β-cells were incubated overnight in RPMI 1640 culture medium with 10% added sera [61], and changes in $[Ca^{2+}]_i$ were recorded, subsequent to depolarization with 25 mM KCl. The five T1D sera that induced an enhanced $[Ca^{2+}]_i$ response were centrifuged and the supernatant was passed through a 0.45 mm sterile filter. Samples were loaded on Sep-Pak C_{18} (Waters, MA) preconditioned with 0.1% TFA. After a wash with 0.1% TFA, proteins were eluted with 60% acetonitrile in 0.1% TFA and then lyophilized. Batches of one milligram of the lyophilized sample were dissolved in 500 µl 0.1% TFA, centrifuged and injected into an HPLC with a Vydac C_{18} (0.46 x 25 cm) column (Grace Vydac, Hesperia, CA).

The separation was by use of a linear gradient of 20-60% acetonitrile in 0.1% TFA for 40 min at 1 mL/min.

Protein molecular weights were determined by electrospray mass spectrometry (ESMS) on an Autospec hybrid tandem mass spectrometer (Micromass plc, Manchester, UK) operated in the positive ion mode. Samples (16 pmol/μL) were introduced to the ES interface by either continuous infusion or loop injection at a flow rate of 3 μL/min.

2.7 Preparation of cells and media

Pancreatic islets were isolated by a collagenase technique and cell suspensions were prepared as described by Lernmark [63]. Cells were seeded onto glass cover slips and cultured at 37°C in a humidified atmosphere of 5% CO_2 in air, or used as cell suspensions.

The basal medium used both for isolation of cells and for experiments was a HEPES buffer (pH 7.4), containing (in mM): 125 NaCl, 5.9 KCl, 1.3 CaCl2, 1.2 $MgCl_2$, 25 HEPES. Bovine serum albumin was added to the medium at a concentration of 1 mg/ml. For cell culture, RPMI 1640 medium was supplemented with 100 μg/ml streptomycin, 100 IU penicilliṇ and 10% fetal calf serum, normal human serum or diabetic human serum.

2.8 Measurements of $[Ca^{2+}]_i$ and insulin release

Cells, attached to cover slips, were pretreated with the different compounds as described in the results section (paper IV and V) and then incubated in basal medium with 2 μM fura-2AM (Molecular Probes, Eugene, OR) for 30 minutes. The cover slips were mounted as the bottom of an open chamber and cells were perifused with medium. Fluorescence signals were recorded with a SPEX Fluorolog-2 system connected to an inverted Zeiss Axiovert epifluorescence microscope. The excitation and emission wavelengths were 340/380 and 510 nm, respectively. The results are presented as 340/380 excitation ratios, directly representative of $[Ca^{2+}]_i$ [64].

Cells in suspension were incubated overnight with 50, 100 or 150 mg/L TTR (Sigma) and 1 or 2 μg/mL purified TTR monomer. Control cells were incubated with the vehicle (water) of TTR. Dynamics of insulin release were studied by perifusing islet cell aggregates mixed with Bio-Gel P4 polyacrylamide beads (Bio-Rad) in a 0.5 ml column at 37°C [65]. The flow rate was 0.2mL/min, and 2 minutes fractions were collected and analyzed for insulin by a radioimmunoassay using a rat insulin standard (Novo Nordisk).

2.9 Patch clamp

Whole-cell Ca^{2+} currents were recorded by use of the perforated-patch variant of the whole-cell patch-clamp recording technique [66] to eliminate the loss of soluble cytoplasmic components. Electrodes were filled with (in mM): 76 Cs_2SO_4, 1 $MgCl_2$, 10 KCl, 10 NaCl, and 5 HEPES (pH 7.35), as well as amphotericin B (0.24 mg/mL) to permeabilize the cell membrane and allow low-resistance electrical access without breaking the patch. Pancreatiç β-cells were incubated in RPMI 1640 medium with apoCIII (10 μg/mL) or vehicle overnight. The cells were bathed in a solution containing (in mM): 138 NaCl, 10 tetraethylammonium chloride, 10 $CaCl_2$, 5.6 KCl, 1.2 $MgCl_2$, 5 HEPES and 3 D-glucose (pH 7.4). Whole-cell currents induced by voltage pulses (from a holding potential of -70 mV to several clamping potentials from -60 to 50 mV in 10 mV increments, 100 ms, 0.5 Hz) were filtered at 1 kHz and recorded. All recordings were made with an Axopatch 200 amplifier (Axon Instruments, Foster City, California) at room temperature (about 22°C). Acquisition and analysis of data were done using the software program pCLAMP6 (Axon Instruments, Foster City, California).

2.10 Flow cytometric analysis of cell death

RINm5F cells were cultured for 36 h in the presence of 10% control serum, control serum and 40 μg/mL apoCIII, or T1D serum with or without 100 or 200 μg/mL anti-apoCIII. The whole cell population was collected, stained with EGFP-conjugated Annexin V and propidium iodide (PI) (BD PharMingen), and analyzed on a FACscan using CELLQuest acquisition software (Becton Dickinson, Immunocytometry System). FACS gating, based on forward and side scatter, was used to exclude cellular debris and autofluorescence. Typically 10 000 cells were selected for analysis.

3 RESULTS

3.1 Paper I:

This study was carried out to identify the target organ(s) of VIP in vivo when administrated intravenously. In vivo distribution of ^{131}I-VIP was studied using a rat model in combination with a gamma camera. During the first minute, the radioactivity was accumulated in the lungs and then redistributed into the kidneys, gastric mucosa, liver and small intestine; this was observed by the gamma camera and established by a gamma counter.

^{131}I-VIP was eliminated rapidly from the blood with a half-life of 0.44±0.05 (min±SD), while in lung the elimination half-life was determined to be 2.3±0.8 (min±SD). The radioactivity was cleared from the lungs by biphasic elimination, one short [0.9±0.2 (min±SD)], the other longer [20.6±1.5 (min±SD)] Fig. 1.

Figure 1

Pharmakokinetics of the radioactivity in the rat lungs (biphasic elimination)

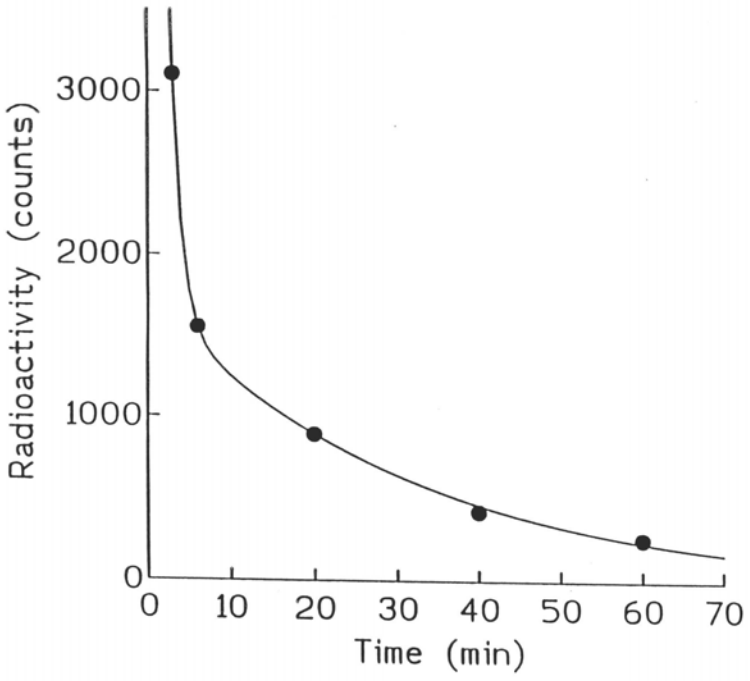

From the rat sacrificed after 20 min, extract of lung tissue had intact ^{131}I-VIP representing 2% of the tissue radioactivity, as identified by coelution with the iodinated VIP. No intact iodinated VIP was found in the rat lung tissue beyond that time point. When 100 fold

unlabeled VIP was coinjected with a trace amount of ^{131}I-VIP, the radioactivity in the lung was 6-fold less when compared to the injection of ^{131}I-VIP (calculated as the ratio lung/whole body).

3.2 Paper II:

This study investigates liposomal ^{131}I-VIP half-life and biodistribution when administrated intravenously into the rats.

The liposomes used, (600nm) in size, were stable and did not form any aggregates at +4°C for 22 days. ^{131}I-VIP encapsulated in liposomes and administrated intravenously into the rats showed higher accumulation at 10 min, in the lungs (per mL tissue) than that observed after the administration of ^{131}I-VIP Fig. 2.

Figure 2

An image of the rat 10 min post injection of liposomal ^{131}I-VIP (left) and ^{131}I-VIP (right).

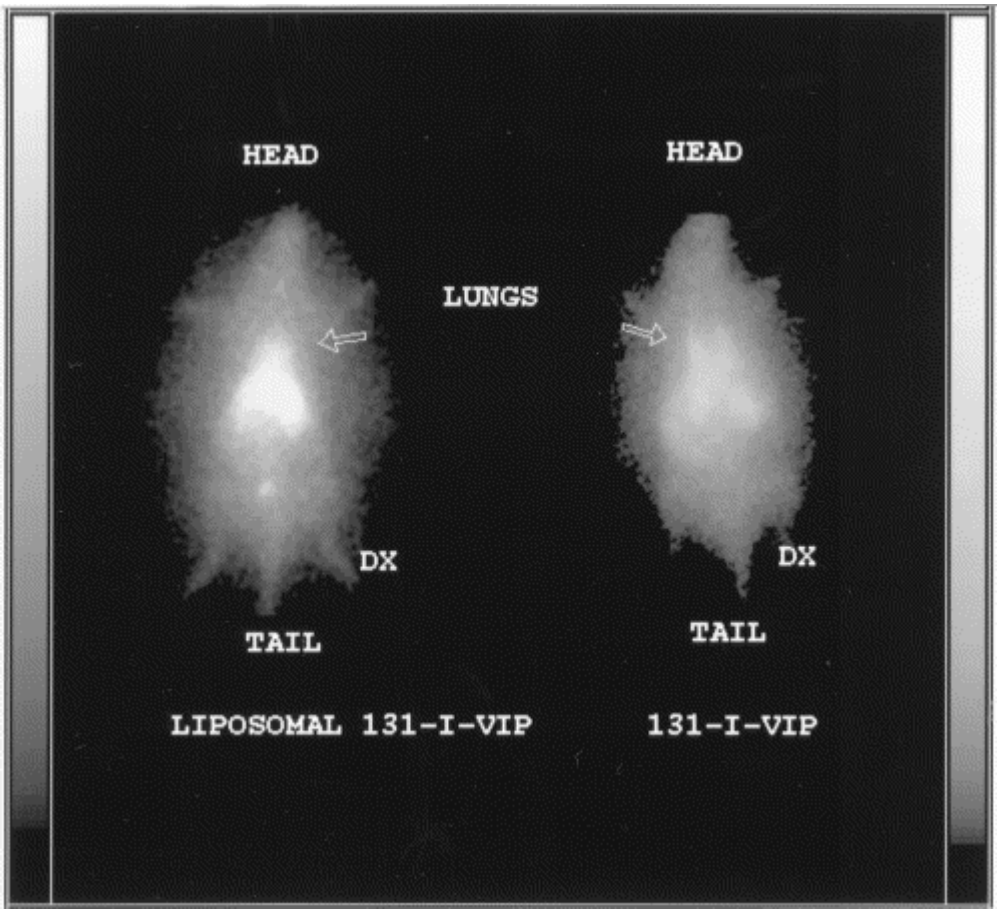

The distribution determined by a gamma camera was established and was in agreement with that obtained by counting the radioactivity in the removed organs. The elimination half-life of liposomal ^{131}I-VIP in blood, 5.29 min, was eight-fold higher than that of ^{131}I-VIP. The radiolabelled VIP encapsulated in liposomes, as well as the radiolabelled VIP, was displaced from the rat lungs by an intravenous administration of an excess of non-labelled VIP (200 μg). A scan after 24 hr showed that the radioactivity remaining after the administration of ^{131}I-VIP and liposomal ^{131}I-VIP was localized to the thyroid gland, stomach and urine bladder. This indicates that the encapsulation of VIP in liposomes prolongs its half-life in the blood.

3.3 Paper III:

Somatostatin and VIP immunoreactivities as well as their respective receptors were analysed in human neuroblastoma SH-SY5Y xenografts in nude rats. The therapeutic effects of VIP, a somatostatin analogue ^{111}In-pentetreotide and 13-cis-retinoic acid were analysed with respect to the in vivo expression of somatostatin and VIP receptors. This selection was due to the fact that the SH-SY5Y cell line has been reported to have an autocrine expression of VIP receptors and also to respond to retinoic acid with upregulation of VIP receptors [38, 42]. The SH-SY5Y xenografts grown in nude rats showed only a low level of somatostatin immunoreactivity (0.08 pmol/g). However, all xenografts in rats showed positive scans for ^{111}In-pentetreotide, indicating the presence of high affinity somatostatin receptors in tumour tissue. Expression of somatostatin receptors, but low levels of somatostatin peptide concentrations in the xenografts, promoted us to try treatment with the somatostatin analogue ^{111}In-pentetreotide, compared with VIP and 13-cis-retinoic acid treatment. All treated rats showed positive scans for ^{111}In-pentetreotide indicating high-affinity somatostatin receptors. Rats treated with ^{111}In-pentetreotide or VIP showed higher uptake in tumour tissue of ^{131}I-VIP than rats receiving treatment with retinoic acid or no treatment at all. From the dynamic scans of the gamma camera, it was observed that rats receiving ^{111}In-pentetreotide in the higher dose range showed more intense in vivo labelling of tumour tissue for both ^{111}In-pentetreotide and ^{131}I-VIP compared to control rats and rats receiving 13-*cis*-retinoic acid.

Thus, specific somatostatin analogues were not only useful in target therapy but can also be used to facilitate receptor scintigraphy since they upregulate peptide receptors.

3.4 Paper IV:

Sera from newly diagnosed T1D patients have been shown to increase the activity of voltage-gated L-type Ca^{2+}-channels and induce apoptosis in β-cells [61]. To isolate the factor responsible for the observed effect we used sera from newly diagnosed T1D patients. Five positive sera were pooled, concentrated and fractionated by HPLC. When testing the fractions in pancreatic β-cells from ob/ob mice one fraction (the bar no. 3, fig 3 a), eluting between 52-60% acetonitrile, induced a higher increase in $[Ca^{2+}]_i$ when the cells were depolarized. The component(s) in this fraction were purified further using repeated HPLC (Fig. 3b, d). All fractions obtained from these steps of purification were also tested for effects on isolated β-cells. The isolated protein that induced increase in $[Ca^{2+}]_i$ (the bar in Fig. 3d) was characterized. Sequence information was obtained by both C-terminal and N-terminal degradations in ABI 494C and cLC sequencers. The sequences obtained were identical to those of apoCIII for 20 N-terminal and 5 C-terminal residues.

Figure 3

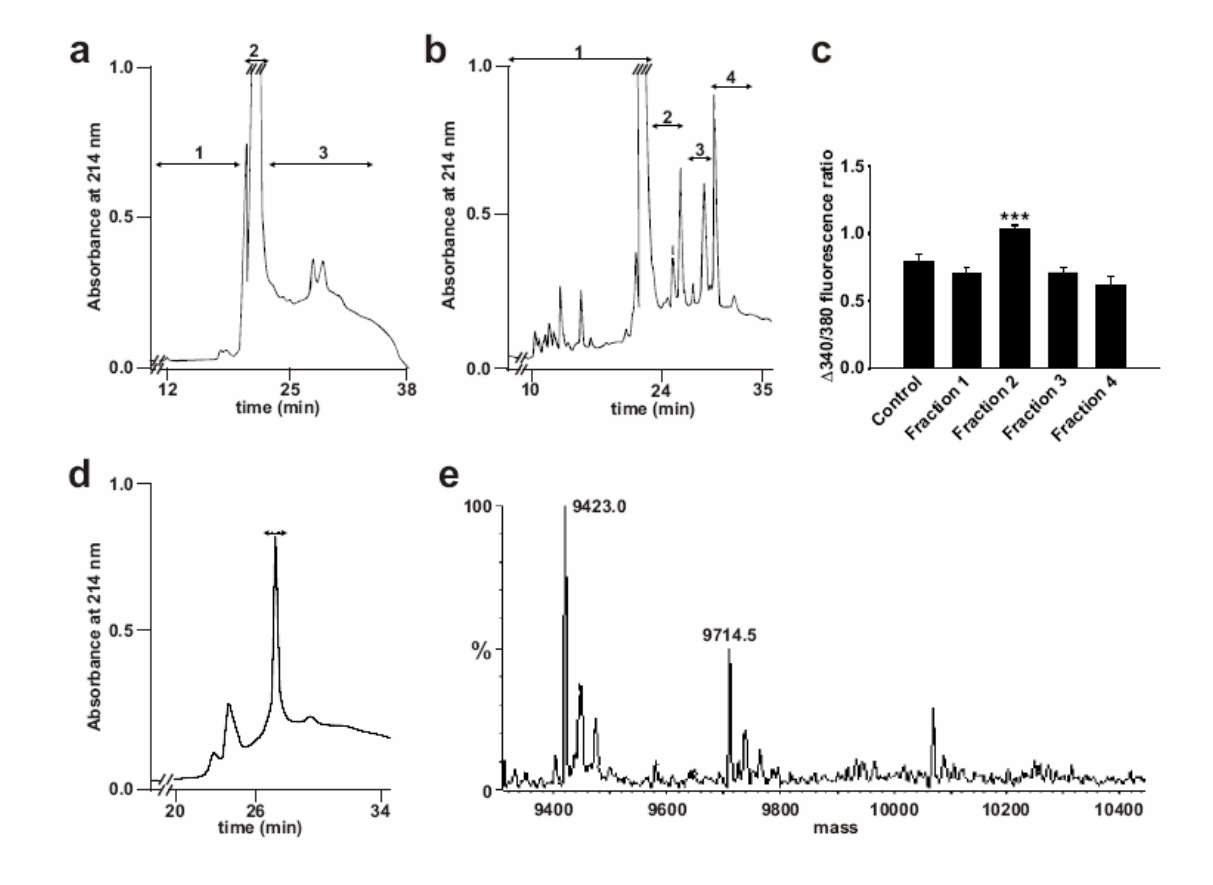

The purified apoCIII fraction was analyzed by mass spectrometry for subcomponent identification. The major components had apparent masses of 9423 and 9714 Da (fig 3e), but non-glycosylated apoCIII has a mass of 8765 Da. To determine the position of the possible modification of the apoCIII fraction, it was digested with trypsin. The resulting fragments were separated by HPLC using a Vydac C_8 (2.1 x 150 mm). The separated fragments masses were measured using ESMS. Among the fragment masses observed for apoCIII, the only difference compared to theoretical tryptic peptide masses, was for the C-terminal residues. However, a galactose-N-acetyl galactosamine modification has been described [67], resulting in a theoretical mass of 9420 Da for $apoCIII_1$ and 9712 Da for $apoCIII_2$. Thus the observed masses of 9423 and 9714 Da (fig 3e) correspond to the mono- and di-glycosylated forms of apoCIII.

Our study shows that the levels of apoCIII isolated from T1D sera were four fold higher than from control sera. This is in agreement with earlier results that found apoCIII concentrations to be higher in diabetic patients than in normal controls [68-70]. ApoCIII increased $[Ca^{2+}]_i$ in pancreatic β–cells and induced Ca^{2+} dependent programmed cell death. Polyclonal antisera against human apoCIII blocked the activity of apoCIII and T1D sera. The antibody itself had no activity. Cell death in the cell population exposed to T1D sera was prevented by the addition of anti-apoCIII. The stimulatory effect of apoCIII on the voltage-gated Ca^{2+}-channel was analysed in β-cells using the patch clamp technique. ApoCIII treated cells showed larger Ca^{2+}-channel currents than control cells within the physiological range of -10 to 10 mV, from a holding potential of -70 mV. These data suggest that increased levels of apoCIII in T1D sera could have cytotoxic effects on pancreatic β-cells in a Ca^{2+} dependent manner.

3.5 Paper V:

TTR is involved in the transport of thyroxine (T4) and retinol-binding protein (RBP) in cerebrospinal fluid (CSF) and serum. It exists mainly as a tetramer, with only a small amount of TTR monomer, *in vivo*. Levels of TTR were shown to decrease in diabetic patients, while we observed that a 14 kDa band on SDS-PAGE, representing TTR monomer, was of a higher intensity in T1D patients than in controls.

The identification of TTR was carried out from diabetic sera that induced a higher increase $[Ca^{2+}]_i$ in pancreatic β–cells than sera from controls. Briefly samples were centrifuged and the supernatant was passed through a sterile filter before concentrating and desalting on Sep-Pak C_{18} .

The sample was analysed by two separate SDS-PAGEs. One gel was stained with Coomassie Brilliant Blue and one was blotted on PVDF membrane and stained lightly. The band at 14 kDa was cut out and in-gel digested. The tryptic fragments were analysed by matrix assisted laser desorption/ionization (MALDI). The fingerprint pattern suggested the presence of TTR. This result was confirmed by running the band cut out from the PVDF membrane on an amino acid sequencer 15 cycles from the N-terminal.

Changes in cytoplasmic free Ca^{2+} concentration, $[Ca^{2+}]_i$, in β-cells pretreated with TTR (tetramer) was measured at concentrations of 50, 100, and 150 μg/mL. Only the concentrations of 100 and 150 μg/mL induced a pronounced increase in $[Ca^{2+}]_i$ and was paralleled by changes in insulin release. TTR monomer was purified from TTR by HPLC and was tested at concentrations of 1 and 2 μg/mL. Both concentrations gave pronounced increase in $[Ca^{2+}]_i$ compared to controls. Although none of the monomer concentrations had effects on insulin secretion, basal insulin secretion was significantly higher in cells treated with 2 μg/mL. This could have harmful effects on β-cells, but neither the tetrameric TTR (150 μg/mL) nor monomeric TTR (2 μg/mL) did induce cell death.

These data suggests that in T1D patients serum levels of TTR decrease under conditions where the tetramer form dissociates into the monomer form. These changes in TTR are associated with increases in both $[Ca^{2+}]_i$ and insulin release.

4 DISCUSSION

4.1 Papers I-III

Early diagnosis of cancer is important for treatment and long-time survival. Receptor imaging using radiolabeled peptides has been found to be a promising diagonstic tool in several cases [29, 71].

Both somatostatin and VIP receptors are present in a number of tumours [72]. A somatostatin-labeled analogue, ^{111}In-pentetreotide, is now routinly used in diagnosis. However, its clinical use is limited because of several factors, i.e. its biodistribution, the complicated physiological function, and the presence of several receptor subtypes [73]. Alternative peptides, with tumours expressing their receptors, can be a useful tool in diagnosis.

We have studied the in vivo distribution of ^{131}I-VIP in the rat with a gamma camera. Radioiodinated VIP maintains a high biological activity as determined by cAMP formation in receptor expressing tumour cell lines [74]. Dynamic scans of the uptake of the radioactivity

showed that ^{131}I-VIP, when administrated iv, is rapidly eliminated from the circulation and accumulated in the lungs during the first minute. A low uptake and almost no accumulation in the lungs was seen when a large amount of non-labeled VIP was coinjected with ^{131}I-VIP. After the initial uptake, the radioactivity is cleared from the lungs by biphasic elimination.

These results confirm the presence of a high number of specific VIP receptors in rat lung [75]. The data are also in good agreement with the results reported by Barrocliffe et al. [76], showing that the lungs play an important role in the clearence of iodinated VIP from circulation after intravenously administration. The regression analysis of the concentration of intact ^{131}I-VIP obtained by HPLC analysis in lungs and blood showed that the elimination half-life was longer in lungs (2.34 min) than in blood (0.45 min). The chromatographic analysis showed that the radioactivity found in the kidneys, liver, intestines and colon did not correspond to intact ^{131}I-VIP at any of the times studied. The short half-life of VIP is due to its rapid degradation by serum components [77, 78], limits its clinical use.

Numerous attempts have been carried out to stabilize the peptide by chemical modification or by modification the amino acid sequence [79]. None of these forms has reached clinical use because of low activity of the modified analogues.

To overcome the short half-life of VIP in circulation, we encapsulated ^{131}I-VIP in liposomes and studied the biodistribution after intravenous adminstration in a rat. The liposomes are non-toxic drug carriers where both hydrophilic and hydrophobic molecules can be entrapped. The properties of liposomes depend on their size, chemical composition, and charge. Large liposomes target primarily the liver and spleen while very small liposomes target bone marrow [80, 81]. They offer also sustained release in the blood when administered intravenously [82].

We compared both ^{131}I-VIP and encapsulated ^{131}I-VIP and we have shown that:

1) When VIP was encapsulated in liposomes, a two-fold higher exposure was found than when free VIP, in blood and lung, was used. Blood and lung exposure was expressed as AUC.
2) A three-fold longer half-life in lungs was observed after intravenous administration of liposomal VIP than after an intravenous administration of VIP.
3) An eight-fold higher half-life was obtained in blood after administration of liposomal VIP than after administration of VIP.

Our results are consistent with other studies showing that encapsulation of VIP in liposomes enhanced and prolonged its biological activity. These studies also showed that liposomes protects VIP from rapid degradation both in vivo and in vitro [83-85].

Liposomal encapsulation of VIP represents an efficient delivery form, protecting VIP from enzymatic degradation in the blood. It may also sustain the release into the circulation. These mechanisms seem to offer important therapeutic advantages over VIP delivered in its native form.

In vitro studies have shown that VIP may induce growth inhibition and differentiation of malignant neuroblastoma cell lines [86]. Expressions of receptors specific for VIP are necessary for the biological effects of VIP. VIP receptors have been previously detected on neuroblastoma cells [38]. Data implicate that VIP-induced differentiation of neuroblastoma cells markedly increased VIP receptor expression [40].

We have used a nude rat model with the neuroblastoma cell line SH-SY5Y injected on the lateral side of each hind leg. The SH-SY5Y grown in the rats showed a low level of somatostatin immunoreactive concentration and the somatostatin receptor scintigraphy showed tumour tissue expressing the somatostatin receptor. This fact prompted us to compare somatostatin, VIP and 13-*cis*-retinoic acid in the treatment of those tumours.

All treated rats showed positive scans for ^{111}In-pentetreotide, which indicated high affinity receptors for somatostatin. Using ^{131}I-VIP to image tumours in treated rats, higher uptake was observed in rats treated with ^{111}In-pentetreotide or VIP than in rats receiving treatment with 13-cis-retinoic acid or in controls. This implies that SH-SY5Y xenografts showed an increase in scintigraphic detection of somatostatin and VIP receptors in vivo when treated with somatostatin analogue or VIP. The higher tumour uptake may in part be due to an upregulation of VIP receptors on tumour cells. Previous studies showed that VIP synthesis is increased in neuroblastoma cells by differentiation induced by 13-cis-retinoic acid and VIP [86]. The high affinity binding sites for somatostatin and VIP in the treated rats appears to be useful for diagnosis. In summary, we show that:

- VIP has a short half-life, when administrated intravenously, in *vivo* and targets the lungs.
- Encapsulation of VIP in liposomes protects it from rapid degradation and elongates its half-life in vivo eight-fold.
- VIP can be used as an agent to detect tumours in a rat model.

Even though we did not have the opportunity to expand our studies for tumour imaging in humans, Virgolini and colleges have demonstrated the potential use of VIP in imaging a number of intestinal adeno-carcinomas and endocrine tumours. However stable analogues that have high affinity to both VIP receptors are still not available.

4.2 Papers IV-V

The major difficulties in identifying proteins from serum or plasma is derived from the fact that a small number of proteins such as albumin, alpha2-macroglobulin, transferrin, and immunoglobulins, may represent as much as 80% of the total serum protein. The large quantity of these proteins makes it difficult to identify other proteins in serum especially if the amount of sera is limited as in our case.

Sera from newly diagnosed T1D patients have been shown to increase the activity of voltage-gated L-type Ca^{2+}-channels in β-cells resulting in increased $[Ca^{2+}]_i$. This increase promoted Ca^{2+}-induced apoptosis [61]. Identification of the subcomponents of the sera that cause such effects could be of importance in the outcome of the disease.

T1D diabetic sera were collected and tested for increase in $[Ca^{2+}]_i$. The positive sera were pooled, concentrated and fractionated. The active fractions, being responsible for the increase in $[Ca^{2+}]_i$, has been identified to be apoCIII and TTR.

It is known that the levels of apoCIII differ in diabetic patients versus healthy individuals. In poorly controlled type 1 diabetic patients the levels of apoCIII were largely increased, and returned to normal when the glycaemic control was improved [69, 87]. It is not specified whether the increase includes both the sialylated and non-sialylated isoforms. Furthermore, there are no previous reports on the effects of apoCIII on pancreatic β-cells and $[Ca^{2+}]_i$.

Human TTR was the first serum protein for which the amino acid sequence and 3D structure were determined. TTR is a serum protein that transports thyroxine and retinol-binding protein. It exists mainly as a stable tetramer under physiological conditions, but a small amount of monomer has recently been found *in vivo* in normal individuals. TTR is associated with two medical disorders: familial amyloidotic polyneuropathy (FAP) caused by mutations within the protein, and senile systemic polyneuropathy (SSA) that involves the native protein. In the northern parts of Sweden, FAP is prevalent and is also referred to as "Skelleftesjukan". It is also a marker of malnutrition and chronic inflammation.

Commercially available apoCIII and TTR were tested and shown to stimulate Ca^{2+} influx in a similar manner to the fractions isolated from the T1D sera. The activity of voltage-gated Ca^{2+}-channels was analyzed in mouse β-cells incubated with apoCIII or TTR.

ApoCIII/TTR treated cells displayed larger Ca^{2+}-channel currents than control cells during depolarizations in the range -10 to 10 mV, from a holding potential of –70 mV. These data demonstrate that apoCIII/TTR modulated the activity of the voltage-gated L-type Ca^{2+}-

channel and that the effect occurred in the range of physiological depolarization [88]. It is known that mouse β-cells contain exclusively L-type Ca^{2+}-channels [89]. There was a higher percentage of dead cells in the cell population exposed to apoCIII but not to TTR. Co-incubation of β-cells with a polyclonal antibody raised against apoCIII blocked the activity of both the commercial apoCIII and the diabetic sera. The relative amounts of apoCIII in T1D serum and control serum respectively, were evaluated by comparisons of the peak area corresponding to apoCIII in the second HPLC and showed on average four-fold higher in serum from T1D patients. This suggests that apoCIII/TTR have an effect on pancreatic β-cell stimulus-secretion coupling, specifically increasing the activity of the voltage-gated L-type Ca^{2+}-channel in T1D.

The study of the molecular mechanisms and pathophysiological events by which apoCIII/TTR can affect β-cells might be of great importance for the development of new insights for T1D.

5 ACKNOWLEDGEMENTS

A Word of Thanks

I thank you all for your goodness
For your kindly thought of me
So here's my heart's acknowledgement
In simple words expressed
May God bless and thank you all
In the way that he knows best

I must be a lucky person to be surrounded by such good, kind and talented people who supported and helped me through my thesis. I wish to express my sincere gratitude to the following people:

- ***My supervisors***

- **Mats Andersson**, for supplying me with professional guidance, encouragement, excellent teaching, creative suggestions, fruitful discussions, sharing your wide scientific knowledge with me and our long friendship.
- **Hans Jörnvall,** for brilliant guidance, providing me excellent working environment, help whenever needed, vast knowledge of protein science and for arranging great scientific lab meetings. You are special, and I am truly grateful for your support.

Per-Olof Berggren, for introducing me into the field of Ca^{2+} ions and β-cells, giving me the opportunity to take part in such an interesting field of research, for your stimulating intellect and positive provocative attitude where no mountains are too high to climb.

Lisa Juntti-Berggren, for your inspiring positive attitude, taking time to discuss with me both research and other matters.

Moustapha Hassan, for initiating my thesis, professional guidance in radiolabelled tracers, animal models, pharmacokinetics and being a close reliable friend.

Per Kogner, for the knowledge on neuropeptides in neurotumours and for fruitful discussions which always gave me a better view.

Jaroslaw Szecowka, for introducing me to **P-O Berggren** and the field of diabetes, travelling with me throughout Poland and beginning such a dear friend despite the distances between us.

Sami Said, the father of **VIP**, for supporting me many years at **Viktor´s Lab**, and all the knowledge about VIP.

Andreas Jonsson, the guy with a golden heart and ambitious goals, "my little brother".

The people from "**Viktor´s Lab**": **Birgitta Agerberth, Guro Gafvelin, Jan Wiberg, Johnny Söderlund, Åke Norberg, Mats Carlquist, Maj-Britt Marin, Rannars Sillard, Elo Eriste, Louise Melin, J-C Marie, Zheng-wang Chen and Delphi Post,** thank you all for the memorable years, I am fortunate to have had such wonderful, intelligent and helpful lab mates.

Previous and present room mates: **Charlotta Filling, Valentina Bonetto, Sam Tryggvason, Theres Jägerbrink and Susanne Vollmer**, for support help and friendship.

Previous an present PhD students: **Erik Nordling, Yvonne Kallberg, Magnus Gustafsson, Ermias Melles, Margareta Stark, Jing Li, Annika Norin, Naeem Shafqat, Yuqin Wang, Malin Hult, Johan Lengqvist, Daniel Hirschberg, Anna Päiviö, Patrik Strömberg, Jesper Hedberg, Maria Tollin, Naeem Shafqat, Johan Nilsson, Andreas Almlén, Madalina Oppermann, Juan Astorga-Wells, Xiaoqiu Wu, Waltteri Hosia, Gudmundur Bergsson, Mikael Henriksson, Peter Bergman, Shah Zaltash,** for their help, nice discussions about science and life, and for creating a friendly working environment at HEJ-lab.

Previous and present people at Chemistry I: **William J. Griffiths, Tomas Bergman, Lars Hjelmqvist, Jawed Shafqat, Jan Sjövall, Åke Rökaeus, Udo Oppermann, Jenny Samskog, Jan Johansson and Bengt Persson,** for nice discussions about science and sharing of your outstanding knowledge.

Jan-Olof Höög´s group: **Margareta Brandt** and **Claudia Staab**, for being so friendly.

From MTC: **Katrin Pütsep, Birgitta Wallström, Charlotta Linde and Jenny Karlsson**, for wonderful collaboration and being so kind and helpful.

Techincians "**The Ladies**": **Ella Cederlund, Carina Palmberg, Marie Ståhlberg, Monica Lindh, Gunvor Alvelius, Irene Byman and Eva Mårtensson** for great help and excellent technical expertise.

Our excellent secretaries: **Ingegerd Nylander** and **Ann-Margareth Jörnvall**, for their great help and kindness.

Teaching aid at MBB: **Susanne Rothstein, Sussi Björkholm** and **Ulf Eriksson** for their kind help and excellent expertise.

Work shop & computers: **Sören Lundmark, Svante Backlund, Jan Hallensjö** and **Anders Lundsjö** for their help and support.

Angelika Arribada, for taking care of glassware, dry ice and autoclaving, and for being a helpful person.

Rolf Luft Center for Diabetes Research: **Nancy Dekki, Ioulia Appelskog, Martin Köhler, Sabine Uhles, Tilo Moede, Barbara Leibiger, Ingo Leibiger, Gabriela Imreh, Sergei Zaitsev, Christopher Barker, Christina Bark, Jenny Johansson, Dominic-Luc Webb and Shao-Nian Yang,** for excellent collaboration and being so nice and helpful.

From Dept. of Hospital Physics, KS: **Hans Jacobsson, Stig Larsson, Per-Olof Schnell Cathrine Jonsson**, for excellent expertise help with gamma camera, radiotracers and being wonderful people to work with.

From Matrix Biology: **Ari Tuuttila, Marko Sankala, Timo Pikkarainen, Stefania Cotta Doné** and **Matatoshi Nukui**, for being good friends and help both in scientific and computer issues.

From Chemistry II: **Cecila Ross**, for being such a nice person and all the PhD parties…never mind United, LIVERPOOL is the club.

For outside KI, I would like to thank:

Aadel , Azza, Badr, Mohamed, and **Belal-Abdel Aziz**, for support and being family for me in Sweden.

My friends from school "**ESC"** for their care, help and love.

Hani El Sineity, my school friend who was always there with care, encouragement and a helping hand.

From Kampementshallen: **Janolof Hansson, Lars Hasselqvist and Eric Malmström**, for their support, kindness and friendship.

Finally, I would like to acknowledge my **mother, father, Sara, Josef and Mariam** for their great support, encouragement, love and care.

A Special acknowledgement

To the late Viktor Mutt who taught me the principles of protein purification. Thank you Viktor for all the wonderful years I spent at your laboratory, and may your soul rest in peace.

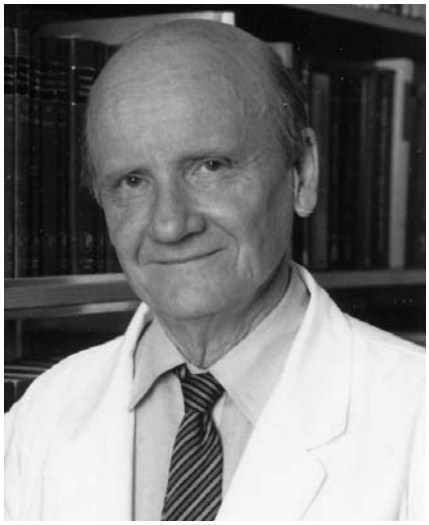

Viktor Mutt

6 REFERENCES

1. Bayliss, W.M. and E.H. Starling, *The mechanism of pancreatic secrection.* J. Physiol. Lond., 1902. **28**, 325-353.
2. Mutt, V., *Preparation of highly purified secretin.* Ark. Kemi, 1959. **15**, 69-74.
3. Mutt, V., J.E. Jorpes, and S. Magnusson, *Structure of porcine secretin. The amino acid sequence.* Eur J Biochem, 1970. **15**, 513-519.
4. Said, S.I. and V. Mutt, *A peptide fraction from lung tissue with prolonged peripheral vasodilator activity.* Scand J Clin Lab Invest Suppl, 1969. **107**, 51-56.
5. Said, S.I. and V. Mutt, *Polypeptide with broad biological activity: isolation from small intestine.* Science, 1970. **169**, 1217-1218.
6. Jornvall, H., V. Mutt, and M. Persson, *Structural similarities among gastrointestinal hormones and related active peptides.* Hoppe Seylers Z Physiol Chem, 1982. **363**, 475-483.
7. Sherwood, N.M., S.L. Krueckl, and J.E. McRory, *The origin and function of the pituitary adenylate cyclase-activating polypeptide (PACAP)/glucagon superfamily.* Endocr Rev, 2000. **21**, 619-670.
8. Steiner, D.F., *Evidence for a precursor in the biosynthesis of insulin.* Trans N Y Acad Sci, 1967. **30**, 60-68.
9. Sachs, H. and Y. Takabatake, *Evidence for a Precursor in Vasopressin Biosynthesis.* Endocrinology, 1964. **75**, 943-948.
10. Said, S.I., *VIP as a modulator of lung inflammation and airway constriction.* Am Rev Respir Dis, 1991. **143**, S22-24.
11. Said, S.I., *Vasoactive intestinal polypeptide (VIP) in asthma.* Ann N Y Acad Sci, 1991. **629**, 305-318.
12. Klimaschewski, L., *VIP -- a 'very important peptide' in the sympathetic nervous system?* Anat Embryol (Berl), 1997. **196**, 269-277.
13. Ganea, D. and M. Delgado, *Vasoactive intestinal peptide (VIP) and pituitary adenylate cyclase-activating polypeptide (PACAP) as modulators of both innate and adaptive immunity.* Crit Rev Oral Biol Med, 2002. **13**, 229-237.
14. Saito, K., K. Yamatani, H. Manaka, K. Takahashi, M. Tominaga, and H. Sasaki, *Role of Ca2+ on vasoactive intestinal peptide-induced glucose and adenosine 3',5'-monophosphate production in the isolated perfused rat liver.* Endocrinology, 1992. **130**, 2267-2273.
15. Christophe, J.P., T.P. Conlon, and J.D. Gardner, *Interaction of porcine vasoactive intestinal peptide with dispersed pancreatic acinar cells from the guinea pig. Binding of radioiodinated peptide.* J Biol Chem, 1976. **251**, 4629-4634.
16. Desbuquois, B., *The interaction of vasoactive intestinal polypeptide and secretin with liver-cell membranes.* Eur J Biochem, 1974. **46**, 439-450.
17. Bataille, D., G. Rosselin, and P. Freychet, *Interactions of glucagon, gut glucagon, vasoactive intestinal polypeptide and secretin with their membrane receptors.* Isr J Med Sci, 1975. **11**, 687-692.
18. Lutz, E.M., W.J. Sheward, K.M. West, J.A. Morrow, G. Fink, and A.J. Harmar, *The VIP2 receptor: molecular characterisation of a cDNA encoding a novel receptor for vasoactive intestinal peptide.* FEBS Lett, 1993. **334**, 3-8.
19. Svoboda, M., M. Tastenoy, J. Van Rampelbergh, J.F. Goossens, P. De Neef, M. Waelbroeck, and P. Robberecht, *Molecular cloning and functional characterization of a human VIP receptor from SUP-T1 lymphoblasts.* Biochem Biophys Res Commun, 1994. **205**, 1617-1624.

20. Inagaki, N., H. Yoshida, M. Mizuta, N. Mizuno, Y. Fujii, T. Gonoi, J. Miyazaki, and S. Seino, *Cloning and functional characterization of a third pituitary adenylate cyclase-activating polypeptide receptor subtype expressed in insulin-secreting cells.* Proc Natl Acad Sci U S A, 1994. **91**, 2679-2683.
21. Reubi, J.C., *Regulatory peptide receptors as molecular targets for cancer diagnosis and therapy.* Q J Nucl Med, 1997. **41**, 63-70.
22. Brenneman, D.E., J. Hauser, C.Y. Spong, T.M. Phillips, C.B. Pert, and M. Ruff, *VIP and D-ala-peptide T-amide release chemokines which prevent HIV-1 GP120-induced neuronal death.* Brain Res, 1999. **838**, 27-36.
23. Said, S.I. and K.G. Dickman, *Pathways of inflammation and cell death in the lung: modulation by vasoactive intestinal peptide.* Regul Pept, 2000. **93**, 21-29.
24. Goldenberg, D.M., F. DeLand, E. Kim, S. Bennett, F.J. Primus, J.R. van Nagell, Jr., N. Estes, P. DeSimone, and P. Rayburn, *Use of radiolabeled antibodies to carcinoembryonic antigen for the detection and localization of diverse cancers by external photoscanning.* N Engl J Med, 1978. **298**, 1384-1386.
25. Serafini, A.N., *From monoclonal antibodies to peptides and molecular recognition units: an overview.* J Nucl Med, 1993. **34**, 533-536.
26. De Jager, R., H. Abdel-Nabi, A. Serafini, A. Pecking, J.L. Klein, and M.G. Hanna, Jr., *Current status of cancer immunodetection with radiolabeled human monoclonal antibodies.* Semin Nucl Med, 1993. **23**, 165-179.
27. Behr, T.M., S. Memtsoudis, R.M. Sharkey, R.D. Blumenthal, R.M. Dunn, S. Gratz, E. Wieland, K. Nebendahl, H. Schmidberger, D.M. Goldenberg, and W. Becker, *Experimental studies on the role of antibody fragments in cancer radio-immunotherapy: Influence of radiation dose and dose rate on toxicity and anti-tumor efficacy.* Int J Cancer, 1998. **77**, 787-795.
28. Reubi, J.C., B. Waser, J.C. Schaer, and R. Markwalder, *Somatostatin receptors in human prostate and prostate cancer.* J Clin Endocrinol Metab, 1995. **80**, 2806-2814.
29. Reubi, J.C., S.J. Lamberts, and E.P. Krenning, *Receptor imaging of human diseases using radiolabeled peptides.* J Recept Signal Transduct Res, 1995. **15**, 379-392.
30. Kogner, P., *Neuropeptides in neuroblastomas and ganglioneuromas.* Prog Brain Res, 1995. **104**, 325-338.
31. Virgolini, I., M. Raderer, A. Kurtaran, P. Angelberger, S. Banyai, Q. Yang, S. Li, M. Banyai, J. Pidlich, B. Niederle, and et al., *Vasoactive intestinal peptide-receptor imaging for the localization of intestinal adenocarcinomas and endocrine tumors.* N Engl J Med, 1994. **331**, 1116-1121.
32. Reubi, J.C., *Peptide receptors as molecular targets for cancer diagnosis and therapy.* Endocr Rev, 2003. **24**, 389-427.
33. Behr, T.M., M. Gotthardt, A. Barth, and M. Behe, *Imaging tumors with peptide-based radioligands.* Q J Nucl Med, 2001. **45**, 189-200.
34. Borgstrom, P., M. Hassan, E. Wassberg, E. Refai, C. Jonsson, S.A. Larsson, H. Jacobsson, and P. Kogner, *The somatostatin analogue octreotide inhibits neuroblastoma growth in vivo.* Pediatr Res, 1999. **46**, 328-332.
35. Wang, H.L., W.T. Chang, A.H. Li, T.H. Yeh, C.Y. Wu, M.S. Chen, and P.C. Huang, *Functional analysis of connexin-26 mutants associated with hereditary recessive deafness.* J Neurochem, 2003. **84**, 735-742.
36. Tonini, G.P. and M. Romani, *Genetic and epigenetic alterations in neuroblastoma.* Cancer Lett, 2003. **197**, 69-73.
37. McConville, C.M. and J. Forsyth, *Neuroblastoma - a developmental perspective.* Cancer Lett, 2003. **197**, 3-9.

38. Muller, J.M., S.J. Lolait, V.C. Yu, W. Sadee, and J.A. Waschek, *Functional vasoactive intestinal polypeptide (VIP) receptors in human neuroblastoma subclones that contain VIP precursor mRNA and release VIP-like substances.* J Biol Chem, 1989. **264**, 3647-3650.
39. O'Dorisio, M.S., D.J. Fleshman, S.J. Qualman, and T.M. O'Dorisio, *Vasoactive intestinal peptide: autocrine growth factor in neuroblastoma.* Regul Pept, 1992. **37**, 213-226.
40. Pence, J.C. and N.A. Shorter, *The autocrine function of vasoactive intestinal peptide on human neuroblastoma cell growth and differentiation.* Arch Surg, 1993. **128**, 591-595.
41. Sucov, H.M. and R.M. Evans, *Retinoic acid and retinoic acid receptors in development.* Mol Neurobiol, 1995. **10**, 169-184.
42. Waschek, J.A., J.M. Muller, D.S. Duan, and W. Sadee, *Retinoic acid enhances VIP receptor expression and responsiveness in human neuroblastoma cell, SH-SY5Y.* FEBS Lett, 1989. **250**, 611-614.
43. Kogner, P., P. Borgstrom, P. Bjellerup, F.H. Schilling, E. Refai, C. Jonsson, C. Dominici, E. Wassberg, H. Bihl, H. Jacobsson, E. Theodorsson, and M. Hassan, *Somatostatin in neuroblastoma and ganglioneuroma.* Eur J Cancer, 1997. **33**, 2084-2089.
44. Matthay, K.K., J.G. Villablanca, R.C. Seeger, D.O. Stram, R.E. Harris, N.K. Ramsay, P. Swift, H. Shimada, C.T. Black, G.M. Brodeur, R.B. Gerbing, and C.P. Reynolds, *Treatment of high-risk neuroblastoma with intensive chemotherapy, radiotherapy, autologous bone marrow transplantation, and 13-cis-retinoic acid. Children's Cancer Group.* N Engl J Med, 1999. **341**, 1165-1173.
45. Brewer, H.B., Jr., R. Shulman, P. Herbert, R. Ronan, and K. Wehrly, *The complete amino acid sequence of alanine apolipoprotein (apoC-3), and apolipoprotein from human plasma very low density lipoproteins.* J Biol Chem, 1974. **249**, 4975-4984.
46. Fredenrich, A., *Role of apolipoprotein CIII in triglyceride-rich lipoprotein metabolism.* Diabetes Metab, 1998. **24**, 490-495.
47. Ruge, T., G. Wu, T. Olivecrona, and G. Olivecrona, *Nutritional regulation of lipoprotein lipase in mice.* Int J Biochem Cell Biol, 2004. **36**, 320-329.
48. Wu, G., G. Olivecrona, and T. Olivecrona, *The distribution of lipoprotein lipase in rat adipose tissue. Changes with nutritional state engage the extracellular enzyme.* J Biol Chem, 2003. **278**, 11925-11930.
49. Grundy, S.M., I.J. Benjamin, G.L. Burke, A. Chait, R.H. Eckel, B.V. Howard, W. Mitch, S.C. Smith, Jr., and J.R. Sowers, *Diabetes and cardiovascular disease: a statement for healthcare professionals from the American Heart Association.* Circulation, 1999. **100**, 1134-1146.
50. Bar-On, H., P.S. Roheim, and H.A. Eder, *Serum lipoproteins and apolipoproteins in rats with streptozotocin-induced diabetes.* J Clin Invest, 1976. **57**, 714-721.
51. Bar-On, H., Y.D. Chen, and G.M. Reaven, *Evidence for a new cause of defective plasma removal of very low density lipoproteins in insulin-deficient rats.* Diabetes, 1981. **30**, 496-499.
52. Bar-on, H., E. Levy, Y. Oschry, E. Ziv, and E. Shafrir, *Removal defect of very-low-density lipoproteins from diabetic rats.* Biochim Biophys Acta, 1984. **793**, 115-118.
53. Takahashi, T., T. Hirano, K. Okada, and M. Adachi, *Apolipoprotein CIII deficiency prevents the development of hypertriglyceridemia in streptozotocin-induced diabetic mice.* Metabolism, 2003. **52**, 1354-1359.

54. Sladek, F.M., W.M. Zhong, E. Lai, and J.E. Darnell, Jr., *Liver-enriched transcription factor HNF-4 is a novel member of the steroid hormone receptor superfamily.* Genes Dev, 1990. **4**, 2353-2365.
55. Diamond, J., *The double puzzle of diabetes.* Nature, 2003. **423**, 599-602.
56. King, H., R.E. Aubert, and W.H. Herman, *Global burden of diabetes, 1995-2025: prevalence, numerical estimates, and projections.* Diabetes Care, 1998. **21**, 1414-1431.
57. Berggren, P.O., P. Arkhammar, M.S. Islam, L. Juntti-Berggren, A. Khan, H. Kindmark, M. Kohler, K. Larsson, O. Larsson, T. Nilsson, and et al., *Regulation of cytoplasmic free Ca2+ in insulin-secreting cells.* Adv Exp Med Biol, 1993. **334**, 25-45.
58. McConkey, D.J., P. Hartzell, P. Nicotera, and S. Orrenius, *Calcium-activated DNA fragmentation kills immature thymocytes.* Faseb J, 1989. **3**, 1843-1849.
59. Nicotera, P., G. Bellomo, and S. Orrenius, *The role of Ca2+ in cell killing.* Chem Res Toxicol, 1990. **3**, 484-494.
60. Orrenius, S., D.J. McConkey, G. Bellomo, and P. Nicotera, *Role of Ca2+ in toxic cell killing.* Trends Pharmacol Sci, 1989. **10**, 281-285.
61. Juntti-Berggren, L., O. Larsson, P. Rorsman, C. Ammala, K. Bokvist, K. Wahlander, P. Nicotera, J. Dypbukt, S. Orrenius, A. Hallberg, and et al., *Increased activity of L-type Ca2+ channels exposed to serum from patients with type I diabetes.* Science, 1993. **261**, 86-90.
62. Mutt, V. and U. Söderberg, *On the assay of secretin.* Arkiv för kemi, 1959. **15**, 63-68.
63. Lernmark, A., *The preparation of, and studies on, free cell suspensions from mouse pancreatic islets.* Diabetologia, 1974. **10**, 431-438.
64. Kindmark, H., M. Kohler, S. Efendic, P. Rorsman, O. Larsson, and P.O. Berggren, *Protein kinase C activity affects glucose-induced oscillations in cytoplasmic free Ca2+ in the pancreatic B-cell.* FEBS Lett, 1992. **303**, 85-90.
65. Kanatsuna, T., A. Lernmark, A.H. Rubenstein, and D.F. Steiner, *Block in insulin release from column-perifused pancreatic beta-cells induced by islet cell surface antibodies and complement.* Diabetes, 1981. **30**, 231-234.
66. Zaitsev, S.V., I.B. Appelskog, I.L. Kapelioukh, S.N. Yang, M. Kohler, S. Efendic, and P.O. Berggren, *Imidazoline compounds protect against interleukin 1beta-induced beta-cell apoptosis.* Diabetes, 2001. **50 Suppl 1**, S70-76.
67. Ito, Y., J.L. Breslow, and B.T. Chait, *Apolipoprotein C-III0 lacks carbohydrate residues: use of mass spectrometry to study apolipoprotein structure.* J Lipid Res, 1989. **30**, 1781-1787.
68. al Muhtaseb, N., A. al Yousuf, and J.S. Bajaj, *Apolipoprotein A-I, A-II, B, C-II, and C-III in children with insulin-dependent diabetes mellitus.* Pediatrics, 1992. **89**, 936-941.
69. Blackett, P., D.C. Sarale, J. Fesmire, J. Harmon, P. Weech, and P. Alaupovic, *Plasma apolipoprotein C-III levels in children with type I diabetes.* South Med J, 1988. **81**, 469-473.
70. Briones, E.R., S.J. Mao, P.J. Palumbo, W.M. O'Fallon, W. Chenoweth, and B.A. Kottke, *Analysis of plasma lipids and apolipoproteins in insulin-dependent and noninsulin-dependent diabetics.* Metabolism, 1984. **33**, 42-49.
71. Behr, T.M., M. Behe, and W. Becker, *Diagnostic applications of radiolabeled peptides in nuclear endocrinology.* Q J Nucl Med, 1999. **43**, 268-280.
72. Reubi, J.C., B. Waser, J.A. Laissue, and J.O. Gebbers, *Somatostatin and vasoactive intestinal peptide receptors in human mesenchymal tumors: in vitro identification.* Cancer Res, 1996. **56**, 1922-1931.

73. Breeman, W.A., W.H. Bakker, M. De Jong, L.J. Hofland, D.J. Kwekkeboom, P.P. Kooij, T.J. Visser, and E.P. Krenning, *Studies on radiolabeled somatostatin analogues in rats and in patients.* Q J Nucl Med, 1996. **40**, 209-220.
74. Hessenius, C., M. Bader, H. Meinhold, M. Bohmig, S. Faiss, J.C. Reubi, and B. Wiedenmann, *Vasoactive intestinal peptide receptor scintigraphy in patients with pancreatic adenocarcinomas or neuroendocrine tumours.* Eur J Nucl Med, 2000. **27**, 1684-1693.
75. Humphrey, C.S., P. Murray, A.M. Ebeid, and J.E. Fischer, *Hepatic and pulmonary clearance of exogenous vasoactive intestinal peptide in the rat.* Gastroenterology, 1979. **77**, 55-60.
76. Barrowcliffe, M.P., A. Morice, J.G. Jones, and P.S. Sever, *Pulmonary clearance of vasoactive intestinal peptide.* Thorax, 1986. **41**, 88-93.
77. Bernhard, W., E. Bothe-Sandtfort, H. Koop, W. Cassel, and P. Von Wichert, *Degradation of vasoactive intestinal peptide by isolated, ventilated, and perfused rat lungs.* Eur J Clin Invest, 1989. **19**, 506-513.
78. Paul, S., D.J. Volle, C.M. Beach, D.R. Johnson, M.J. Powell, and R.J. Massey, *Catalytic hydrolysis of vasoactive intestinal peptide by human autoantibody.* Science, 1989. **244**, 1158-1162.
79. Bolin, D.R., J. Michalewsky, M.A. Wasserman, and M. O'Donnell, *Design and development of a vasoactive intestinal peptide analog as a novel therapeutic for bronchial asthma.* Biopolymers, 1995. **37**, 57-66.
80. Hassan, Z., C. Nilsson, and M. Hassan, *Liposomal busulphan: bioavailability and effect on bone marrow in mice.* Bone Marrow Transplant, 1998. **22**, 913-918.
81. Hassan, M., Z. Hassan, C. Nilsson, M.A. Rehim, S. Kumlien, B. Elfsson, and N. Kallberg, *Pharmacokinetics and distribution of liposomal busulfan in the rat: a new formulation for intravenous administration.* Cancer Chemother Pharmacol, 1998. **42**, 471-478.
82. Ostro, J.M., *Liposomes from biophysics to therapeutics.* Marcel Dekker Inc., New York, 1987.
83. Gao, X.P., Y. Noda, I. Rubinstein, and S. Paul, *Vasoactive intestinal peptide encapsulated in liposomes: effects on systemic arterial blood pressure.* Life Sci, 1994. **54**, PL247-252.
84. Suzuki, H., Y. Noda, S. Paul, X.P. Gao, and I. Rubinstein, *Encapsulation of vasoactive intestinal peptide into liposomes: effects on vasodilation in vivo.* Life Sci, 1995. **57**, 1451-1457.
85. Sejourne, F., H. Suzuki, H. Alkan-Onyuksel, X.P. Gao, H. Ikezaki, and I. Rubinstein, *Mechanisms of vasodilation elicited by VIP in sterically stabilized liposomes in vivo.* Am J Physiol, 1997. **273**, R287-292.
86. Pence, J.C. and N.A. Shorter, *In vitro differentiation of human neuroblastoma cells caused by vasoactive intestinal peptide.* Cancer Res, 1990. **50**, 5177-5183.
87. Alaupovic, P., W.J. McConathy, J. Fesmire, M. Tavella, and J.M. Bard, *Profiles of apolipoproteins and apolipoprotein B-containing lipoprotein particles in dyslipoproteinemias.* Clin Chem, 1988. **34**, B13-27.
88. Rorsman, P. and G. Trube, *Calcium and delayed potassium currents in mouse pancreatic beta-cells under voltage-clamp conditions.* J Physiol, 1986. **374**, 531-550.
89. Ashcroft, F.M. and P. Rorsman, *Electrophysiology of the pancreatic beta-cell.* Prog Biophys Mol Biol, 1989. **54**, 87-143.

I

Pergamon

0969-8051(93)E0023-X

Nucl. Med. Biol. Vol. 21, No. 6, pp. 865–872, 1994

0969-8051/94 $7.00 + 0.00

In Vivo Dynamical Distribution of ^{131}I-VIP in the Rat Studied by Gamma-camera

MOUSTAPHA HASSAN[1]*, ESSAM REFAI[2], MATS ANDERSSON[2], PER-OLOF SCHNELL[3] and HANS JACOBSSON[4]

[1]Karolinska Pharmacy, Research Department, [2]Department of Medical Biochemistry and Biophysics, Laboratory of Biochemistry II, Karolinska Institute, [3]Department of Hospital Physics, Karolinska Hospital, [4]Department of Diagnostic Radiology, Karolinska Hospital, Stockholm, Sweden

(Accepted 25 November 1993)

The *in vivo* distribution of vasoactive intestinal peptide (VIP) was studied for the first time using a rat model in combination with labeled VIP (^{131}I-VIP) and a gamma-camera. A dynamic scan showed that ^{131}I-VIP was cleared rapidly from the blood circulation. The radioactivity was taken up and accumulated in the lungs during the first minute. During the next 15 min, the radioactivity was slowly removed from the lungs and redistributed into the kidneys, gastric mucosa, liver and small intestine. However, the radioactivity extracted by the lungs was about 6-fold lower during the first minute when a large amount of the non iodinated VIP was coinjected with the ^{131}I-VIP. ^{131}I-VIP was eliminated rapidly from the blood with a half-life of 0.44 ± 0.05 (min ± SD) while in lung the elimination half-life was determined to 2.3 ± 0.8 (min ± SD). Of the radioactivity in the lungs, 2% was found to be intact ^{131}I-VIP after 20 min. In all other organs the radioactivity found was assumed to be low molecular weight fragments of ^{131}I-VIP. We suggest that lungs play an important role to extract VIP from the circulation after an i.v. administration. ^{131}I-VIP degradation products are redistributed mostly to the kidneys and to the gastric mucosa to be excreted through urine and stomach contents, respectively.

Introduction

Vasoactive intestinal peptide (VIP) is a 28-amino acid peptide isolated from small intestinal mucosa by Said and Mutt in the early 1970's (1970). VIP is a member of the glucagon-secretin family of peptides. It is proposed as a mediator of a variety of physiological processes that include local regulation of blood flow and smooth muscle relaxation in specific mammalian organs (Gozes and Brenneman, 1989; Said, 1982). It has also been shown that VIP acts as a neurotransmitter (Costa *et al.*, 1988; Gozes *et al.*, 1987). Several studies have shown a high hepatic uptake of VIP, while others have shown contradictory results (Gammeltoft *et al.*, 1984; Kitamura *et al.*, 1975; Misbin *et al.*, 1982; Chayvialle *et al.*, 1981). Consequently, uptake and degradation of VIP by the liver might be clinically important especially in patients with liver cirrhosis. In addition, it has recently been reported (Said, 1992) that VIP exerts a protective effect on the lungs against acute inflammatory injury, including asthma.

The effect of VIP is mediated by the binding to specific receptors which involves a secondary messenger system and stimulates the generation of cyclic AMP (Harrelson and McEwen, 1987; Watling and Bristow, 1986). High affinity binding sites for VIP have been described in a number of normal tissues including rat brain (Watling and Bristow, 1986) and liver (Misbin *et al.*, 1982). The human liver cell membrane was found to contain a single class of high-affinity binding sites for VIP (Meunier *et al.*, 1992). VIP and its receptors are involved in many physiological systems in both normal and diseased tissues.

It has also been demonstrated that many types of human neoplasias, especially neuroendocrine tumors, have higher VIP production (Yamaguchi *et al.*, 1992) compared to normal tissues. Other tumors, such as human myeloma cells, small cell lung carcinoma, breast cancer and colonic carcinomas express an increased number of receptors (Muller *et al.*, 1985; Wood *et al.*, 1985; Gespach *et al.*, 1988; Luis and Said, 1990). A potential application of the latter fact may be its use for diagnostic purposes, like for the polypeptide somatostatin. By the synthesis of a stable analogue, octreotide, and its labelling by a proper radionuclide it is used for the depiction of especially neuroendocrine tumors with a gamma-camera (Lamberts *et al.*, 1990). To develop such a technique for VIP, it is necessary to study its normal distribution

*All correspondence should be addressed to: Dr Moustapha Hassan, Karolinska Pharmacy, Box 160, S-171 76 Stockholm, Sweden.

after exogenous administration. However, most of the binding studies reported have been performed in perfused systems, by using organ slices or by autoradiography.

The present study aimed to investigate the dynamic biodistribution of ^{131}I-VIP in the rat. ^{131}I-VIP was injected i.v. into the rat, and the distribution of the radiolabeled compound was dynamically registered by gamma-camera as well as by measuring the organs removed at various times after administration with gamma-counter.

Methods

Iodination and purification

Iodination and purification of ^{131}I-VIP was performed by the chloramine-T method essentially as described for ^{125}I-VIP by Marie *et al.* (1984) and Martin *et al.* (1986). VIP (25 nmol in 500 μL 0.3 M phosphate buffer, pH 7.6) was mixed with 10 nmol carrier free Na^{131}I (The Radiochemical Centre, Amersham, U.K.). The reaction was started with 355 nmol chloramine-T and terminated after 20–30 s with 1052 nmol metabisulfite. Unreacted iodine, chloramine-T and metasulfite were eliminated by passing the reaction mixture through Sep-Pak (C-18, Millipore) previously equilibrated with 10% acetonitrile in 0.1% trifluoroacetic acid (TFA). ^{131}I-VIP was eluted with 2 mL 60% acetonitrile in 1% TFA. The volume was reduced by evaporation (N_2). Separation from iodinated products was performed using reversed phase liquid chromatography (HPLC) with a C18 Vydac column (0.46 × 25 cm). The HPLC was run in isocratic mode with a mobile phase containing 27% acetonitrile in 0.1% TFA for 10 min followed by a linear gradient 27–40% acetonitrile for 60 min with a flow rate of 1 mL/min.

Fractions of 1.0 mL were collected and measured by a gamma-counter (LKB-Wallac, Bromma, Sweden). The first fraction after the unlabeled VIP was collected and dried using N_2, the fraction was stored at −20°C until use.

Animals

Male Sprague–Dawley rats (250–300 g) were obtained from ALAB (Sollentuna, Sweden). Food pellets and water were available *ad libitum*. All animals were anaesthetized with pentobarbital (50 mg/kg).

Dynamic planar imaging and biodistribution

^{131}I-VIP, VIP (250 μg) + ^{131}I-VIP or Na ^{131}I was dissolved in physiological saline and injected i.v. (6 MBq in 0.2 mL) into the rats. The rat was placed and injected on a gamma-camera (400 AZ Maxicamera, General Electric, Milwaukee, WI) equipped with high energy collimator and on line to a computer (PDP 11/73, Digital Eq., Maynard, MA). For the whole rat, dynamic planar images were acquired during the first 300 s in frames of 5 s after the injection (time zero) followed by imaging for 20, 40 or 60 min.

Rats were killed at various time points (20, 40 and 60 min, respectively). Different organs were taken and washed with physiological saline to remove blood. About 0.5 g of the tissue was placed in test tubes to determine the radioactivity with a gamma-counter (1282 Compugamma, LKB-Wallac, Bromma, Sweden). The amount radioactivity in each organ was calculated per gram wet tissue as a percent of the total injected amount of radiolabeled VIP.

Extraction of intact ^{131}I-VIP

The rats were killed by ether at various times (2, 3, 6, 10, 20, 40 and 60 min) to study the distribution and elimination half-life. About 1 g of lungs, liver, blood/or plasma, kidneys and small intestine was removed and kept at −20° C until assay. The tissues were homogenized (2 × 20 s) with Ultra-turrax (IKA, Staufen, Germany) homogenizer and extracted by 10 mL/g 0.2 M acetic acid for 90 min. After centrifugation (20000 ***g*** for 20 min), the supernatant was removed and passed through a Sep-Pak C-18 pre-equilibrated with 0.1% TFA. The Sep-Pak was washed with 5 mL 0.1% TFA and the bound radioactivity was eluted with 60% acetonitrile in 0.1% TFA. The elution procedure was repeated twice and the pooled fractions were evaporated by lyophilization. The radioactivity extracted from the different tissues was within the range 75–90 %. The residues were dissolved in 150 μL 0.1% TFA, centrifuged at 10 000 ***g*** and injected into reversed phase HPLC with Vydac C18 column (0.46 × 25 cm). The samples were eluted with a linear gradient of 20–40% acetonitrile in 0.1% TFA for 30 min. Fractions of 0.5 mL were collected for assaying the radioactivity. The labeled VIP obtained from organ extraction was identified by the coelution with reference of non iodinated VIP on the same HPLC system.

Results

Iodination of VIP was performed according to the procedure described by Marie *et al.* (1984) and Martin *et al.* (1986) for the preparation of mono ^{125}I-VIP. The subsequent purification resulted in a HPLC profile similar to that obtained in the purification of [mono[^{125}I]iodo-Tyr^{10}, MetO^{17}]-VIP. Each rat received about 6 MBq of ^{131}I-VIP as an i.v. injection, approx. corresponding to 0.15 nmol. Assuming a blood volume of 12 mL, the injected amount will correspond to a final concentration of 12 nM VIP in the animal blood.

After i.v. injection of ^{131}I-VIP, the radioactivity was removed from the injection site and reached a maximum in the lungs within the first minute (Fig. 1). The radioactivity was slowly removed from the lungs and redistributed into the kidneys (Fig. 2). The dynamic scan of the rat [Fig. 3(A)] showed that ^{131}I-VIP was almost completely cleared from the circulation and

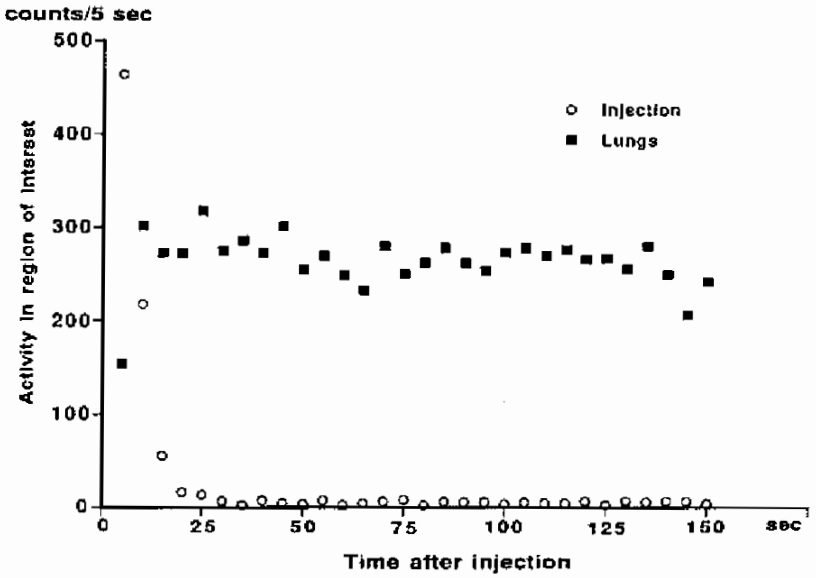

Fig. 1. Disappearance of the radioactivity from the injection site and the distribution into the rat lungs after i.v. administration of ^{131}I-VIP.

largely accumulated in the lungs during the first minute. Thereafter, a continuous scanning showed the redistribution of the radioactivity into the kidneys, stomach and intestine [Fig. 3(B)]. However, the radioactivity was 6-fold higher in the lungs (calculated as ratio lung/whole body) compared to that ratio obtained after coinjecting 100-fold of non labeled VIP and trace amount of ^{131}I-VIP. In the later case the radioactivity after 1 min was more located in the abdomen region [Fig. 3(C)].

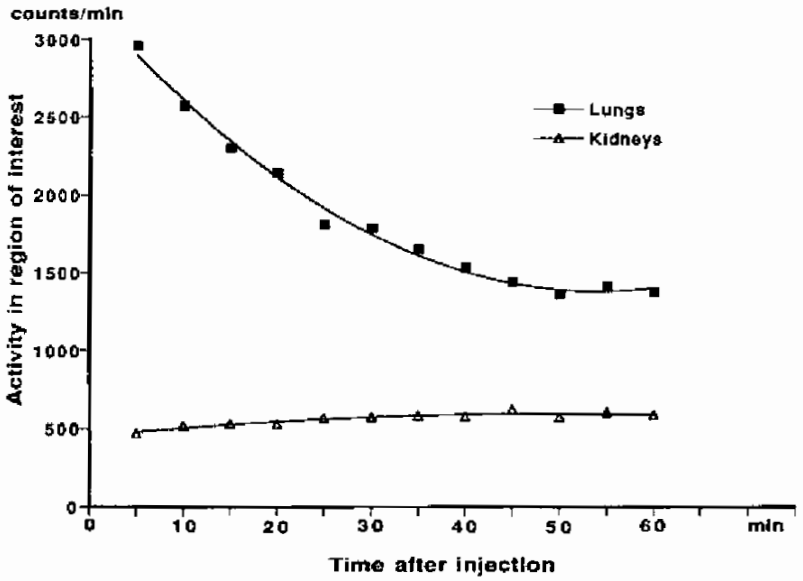

Fig. 2. Elimination of the radioactivity from the rat lungs and accumulation in the kidneys.

Table 1 shows the distribution of the radioactivity in the removed tissues at different time intervals after injecting ^{131}I-VIP. The radioactivity in the lung after 20 min is about 8% of the injected activity per gram lung tissue. This amount corresponds to 870% of that radioactivity found in peripheral blood. During the next 20 min, the pulmonary radioactivity declined to reach about 3% of the injected amount (420% compared to peripheral blood). At 60 min the remained radioactivity was measured to 260% of that in blood (Table 1). Most organs exhibited radioactivity less than 1% (Table 1) of the injected amount per gram tissue. Radioactivity was very low in both brain and cerebellum. However, an increase of the radioactivity in stomach from 0.6% at 20 min to 1.7% at 60 min was observed. Also, radioactivity in stomach contents increased about 7-fold between 20 to 60 min. The distribution of ^{131}I in the rat (Table 1) was considerably different from that obtained at 20 min for ^{131}I-VIP. Especially the pulmonary uptake was found to be only 0.34% compared to about 8% (VIP). Also, kidneys showed significantly lower activity. However, the target organ seems to be the stomach with a value of 490% compared to blood, also in the urine the activity was detected to 430%. In contrast, the radioactivity in the stomach contents was not higher when ^{131}I was administered.

Extraction of lungs from the rats sacrificed at 20 min showed that about 2% of the radioactivity in the lung is intact ^{131}I-VIP, which was identified by the

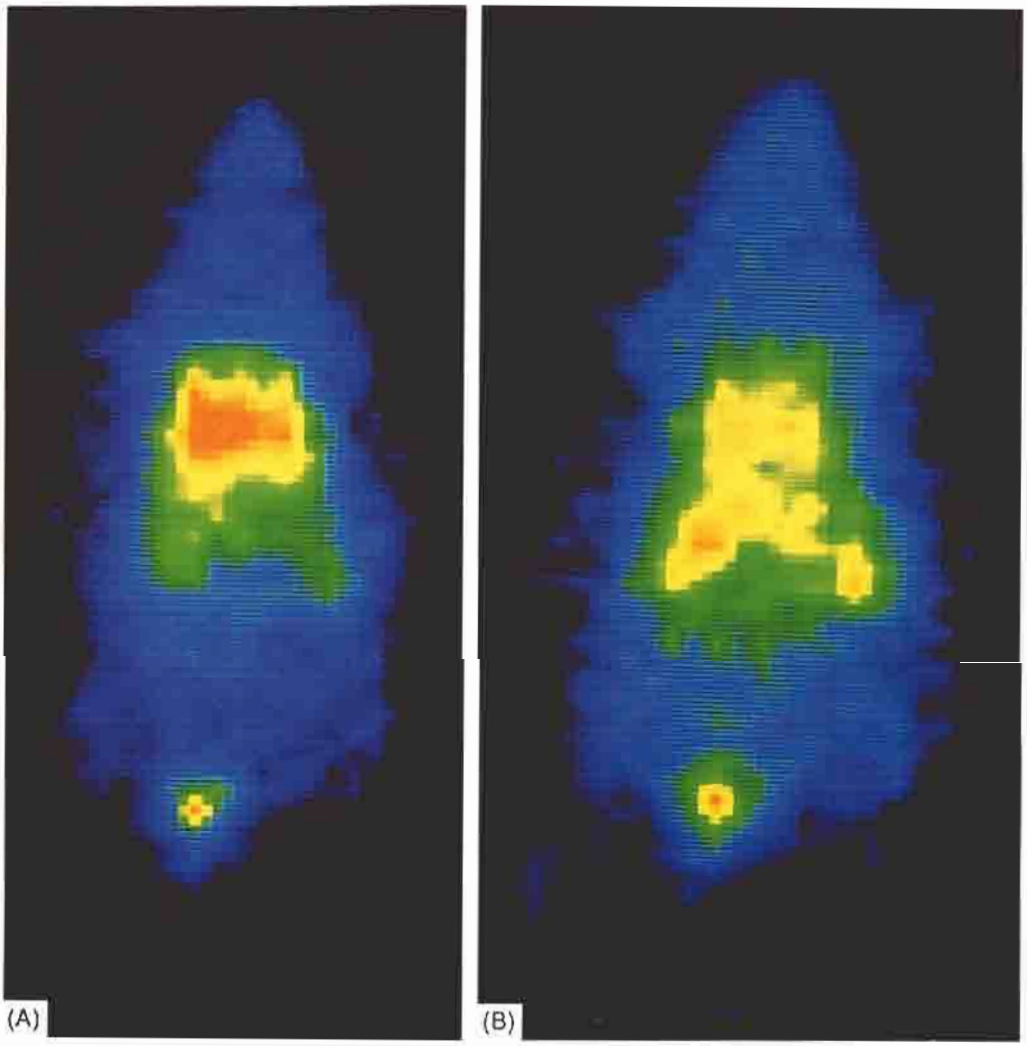

Fig. 3(A)–(B).—*legend opposite.*

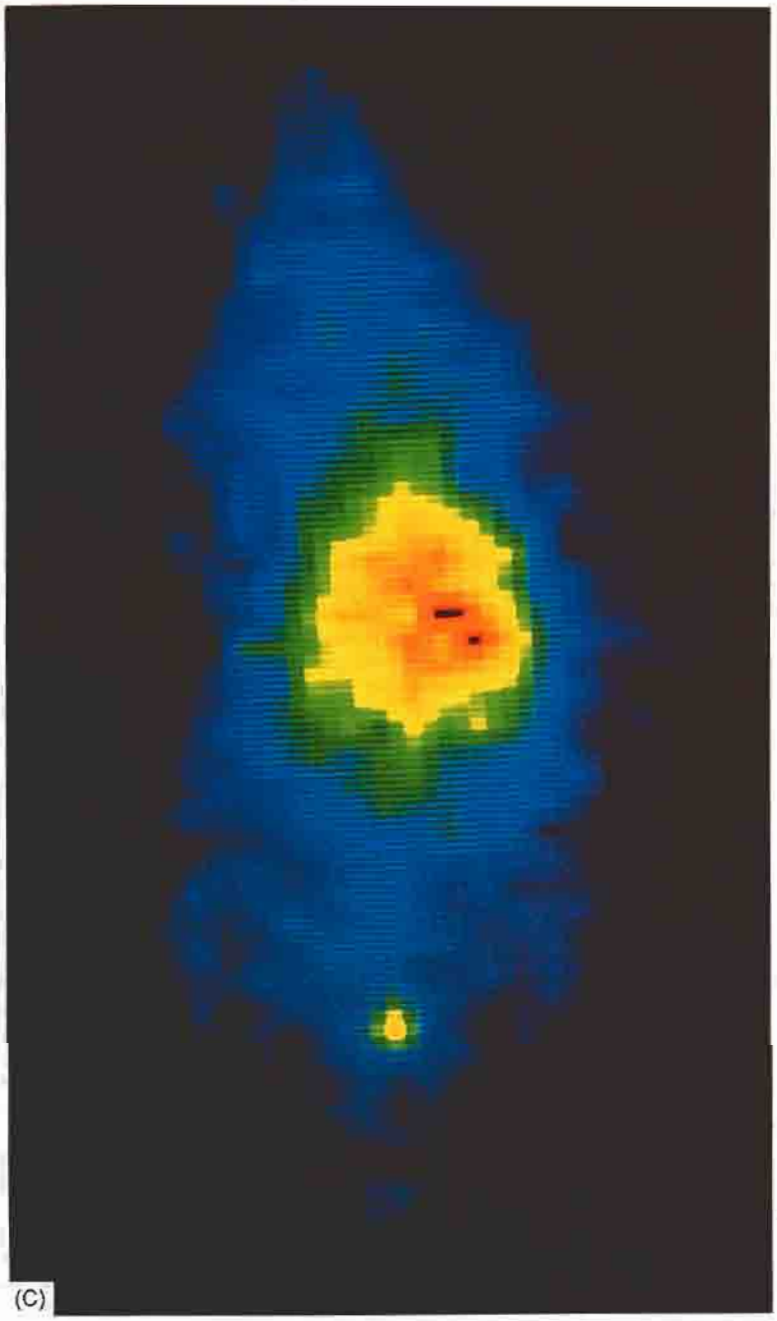

Fig. 3(C)

Fig. 3. (A) An image of the rat 1 min after injection of ^{125}I-VIP showing the accumulation of the radioactivity in the lungs. (B) An image of the rat 10 min after injection of ^{125}I-VIP showing the redistribution of the radioactivity from the lungs to the kidneys. (C) An image of the rat 1 min after coinjection of a large amount of non labeled VIP and a trace amount of ^{125}I-VIP showing higher distribution of the radioactivity to the abdomen region and a very low distribution to the lungs.

Table 1.

Organ	Radioactivity/g (20 min) % of TRA	Radioactivity/g (20 min) % of Blood	Radioactivity/g (40 min) % of TRA	Radioactivity/g (40 min) % of Blood	Radioactivity/g (60 min) % of TRA	Radioactivity/g (60 min) % of Blood	^{131}I/g 20 min % of TRA	^{131}I/g 20 min % of Blood
Lung	7.90	870	3.20	420	2.10	260	0.34	56
Liver	0.60	69	0.47	63	0.40	49	0.25	41
Blood	0.91	100	0.75	100	0.80	100	0.60	100
Spleen	0.32	35	0.30	41	0.27	34	0.17	29
Small intestine	0.36	40	0.50	66	0.44	55	0.28	45
Large intestine	0.23	25	0.34	46	0.76	94	0.80	131
Kidney	2.17	238	2.04	270	1.46	181	0.32	53
Heart	0.29	31	0.36	48	0.23	28	0.15	24
Pancreas	0.43	47	0.36	48	0.30	37	0.17	28
Stomach	0.60	65	1.0	133	1.70	208	3.00	486
Stomach contents	0.67	74	1.10	140	4.70	586	0.23	38
Urine	0.60	65	7.20	962	5.40	666	2.60	431
Urine bladder	0.43	47	0.40	52	0.80	94	—	-
Brain	0.10	11	0.04	5	0.05	7	0.03	6
Cerebellum	0.10	11	0.13	18	0.06	8	0.06	10

% of TRA: % of total radioactivity.
Radioactivity/g (× min): The radioactivity obtained/g organ after injection of ^{131}I-VIP (20, 40 and 60 min).

coelution with reference of non iodinated VIP on HPLC. However, no ^{131}I-VIP was found in the extractions of the lungs taken at 40 and 60 min. Also, no iodinated VIP was found in the other tested organs i.e. liver, blood, small intestine and kidney at 20, 40 and 60 min. The elimination half-life of ^{131}I-VIP was determined in blood and lungs from the rats sacrificed at 2, 3, 6, 10 and 20 min resulting in half-lives of 0.45 ± 0.05 and 2.3 ± 0.8 (min ± SD), respectively.

Moreover, the radioactivity was cleared by biphasic elimination (Fig. 4) from the lungs with a shorter half-life (0.9 ± 0.2; min ± SD) and thereafter, a longer one (20.6 ± 1.5; min ± SD). These values were determined from rats killed at all times studied and were in agreement with that obtained from gamma-camera.

Discussion

Previous investigations and reports have shown that VIP and its receptors are presented in many tissues. VIP administered to humans by inhalation protected against histamine-induced bronchoconstriction but did not change airway conductance because of the rapid enzymatic breakdown of the VIP (Altiere *et al.*, 1984). Similar observations were also reported in animals (Diamond *et al.*, 1983; Barrowcliffe *et al.*, 1986). On the other hand, when VIP was administered i.v., contradictory results concerning the ability of VIP as a bronchodilator were reported in man (Palmer *et al.*, 1986; Morice *et al.*, 1983). This effect on the lung airways after injecting a higher dose of VIP (Morice *et al.*, 1983) can probably be explained by the short elimination half-life of VIP in the lung as reported in both man and animals (Bloom *et al.*, 1977; Chyvialle *et al.*, 1981).

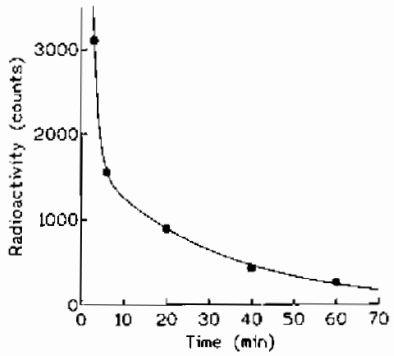

Fig. 4. The elimination of the radioactivity from the rat lungs according to a biphasic model.

The *in vivo* distribution of ^{131}I-VIP was studied for the first time in combination with gamma-camera. Dynamic scans of the uptake of radioactivity showed that ^{131}I-VIP is eliminated from the circulation and accumulated in the lungs during the first minute [Fig. 1, 3(A)]. On the other hand a low uptake and almost no accumulation in the lungs was seen when a large amount of non labeled VIP was coinjected with ^{131}I-VIP [Fig. 3(C)] which most likely must due to a blockade of VIP receptors in the lungs. The present results confirm the presence of a high number of specific receptors in the lungs reported in rat (Humphrey *et al.*, 1979; Veliçelebi *et al.*, 1988; Paul *et al.*, 1988). Also, the results are in good agreement with the results reported by Barrowcliffe *et al.* (1986) that the lungs play an important role in the clearance of iodinated-VIP from the circulation after an i.v. administration. Bernhard *et al.* (1989) have reported that VIP is taken up by the lungs in a perfusion system and the degradation products formed were re-extruded into the perfusate. These results can explain our observation of the accumulation of the radioactivity during the time studied in kidneys [Fig. 2, 3(B)], stomach and stomach contents [Fig. 3(B)] as an excretion route. ^{131}Iodide was found to be distributed mostly to stomach and urine which differs from that obtained for iodinated VIP.

Liver as an organ was suggested to play a major role in the inactivation of VIP in both dog and rat

(Kitamura *et al.*, 1975; Misbin *et al.*, 1982), while other studies in dogs have shown the lack of this role (Strunz *et al.*, 1977). Our finding of a lower radioactivity in liver than that in blood at 20, 40 and 60 min indicates that the liver is less important in the clearance or inactivation of VIP administered by i.v. route. After the initial uptake, the radioactivity is cleared from the lungs by biphasic elimination (Fig. 4). The first elimination half-life is about 1 min, after approx 8–10 min the clearance half-life is longer (20 min) and comparable with that reported for ^{125}I-VIP (19 min) by Barrowcliffe *et al.*, 1986.

The regression analysis of the concentrations of intact ^{131}I-VIP obtained by HPLC analysis in lungs and blood showed that the elimination half-life was longer in lungs (2.34 min) compared to that in blood (0.45 min). This might be due to the attachment of the VIP to its receptor which could prevent its degradation.

The chromatographic analysis showed that the radioactivity found in the kidneys, liver, intestinum and colon did not correspond to intact ^{131}I-VIP at any of the times studied. It is more likely that the radioactivity represents low molecular degradation products of VIP because of its earlier elution on the chromatographic system.

In summary, this study has shown that ^{131}I-VIP injected i.v. into the rat is cleared rapidly from the circulation and accumulated in the lungs while only less than 20% of the injected labeled (VIP) tracer was extracted into the lungs when coinjected with a large amount of non labeled VIP. Also, it was demonstrated that the elimination half-life is longer in lungs compared to blood which most likely reflect a high number of specific receptors. An accumulation of radioactivity was observed at a later time in kidneys, colon intestinum and stomach contents which most probably is due to the degradation products excreted from the lungs. Despite the fast elimination half-life of ^{131}I-VIP, the clinical value to use radiolabeled VIP or VIP analogue as a tumor marker has to be evaluated since it was reported that small cell lung carcinoma cell lines contain high affinity receptors for VIP (Luis and Said, 1990).

References

Altiere R. J., Francis P. B., Küng M. and Diamond L. (1984) Comparative effects of inhaled isoproterenol and vasoactive intestinal peptide on histamine-induced bronchoconstriction in human subjects. *Chest* **86,** 153–154.

Barrowcliffe M. P., Morice A., Jones J. G. and Sever P. S. (1986) Pulmonary clearance of vasoactive intestinal peptide. *Thorax* **41,** 88–93.

Bernhard W., Bothe-Sandtfort E., Koop H., Cassel W. and Von Wichert P. (1989) Degradation of vasoactive intestinal peptide by isolated, ventilated, and perfused rat lungs. *Eur. J. Clin. Invest.* **19,** 506–513.

Bloom S. R., Mitchell S. J., Domschke S., Domschke W., Mitznegg P., Lux G., Strunz U. and Demling L. (1977) VIP infusion in man. *Gut* **18,** 963A.

Chayvialle J. A., Rayford P. L. and Thompson A. C. (1981) Radioimmunoassay study of hepatic clearance and disappearance half-time of somatostatin and vasoactive intestinal peptide in dogs. *Gut* **22,** 732–737.

Costa M., Furness J. B., Gibbins I. L., Morris J. L., Bornstein J. C., Llewellyn-Smith I. J. and Murphy R. (1988) Colocalization of VIP with other neuropeptides and neurotransmitters in the autonomic nervous system. In Vasoactive intestinal peptide and related peptides (Edited by Said S. I. and Mutt V.). *Ann. NY Acad. Sci.* **527,** 103–109.

Diamond L., Szarek J. L., Gillespie M. N. and Altiere R. J. (1983) In vivo bronchodilator activity of vasoactive intestinal peptide in the cat. *Am. Rev. Respir. Dis.* **128,** 827–832.

Domschke S., Domschke W., Bloom S. R., Mitznegg P., Mitchell S. J., Lux G. and Strunz U. (1978) Vasoactive intestinal peptide in man: pharmacokinetics, metabolic and circulatory effects. *Gut* **19,** 1049–1053.

Gammeltoft S., Staun-Olsen P., Ottesen B. and Fahrenkrug J. (1984) VIP receptors in pig liver cells: binding characteristics and role in degradation. *Peptides* **5,** 367–370.

Gespach C., Bawab W., de Cremoux P. and Cavlo F. (1988) Pharmacology, molecular identification and functional characteristics of vasoactive intestinal peptide rceptors in human breast cancer cells. *Cancer Res.* **48,** 5079–5083.

Gozez I., Shani Y. and Rosténe, W. H. (1987) Developmental expression of the VIP-gene in the brain and intestine. *Molec. Brain Res.* **2,** 137–148.

Gozez I. and Brenneman D. E. (1989) VIP: molecular biology and neurobiological function. *Molec. Neurobiol.* **3,** 201–236.

Harreison A. L. and McEwen B. S. (1987) Hypophysectomy increase vasoactive intestinal peptide-stimulated cyclic AMP generation in the hippocampus of the rat. *J. Neurosci.* **7,** 2807–2810.

Humphrey C. S., Murray P., Ebeid A. M. and Fischer J. E. (1979) Hepatic and pulmonary clearance of exogenous vasoactive intestinal peptide. *Gastroenterology* **77,** 55–60.

Kitamura S., Yoshida T. and Said S. I. (1975) Vasoactive intestinal polypeptide: inactivation in liver and potentiation in lung of anesthetized dog (38469). *Proceedings of the Society for Experimental Biology and Medicine* **148,** 25–29.

Lamberts S. W. J., Bakker W. H., Reubi J.-C. and Krenning E. P. (1990) Somatostatin receptor imaging. *In vivo* localization of tumors with a radiolabeled somatostatin analog. *J. Steroid Biochem. Molec. Biol.* **37,** 1079–1082.

Luis J. and Said S. I. (1990) Characterization of VIP- and Helodermin-preferring receptors on human small cell lung carcinoma cell lines. *Peptides* **11,** 1239–1244.

Marie J. C., Boissard C. and Rosselin G. (1984) Purification of monoiodinated vasointestinal peptide (M^{125}I-VIP) by high pressure liquid chromatography (HPLC). *Peptides* **5,** 179–182.

Martin J.-L., Rose K., Hughes G. J. and Magistretti P. J. (1986) [mono[^{125}I]iodo-Tyr^{10}, MetO^{17}]-Vasoactive intestinal polypeptide. *J. Biol. Chem.* **261,** 5320–5327.

Meunier A.-C., Carretier M., El Battari A., Luis J., Karamanos Y. and Muller J.-M. (1992) Characterization of the human liver vasoactive intestinal peptide (VIP) receptor. *Biomed. Res.* **13,** 157–161.

Misbin R. L., Wolf M. M., Morris P., Buynitzky S. J. and McGuigan J. E. (1982) Uptake of vasoactive intestinal peptide by rat liver. *Am. J. Physiol. (Gastrointest. Liver Physiol.)* **243,** 103–111.

Morice A., Unwin R. J. and Sever P. S. (1983) Vasoactive intestinal peptide causes bronchodilatation and protects against histamine-induced bronchoconstriction in asthmatic subjects. *Lancet* **ii,** 1225–1227.

Muller J.-M., El Battari A., Ah-Kye E., Luis J., Ducret F., Pichon J. and Marvaldi J. (1985) Internalization of the

vasoactive intestinal peptide (VIP) in a human adenocarcinoma cell line (HT29). *Eur. J. Biochem.* **159,** 107–114.

Palmer J. B. D., Cuss F. M., Warren J. B., Blank M., Bloom S. R. and Barnes P. J. (1986) Effect of infused vasoactive intestinal peptide on airway function in normal subjects. *Thorax* **41,** 663–666.

Paul S., Chou J. and Said S. I. (1988) Regulatory aspects of the vasoactive intestinal peptide receptors in lung. In: Vasoactive intestinal peptide and related peptides (Edited by Said S. I. and Mutt V.). *Ann. NY Acad. Sci.* **527,** 282–295.

Said S. I. and Mutt V. (1970) Polypeptide with broad biological activity: isolation from small intestine. *Science* **169,** 1217–1218.

Said S. I. (1982) Vasoactive intestinal peptide. In *Advances in Peptide Hormone Research Series*, vol. 1. Raven Press, New York.

Said S. I. (1992) Vasoactive intestinal peptide (VIP) and related peptides as anti-asthma and anti-inflammatory agents. *Biochem. Res.* **13,** 257–262.

Strunz U. T., Walsh J. H., Blom S. R., Thompson M. R. and Grossman M. I. (1977) Lack of hepatic inactivation of canine vasoactive intestinal peptide. *Gastroenterology* **73,** 768–771.

Veliçelebi G., Patthi S., Provow S., Akong M. and Simerson S. (1988) Structural characterization of vasoactive intestinal peptide receptors from rat lung membrane. In: Vasoactive intestinal peptide and related peptides (Edited by Said S. I. and Mutt V.). *Ann. NY Acad. Sci.* **527,** 265–281.

Watling K. J. and Bristow D. R. (1986) $GABA_B$ Receptor-mediated enhancement of vasoactive intestinal peptide-stimulated cyclic AMP production in slices of rat cerebral cortex. *Neurochem.* **46,** 1756–1762.

Wood C. L., O'Dorisio S., Vassalo L. M., Malarkey W. B. and O'Dorisio T. M. (1985) Vasoactive intestinal peptide effects on GH_3 pituitary tumor cells: high affinity binding, affinity labeling and adenylate cyclase stimulation. Comparison with peptide histidine isoleucine and growth hormone-releasing factor. *Reg. Peptides* **12,** 237–248.

Yamaguchi K., Abe K. and Yanaihara N. (1992) Production of VIP and related peptides in neuroendocrine tumors. *Biomed. Res.* **13,** 279–283.

II

Nuclear Medicine & Biology, Vol. 26, pp. 931–936, 1999

ISSN 0969-8051/99/$–see front matter
PII S0969-8051(99)00062-1

Biodistribution of Liposomal ^{131}I-VIP in Rat Using Gamma Camera

Essam Refai,[1] *Cathrine Jonsson,*[2] *Mats Andersson,*[1] *Hans Jacobsson,*[3] *Stig Larsson,*[2] *Per Kogner*[4] *and Moustapha Hassan*[5,6]

[1]DEPARTMENT OF MEDICAL BIOCHEMISTRY AND BIOPHYSICS, KAROLINSKA INSTITUTET, STOCKHOLM, SWEDEN; DEPARTMENTS OF [2] HOSPITAL PHYSICS, [3] DIAGNOSTIC RADIOLOGY, AND [4] CHILDREN CANCER RESEARCH, CHILDREN HOSPITAL, KAROLINSKA HOSPITAL, STOCKHOLM, SWEDEN; DEPARTMENTS OF [5] HEMATOLOGY AND [6] CLINICAL PHARMACOLOGY, HUDDINGE UNIVERSITY HOSPITAL, HUDDINGE, SWEDEN

ABSTRACT. Vasoactive intestinal peptide (VIP), a 28 amino-acid peptide was labeled with ^{131}I and encapsulated into liposomes. ^{131}I-VIP or liposomal ^{131}I -VIP was administered intravenously into the rats. The distribution was studied by a gamma camera and established by counting the radioactivity in the removed organs. The elimination half-life for the liposomal ^{131}I-VIP in both blood and lungs was significantly longer (5.29 and 9.28 min, respectively) than that obtained after the administration of ^{131}I-VIP (0.62 and 3.18 min, respectively). Dynamic scans using a gamma camera after the administration of liposomal ^{131}I-VIP showed a higher uptake of the liposomal form into the lungs compared with ^{131}I-VIP. The lack of VIP in asthmatics has been shown in previous studies. However, the clinical investigations using VIP were disappointing most probably due to the rapid degradation of the peptide in the bronchial tract. This in fact is supported by our previous study, in which we demonstrated that VIP had a half-life of 0.45 min in blood. We conclude that the encapsulation of VIP in liposomes prolongs its elimination half-life in plasma and enhances its uptake in lungs. This observation may increase the clinical use of VIP in both diagnostic and therapy. NUCL MED BIOL 26;8:931–936, 1999. **© 2000 Elsevier Science Inc. All rights reserved.**

KEY WORDS. VIP, Pharmacokinetics, Distribution, Liposomal-VIP, Gamma camera

INTRODUCTION

Vasoactive intestinal peptide (VIP) was discovered and characterized in 1970 by Said and Mutt (21, 22). VIP is a member of the secretin/glucagon family and is present in many animal species with considerable conservation of its amino acid composition. It is generally considered to function as a neuropeptide. The action of VIP is mediated via the binding of VIP to high-affinity *trans*-membrane receptors (VIP-R) on the respective target cells.

VIP has a wide variety of biological activities and is involved in the pathogenesis of several diseases, thus an interesting candidate for the treatment of various disorders (18, 20). In particular, VIP has important pharmacological actions on the respiratory tract, including relaxation of the airway smooth muscle, attenuation of acute inflammation (1, 20), and regulation of mucus secretion (6). It has been suggested that the absence of VIP in asthmatic lung may account for the pathogenesis of bronchial asthma (14). Due to these properties, VIP or analogs thereof, are possible therapeutic agents in bronchial asthma and lung injury (12, 19). However, VIP is sensitive to enzymatic degradation once introduced *in vivo*, by inhalation or intravenously (IV), thus losing its biological activity. This has been observed during several clinical trials for the treatment of asthma (1, 19). The rapid degradation of VIP by the airway peptidases in these trials makes the application of the peptide in its natural form limited.

Address correspondence to: Dr. Moustapha Hassan, Laboratory of Hematology, KFC, Novum, Huddinge University Hospital, 141 86 Huddinge, Sweden; e-mail: hassan@algonet.se.
Received 24 April 1999.
Accepted 5 July 1999.

Many attempts have been made to synthesize stable analogs of VIP by modifying the primary and secondary structure (4). These attempts have shown a variety of biological activities; however, none of these analogs has reached clinical use.

Specific VIP receptors (VIP-R) have been identified in cell membrane preparation (17). Other *in vitro* receptor studies using autoradiography have shown that human carcinomas express VIP-R. These results were of great value for VIP-R imaging of tumors *in vivo* and to predict potential clinical use. Neuroblastoma expressing VIP-R has been visualized using ^{131}I-VIP in a xenograft rat model (5, 10). Furthermore, Virgolini *et al.* (26) have used VIP radiolabeled with iodine (^{123}I) and the fact that tumors overexpress VIP-R for human tumor imaging. Thus the protection of VIP against degradation is of great importance for *in vivo* clinical use because of the rapid half-life in the blood (<1 min) (9).

Liposomes are microscopic structures consisting of one or more concentric lipid bilayers surrounding an aqueous compartment. The liposomes are nontoxic drug carriers in which both hydrophilic and hydrophobic molecules can be entrapped (15). The properties of liposomes depend on their size, chemical composition, and charge. Large liposomes target mostly liver, lungs, and spleen. Liposomes offer also sustained release in the blood when administered IV (15). In the present study we aimed to investigate whether the encapsulation of VIP in large liposomes would change the pharmacokinetics in general and the distribution and uptake by the lungs in particular. We studied the biodistribution of encapsulated ^{131}I-VIP in liposomes in the rat after an IV administration using the gamma camera technique and we evaluated the pharmacokinetics of the liposomal VIP. This study can be a step to overcome the limitations in the clinical use of VIP in its native form.

MATERIALS

VIP was prepared from porcine intestine at the laboratory of Biochemistry II, Karolinska Institute (Stockholm, Sweden). The peptide was tested for its biological activity as described previously (13). Carrier-free Na ^{131}I was from Amersham-Pharmacia (Uppsala, Sweden). Cholesterol, L-α-phosphatidylcholine (Egg, 100 mg/mL) and 1,2-Dioleolyl-sn-Glycero-3-phosphate (monosodium salt, 20 mg/mL) were obtained from Avanti Polar-Lipids (Alabaster, Alabama, USA).

METHODS

Iodination

Iodination and purification of ^{131}I-VIP was performed by the chloramine-T method as described previously (9). Briefly, VIP was mixed with carrier-free Na ^{131}I; the reaction was started by adding chloramine-T (Sigma, St. Louis, MO) and terminated after 20–30 s with metabisulfite. Iodinated VIP was passed through a C_{18} Sep-Pak (Millipore, Bedford, MA) and thereafter further purified by high performance liquid chromatography (HPLC) using a Vydac C_{18} column. Fractions of 1 mL were collected. The radioactive fractions corresponding to the labeled VIP were collected, evaporated under light stream of N_2, and kept at −20°C until further use.

^{131}I-VIP Encapsulation in Liposomes

Lipids (L-α-phosphatidylcholine [EPC]), 1,2-Dioleolyl-sn-Glycero-3-phosphate (DOPA), and cholesterol in the molar ratio 9.45:1:9.45 were dissolved in dichloromethane and ^{131}I -VIP was added. The dichloromethane was evaporated and the mixture of lipids and ^{131}I-VIP formed a thin film coating the inside of a spherical glass vessel. Any trace of solvent was removed under a gentle stream of nitrogen. The mixture was then hydrated with 25 mL of glucose (50 mg/mL, pH 4.0, Pharmacia-Upjohn, Uppsala, Sweden). Multilamellar vesicles were formed by vortexing the lipid-aqueous mixture. The suspension was transferred to an Extruder (LipoFast 50, Avestin, Ottawa, Canada) and extruded under nitrogen pressure, through two stacked polycarbonate filters with a pore size of 600 nm (five times). The average diameter of each liposomal preparation was determined and controlled by dynamic light scattering.

Animals

In all experiments male Sprague–Dawley rats (200–250 g) were obtained from B&K Universal (Sollentuna, Sweden). The animals were kept in a fully climatized room with constant temperature, humidity, and 12-h light/dark cycle. Food pellets and water were available *ad libitum*. All animals were anesthetized with pentobarbital (50 mg/mL). The Animal Care Committee at the Karolinska Institute approved the experimental protocol before experimentation. All experiments designed according to guidelines established by the Committee on the Care and Use of Laboratory Animals of the Institute of Laboratory Animal Resources.

Dynamic Planar Imaging

The rats were placed on one head of a Triad XLT gamma camera (Trionix, Twinsburg, OH) and injected IV with ^{131}I-VIP or liposomal ^{131}I-VIP (20 MBq in 0.2 mL saline). The camera head was equipped with a medium energy general purpose (MEGP) collimator. Dynamic planar images were acquired in a 256 × 256 matrix during the first 5 min (ten 30-s acquisitions) followed by ten 5 min-acquisitions. A new image (5-min acquisition) was acquired 24-h postinjection.

Distribution of Radioactivity, Extraction of Organs, and Identification of Intact ^{131}I -VIP

EXTRACTION OF ORGANS. Rats were injected IV in the tail with liposomal ^{131}I -VIP and sacrificed at various time points (1.5, 2.5, 5, 10, 15, 20, 30, 40, and 60 min). Different organs (lung, blood, kidney, spleen, and liver) were removed immediately, washed with saline to remove blood, and placed in tubes (0.5 g/organ) to determine the radioactivity by a gamma-counter (1282 Compugamma, LKB-Wallac, Sweden).

For the quantification of VIP, 0.2–0.5 g of the organs were removed, washed carefully with saline, and kept at −20°C. These organs were thawed, homogenized with an Ultra-turrax, and then extracted in 0.2 M acetic acid 10 mL/g for 90 min. The supernatant was collected after centrifugation and passed through a preconditioned Sep-Pak C_{18}. The Sep-Pak was washed by 5 mL (10% acetonitrile in 0.1% triflouroacetic acid [TFA]), the bound radioactivity was eluted by 2 mL (60% acetonitrile in 0.1% TFA). The procedure was repeated twice. The two fractions were pooled and the volume was reduced by lyophilization. The samples were dissolved in 150 μL 0.1% TFA, centrifuged, and injected to an HPLC equipped with a Vydac C18 (0.46 × 25 cm) column. The analysis was carried out using a linear gradient of 20–40% acetonitrile in 0.1% TFA in 30 min. The radioactive peak (eluted at the same retention time as that of iodinated VIP) was collected and used for quantification.

DISPLACEMENT. The rat was injected IV with either liposomal ^{131}I-VIP (20 MBq = 0.33 nmol) or ^{131}I-VIP (20 MBq = 0.33 nmol). The distribution of the radioactivity was followed by gamma camera for 3 min (30-s acquisitions). One dose of unlabeled VIP (200 μg, 60 nmol) was injected IV into the rat. Dynamic planar images were acquired during the first 300 s in 10-s frames followed by five 5-min frames.

PHARMACOKINETIC AND STATISTICAL ANALYSIS. Pharmacokinetic modeling and parameter estimates were performed using WinNonlin 1.5 (Statistical Consultants, Lexington, KY). Statistical analysis was performed using Wilcoxon's test (nonparametric, paired, two tailed) and Mann–Whitney's test (nonparametric, unpaired, two tailed). The mean, median, and standard deviation were calculated using Graph Pad In Stat (version 3.0). All values are presented as mean ± SD. A p value < 0.05 was considered to be significant.

RESULTS

The iodination of VIP was performed according to the procedure described previously by Marie *et al.* (11) and modified by Hassan *et al.* (9). The iodinated VIP was subsequently encapsulated in liposomes. The size of liposomes was determined by light scattering to 614 ± 32 nm. The liposomes were stable (did not form any aggregates) for 22 days at +4°C. Each rat was injected IV with a dose of approximately 20 MBq of ^{131}I-VIP or liposomal ^{131}I-VIP. The dynamic distribution of ^{131}I-VIP was monitored by gamma camera. The dynamic scanning showed the accumulation of VIP in the lungs after the administration of both forms. However, the radioactivity in the lungs 10-min after administration of liposomal ^{131}I-VIP was higher than that observed when ^{131}I-VIP was administered (Fig. 1).

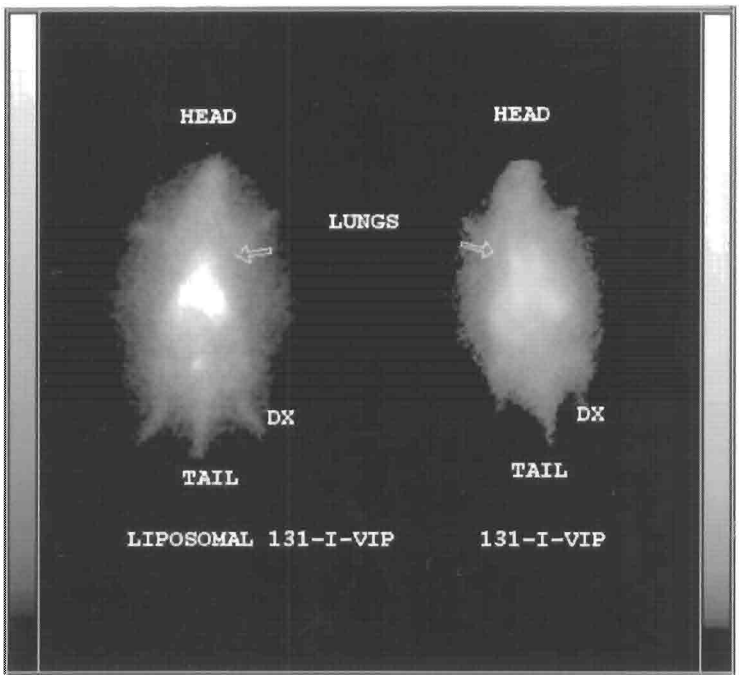

FIG. 1. An image of the rat 10 min postinjection of liposomal ^{131}I-vasoactive intestinal peptide (^{131}I-VIP) (left) and of ^{131}I VIP (right). The image shows a higher accumulation of radioactivity in the lungs at 10 min after the administration of liposomal ^{131}I-VIP compared with that obtained after the administration of ^{131}I VIP.

The elimination of ^{131}I-VIP injected in a liposomal form as well as a nonliposomal form was described by a one-compartment open model (Fig. 2A, 2B). The blood half-life of liposomal ^{131}I-VIP was eightfold higher than that of ^{131}I -VIP, 5.29 ± 0.62 and 0.62 ± 0.05 min, respectively, $p < 0.05$ (Table 1). Likewise, the elimination half-life of ^{131}I-VIP in lungs was three times as fast as compared with that observed after the administration of liposomal ^{131}I-VIP (3.18 ± 0.22 and 9.28 ± 0.76 min, respectively, $p < 0.05$).

A higher exposure to VIP (as expressed as area under the time-concentration curve [AUC]) was observed in blood and lung after the administration of liposomal ^{131}I-VIP compared with that observed after the administration of VIP (Table 1). Significantly ($p < 0.05$) higher clearance values (Cl) in both lungs and blood were observed for ^{131}I-VIP compared with that found for liposomal ^{131}I-VIP.

Figure 3A shows the regional lung uptake of the radioactivity (per milliliter tissue) after the administration of liposomal ^{131}I-VIP and the uptake after the displacement by IV injection of 200 μg unlabeled VIP. As observed, the radioactivity was cleared significantly faster from the lung after the administration of unlabeled peptide compared with the normal clearance of ^{131}I-VIP. As illustrated in Figure 3B, ^{131}I-VIP was likewise displaced by an injection of unlabeled VIP (in the lung).

A scan after 24 h indicated that most of the radioactivity after the administration of liposomal ^{131}I-VIP or ^{131}I-VIP was localized in the thyroid gland, stomach, and urine bladder (data not shown) as reported previously (9). These results were observed by the gamma camera and confirmed by assessing the removed organs at 24 h.

DISCUSSION

Since the isolation of VIP, many investigations, including our previous study (9), have shown that the use of VIP in clinic is limited, which most likely is due to its rapid degradation by enzymes (3) or catalytic antibodies (16). These factors have been described to limit the availability of the peptide at receptor sites. Many attempts have been carried out to stabilize the peptide either by chemical modification in its structure or by modifying the sequence of the amino acids (4). These VIP analogs have shown a variety of biological activities. However, none of these forms has reached clinical use.

In our present study we have shown that: (a) a twofold higher exposure to VIP in both lung and blood (as expressed as AUC) was observed when VIP was administrated as a liposomal encapsulated form compared with the nonencapsulated VIP. (b) Threefold longer elimination half-life was observed after the IV administration of liposomal VIP (in lungs) compared with that found after an IV administration VIP. (c) Eightfold higher half-life in blood after the administration of liposomal VIP compared with VIP. The results obtained after IV administration of the labeled VIP are in agreement with our previous study (9), in which we reported that the elimination half-life time in the lungs (2.34 min) was longer than that of the blood (0.45 min).

Gao *et al.* (7) reported that the encapsulation of VIP in liposomes enhanced its vasoactive effect in hamsters. They showed that duration and magnitude of the hypotensive effect observed in hamsters after the administration of the liposomal VIP was significantly higher than that obtained from nonencapsulated VIP (7). The encapsulation of VIP in large liposomes (600 nm) prolonged its

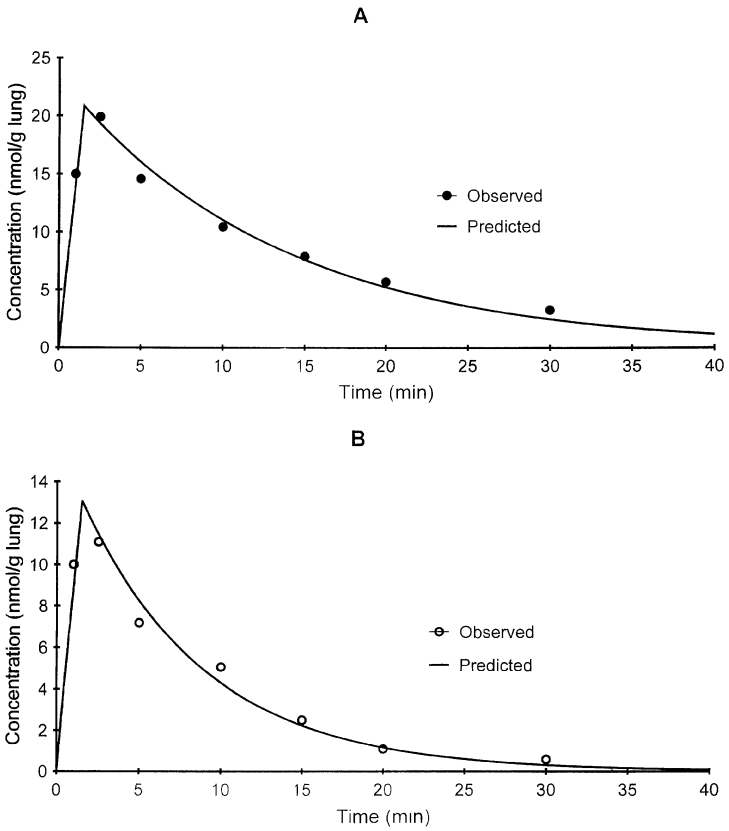

FIG. 2. Concentration–time profile in the rat lungs after the administration of liposomal ^{131}I-vasoactive intestinal peptide (^{131}I-VIP) (A) or ^{131}I-VIP (B) shows the higher exposure to VIP as a liposomal form compared with native VIP.

vasorelaxant effect in the peripheral microcirculation *in vivo* using a hamster cheek pouch animal model (25). Sejourne *et al.* (23) reported that VIP encapsulated in liposomes elicited significant and prolonged vasodilatation in the *in situ* peripheral microcirculation. It has been noted that no leakage of VIP from liposomes occurred during several days and that degradation of VIP by tyrosine was abrogated when VIP was encapsulated in liposomes (7). These studies have shown by indirect evidence that the encapsulation of VIP into the liposomes prolonged its biological activity both *in vivo* and *in vitro*. Our present study supports these investigations and provides direct evidence showing that the encapsulation of VIP into the liposomes may protect the peptide from degradation *in vivo* and subsequently enhance the half-life of the peptide in the blood circulation. This finding may explain the prolonged biological activity observed in previous studies (7, 24, 25).

In the present investigation the use of the gamma camera technique has shown that the uptake of radioactivity in the lungs after the administration of the liposomal ^{131}I-VIP was higher than that observed after the administration of ^{131}I-VIP (Fig. 1). This finding probably could be due to a sustained release of ^{131}I-VIP from

TABLE 1. Pharmacokinetic Parameters for VIP and Liposomal VIP

	VIP		Liposomal VIP	
Parameter	**Blood**	**Lung**	**Blood**	**Lung**
AUC (nmol · min/mL)	50 ± 5.9	158 ± 3.89	109.9 ± 9.7	294.6 ± 18.5
$t_{1/2}$ (min)	0.62 ± 0.05	3.18 ± 0.22	5.29 ± 0.62	9.28 ± 0.76
Cl (mL/min)	2.0 ± 0.2	0.6 ± 0.1	0.9 ± 0.1	0.32 ± 0.02
V_d (L/kg)	4.9 ± 0.7	5.8 ± 0.2	6.9 ± 0.4	4.4 ± 0.2
C_{max}	19.7 ± 2.7	14.8 ± 0.5	13.1 ± 0.7	20.8 ± 0.8

VIP = vasoactive intestinal peptide; AUC = area under the concentration time curve; $t_{1/2}$ = the elimination half-life; Cl = clearence; V_d = distribution volume; C_{max} = maximum concentration.

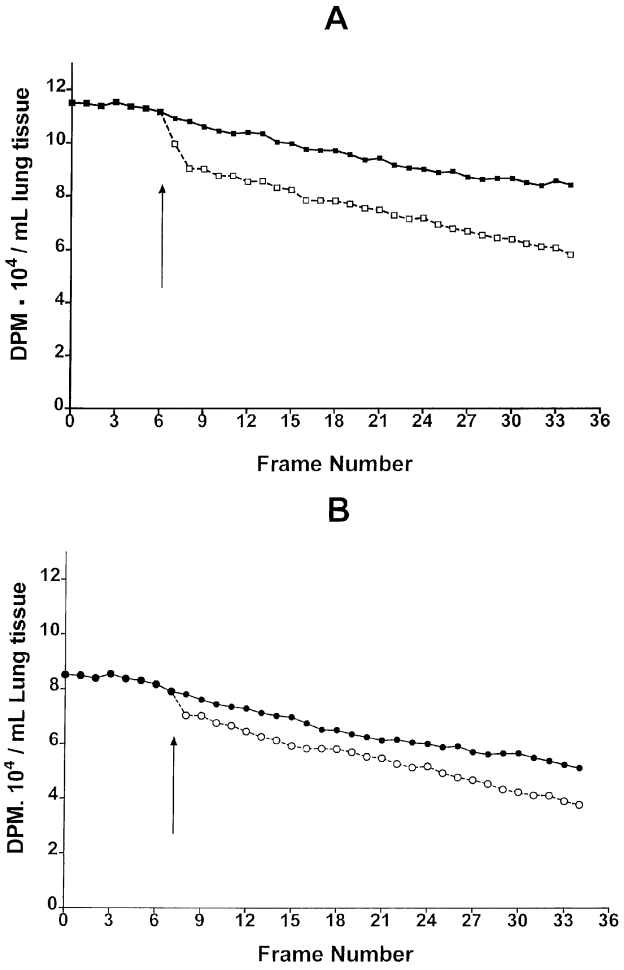

FIG. 3. Displacement experiment where the arrows indicate the time point when 200 μg nonlabeled vasoactive intestinal peptide (VIP) was injected. Frames were taken every 30 s (2 frame/min). A relative number of counts was calculated from a region of interest (of 1 cm^2, which is equal to 1 mL tissue) drawn around a lung area in all animals. One milliliter (gram) of the lung was removed and measured by gamma counter. A correction factor (based on the measured values and the values of the relative count numbers) was obtained. The absolute values of disintegrations per minute (DPM × 10^4/mL) were obtained from the relative number of counts multiplied by the correction factor. (A) Rats injected with liposomal ^{131}I-VIP. ■, Normal dynamic distribution in the rat lung after administration of liposomal ^{131}I–VIP. □, Dynamic distribution postinjection with unlabeled VIP. (B) Rats were injected with ^{131}I–VIP. ●, Normal dynamic distribution in the rat lung after administration of ^{131}I–VIP. ○, Dynamic distribution postinjection with unlabeled VIP.

the liposomes followed by the attachment to its receptors and/or that encapsulation of VIP in liposomes prevents its degradation by circulating enzymes. Recently, it was shown that phospholipids and liposomes could be used to circumvent the rapid degradation process of VIP *in vivo* and *in vitro* (8).

The displacement of ^{131}I-VIP and liposomal ^{131}I-VIP by the nonlabeled VIP (Fig. 2A, 2B) may indicate strongly that encapsulation of VIP in liposomes did not affect its binding to its receptors. This conclusion is in agreement with other investigations showing that VIP encapsulated in liposomes had a prolonged biological activity compared with that observed when the natural VIP was administered to hamsters (7, 25).

The high uptake of VIP by the lungs and the prolonged half-life in both lungs and blood are of an important clinical value, because it was shown that the lungs play a key role in the clearance of VIP from the circulation after an IV administration (2, 9). On the other hand, many clinical attempts did not succeed using VIP in the treatment of acute lung injury, probably due to the rapid degradation of VIP by peptidases in the airway passages when administered by inhalation to humans (3).

In conclusion, this study shows that IV administration of liposomal ^{131}I-VIP into the rat results in a longer half-life in both the lungs and the blood compared with that of ^{131}I-VIP. Liposomal encapsulation of VIP represents an efficient delivery form that appears to offer therapeutic advantages over VIP delivered in its native form. We suggest that the encapsulation of VIP into the liposomes could be useful in the treatment of cardiovascular disorders, asthma, and acute lung injury. This therapy has not reached clinical use most likely because of the short half-life of VIP *in vivo*. However, further studies with other forms of liposomes are urgently needed to establish the pharmacokinetics, pharmacodynamics, and the clinical relevance of using liposomal VIP.

This project was supported by Grant No. 1997/035 from The Swedish Children Cancer Society.

References

1. Barnes P. J. and Dixon C. M. S. (1984) The effect of inhaled vasoactive intestinal peptide on bronchial reactivity to histamine in humans. *Am. Rev. Resp. Dis.* **130,** 162–166.
2. Barrowcliffe M. P., Morice A., Jones J. G. and Sever P. S. (1986) Pulmonary clearance of vasoactive intestinal peptide. *Thorax* **41,** 88–93.
3. Bolin D. R., Cottrell J., Michalewsky J., Garippa R., O'Neil N., Simko B. and O'Donnell M. (1992) Degradation of vasactive intestinal peptide in bronchial alveolar lavage fluid. In: *Vasoactive Intestinal Peptide and Related Peptides* (Edited by Yanaihara N.) pp. 25–30, Kande Chiyodaku, Tokyo. 13.
4. Bolin D. R., Michalewsky J., Wasserman M. A. and O'Donnell M. (1995) Design and development of a vasoactive intestinal peptide analog as a novel therapeutic for bronchial asthma. *Biopolymers* **37(2),** 57–66.
5. Borgström P., Hassan M., Wassbery E., Refai E., Jonsson C., Larsson S., Jacobsson H. and Kogner P. (1999) The somatostatin analouge octreotide inhibits neuroblastoma growth *in vivo*. *Pediat. Res.* **46,** 328–332.
6. Coles S. T., Said S. I. and Reid L. M. (1981) Inhibition by vasoactive intestinal peptide of glycoconjugate and lysozyme secretion by human airways *in vitro*. *Am. Rev. Resp. Dis.* **124,** 531–536.
7. Gao X. P., Noda Y., Rubinstein I. and Paul S. (1994) Vasoactive intestinal peptide encapsulation in liposomes: Effects on systemic arterial blood pressure. *Life Sci.* **54,** 247–252.
8. Gololobov G., Noda Y., Sherman S., Rubinstein I., Baranowska-Kortylewicz J. and Paul S. (1998) Stabilization of vasoactive intestinal peptide by lipids. *J. Pharmacol. Exp. Ther.* **285,** 753–758.
9. Hassan M., Refai E., Andersson M., Schnell P. O. and Jacobsson H. (1994) *In vivo* dynamical distribution of ^{131}I-VIP in the rat studied by gamma-camera. *Nucl. Med. Biol.* **21,** 865–872.
10. Kogner P., Borgström P., Bjelleru P., Schilling F. H., Dominici C., Bihl H., Jacobsson H., Theodorsson E., Wassbery E., Refai E. and Hassan M. (1997) Somatostin in neuroblastoma and ganglioneuroma. *Eur. J. Cancer* **33,** 2084–2089.
11. Marie J. C., Boissard C. and Rosselin G. (1984) Purificaton of monoiodinated vasointestinal peptide (M 125I-VIP) by high pressure liquid chromatography (HPLC). *Peptides* **5,** 179–182.
12. Mojarad M., Grode T. L., Cox C., Kimmel G. and Said S. I. (1985) Differential responses of human asthmatics to inhaled vasoactive intestinal peptide (VIP). *Am. Rev. Resp. Dis.* **131,** Supp A281.
13. Mutt V. and Söderberg U. (1959) On the assay of secretin. *Arkiv för kemi* **15,** 63–68.
14. Ollerenshaw S., Jarvis D., Woolcock A., Sullivan C. and Schieber T. (1989) Absence of immunoreactive vasoactive intestinal polypeptide in tissue from the lungs of patients with asthma. *N. Engl. J. Med.* **320,** 1244–1248
15. Ostro J. M. (1987) *Liposomes from Biophysics to Therapeutics*. Marcel Dekker, New York.
16. Paul S., Volle D. J., Beach C. M., Johnson D. R., Powell M. J. and Massey R. J. (1989) Catalytic hydrolysis of vasoactive intestinal peptide by human autoantibody. *Science* **244,** 1158–1162
17. Said S. I. (Ed.) (1982) *Vasoactive Intestinal Peptide. Advances in Peptide Hormone Research Series*. Raven Press, New York.
18. Said S. I. (1991) Vasoactive intestinal peptide. Biological role in health and disease. *Trends Endocrinol. Metab.* **2,** 107–112.
19. Said S. I. (1991) VIP in asthma. *Ann. NY Acad. Sci.* **629,** 305–318.
20. Said S. I. (1992) Vasoactive intestinal peptide (VIP) and related peptides as anti-asthma and anti-inflamatory agents. *Biomed. Res.* **13**(suppl. 2), 257–262.
21. Said S. I. and Mutt V. (1970) Polypeptide with broad biological activity. Isolation from small intestine. *Science* **169,** 1217–1218.
22. Said S. I. and Mutt V. (1972) Isolation from procine-intestinal wall a vasoactive octacosapeptide related to secretin and glucagon. *Eur. J. Biochem.* **28,** 199–204.
23. Sejourne F., Suzuki H. and Alkan-Onyuksel H. (1997) Mechanisms of vasodilation elicited by VIP in sterically stabilized liposomes *in vivo*. *Am. J. Physiol* **271,** 282–287.
24. Suzuki H., Noda Y., Gao X. P., Alkan-Onyuksel H., Paul S. and Rubinstein I. (1996) Encapsulation of VIP into liposomes restore vasorelation in hypertension. *Am. J. Physiol* **271,** 282–292.
25. Suzuki H., Noda Y., Paul S., Gao X. P. and Rubinstein I. (1995) Encapsulation of vasoactive intestinal peptide into liposomes: Effects on vasodilation *in vivo*. *Life Sci.* **57,** 1451–1457.
26. Virgolini I., Raderer M., Kurtaran A., Angelberger P., Banyai S., Wang Q., Shuren L., Banyai M., Pidlich J., Niederle B., Scheithauer W. and Valent P. (1994) Vasoactive intestinal peptide-receptor imaging for the localization of intestinal adenocarcinmoas and endocrine tumors. *N. Engl. J. Med.* **331,** 1116–1121.

III

European Journal of Cancer

Somatostatin in Neuroblastoma and Ganglioneuroma

P. Kogner[1,2] P. Borgström[1,2] P. Bjellerup,[2] F.H. Schilling,[9] E. Refai,[5] C. Jonsson,[3] C. Dominici,[11] E. Wassberg,[8] H. Bihl,[10] H. Jacobsson,[4] E. Theodorsson[7] and M. Hassan[6]

[1]Childhood Cancer Research Unit, Dept. of Woman and Child Health; [2]Peptide Research Laboratory, Dept. of Laboratory Medicine; [3]Dept. of Hospital Physics; [4]Dept. of Radiology; [5]Dept. of Medical Biochemistry and Biophysics; [6]Karolinska Pharmacy, Karolinska Institute, Karolinska Hospital, S-171 76 Stockholm; [7]Dept. of Clinical Chemistry, University of Linköping; [8]Dept. of Anatomy, Biomedical Centre, University of Uppsala, Sweden; [9]Paediatric Oncology-Haematology, Olga Hospital, Stuttgart; [10]Dept. of Nuclear Medicine, Katharinen Hospital, Stuttgart, Germany; and [11]Dept. of Paediatrics, University, 'La Sapienza', Rome, Italy

Reprinted from European Journal of Cancer Vol. 33, No. 12

Pergamon

European Journal of Cancer, Vol. 33, No. 12, pp. 2084–2089, 1997

Printed in Great Britain
0959-8049/97 $17.00+0.00

PII: S0959-8049(97)00212-8

Original Paper

Somatostatin in Neuroblastoma and Ganglioneuroma

P. Kogner[1,2] P. Borgström[1,2] P. Bjellerup,[2] F.H. Schilling,[9] E. Refai,[5] C. Jonsson,[3] C. Dominici,[11] E. Wassberg,[8] H. Bihl,[10] H. Jacobsson,[4] E. Theodorsson[7] and M. Hassan[6]

[1]Childhood Cancer Research Unit, Dept. of Woman and Child Health; [2]Peptide Research Laboratory, Dept. of Laboratory Medicine; [3]Dept. of Hospital Physics; [4]Dept. of Radiology; [5]Dept. of Medical Biochemistry and Biophysics; [6]Karolinska Pharmacy, Karolinska Institute, Karolinska Hospital, S-171 76 Stockholm; [7]Dept. of Clinical Chemistry, University of Linköping; [8]Dept. of Anatomy, Biomedical Centre, University of Uppsala, Sweden; [9]Paediatric Oncology-Haematology, Olga Hospital, Stuttgart; [10]Dept. of Nuclear Medicine, Katharinen Hospital, Stuttgart, Germany; and [11]Dept. of Paediatrics, University, 'La Sapienza', Rome, Italy

Neuroblastoma, a childhood tumour of the sympathetic nervous system, may in some cases differentiate to a benign ganglioneuroma or regress due to apoptosis. Somatostatin may inhibit neuroblastoma growth and induce apoptosis *in vitro* and was therefore investigated. Using a radioimmunoassay, we found that all ganglioneuromas contained high somatostatin concentrations (> 16 pmol/g), significantly higher than neuroblastomas ($n = 117$, median 2.8 pmol/g), healthy adrenals, Wilms' tumours, phaeochromocytomas and other neuroendocrine tumours ($P < 0.001$). Neuroblastomas contained more somatostatin than control tumours ($P < 0.001$–0.05). Neuroblastomas amplified for the *MYCN* oncogene contained less somatostatin than non-amplified tumours (1.2 pmol/g versus 4.0 pmol/g, respectively; $P = 0.026$). In a clinically unfavourable neuroblastoma subset (age > 12 months, stage 3 or 4) 16 children with high concentrations of somatostatin in primary tumours had a better prognosis than 23 with low somatostatin (46.7% versus 0% survival at 5 years, $P < 0.005$). Scintigraphy using ^{111}In-pentetreotide identified tumours expressing high-affinity somatostatin receptors *in vivo*. However, no significant correlation was found between somatostatin receptor expression and peptide content in 15 tumours. Similarly, human SH-SY5Y neuroblastoma xenografts grown in nude rats showed low somatostatin concentrations, but were positive for somatostatin receptor scintigraphy. Treatment of these rats with the somatostatin analogue octreotide seemed to upregulate *in vivo* receptor expression of somatostatin and vasoactive intestinal peptide more effectively than 13-*cis* retinoic acid. In conclusion, somatostatin in neuroblastoma is associated with differentiation to benign ganglioneuromas *in vivo* and favourable outcome in advanced tumours. Furthermore, somatostatin receptor scintigraphy may identify tumours with high-affinity receptors in children that might benefit from targeted therapy using synthetic somatostatin analogues. © **1997 Published by Elsevier Science Ltd.**

Key words: somatostatin, neuroblastoma, ganglioneuroma, ganglioneuroblastoma, octreotide, vasoactive intestinal peptide, neuropeptide Y, retinoic acid, prognosis, xenograft, autocrine
Eur J Cancer, Vol. 33, No. 12, pp. 2084–2089, 1997

INTRODUCTION

NEUROBLASTOMA IS an embryonal tumour of neural crest origin with an extraordinary clinical and biological heterogeneity. The clinical outcome, ranges from differentiation to ganglioneuroma, or regression due to apoptosis after no or minimal therapy in the most favourable subset, to tumour progression and poor clinical outcome despite intensive therapy in the most unfavourable subset. Neuropeptides, a class of regulatory peptides produced by neural cells and acting as neurotransmitters,

Correpondence to P. Kogner.

may have clinical and biological significance in neuroblastoma and ganglioneuroma tumours. Neuropeptides may both cause specific symptoms as well as regulate cellular growth and differentiation [1].

Somatostatin (SOM), or somatotropin-release inhibiting factor (SRIF), is extensively distributed in the human body including the central and peripheral nervous systems, the gastrointestinal tract and various exocrine and endocrine glands [2, 3]. SOM is a cyclic neuropeptide with two different biological active forms (SOM-14 and SOM-28) derived from a 92 amino acid precursor, presomatostatin. Both SOM-14 and SOM-28 bind with high affinity to five known G protein-coupled SOM-receptor subtypes displaying a widespread, overlapping but characteristic pattern of expression with evidence that several subtypes may be co-expressed in certain cells [4]. SOM was shown to have growth inhibitory effects on malignant neuroendocrine cells *in vitro* and long-acting analogues have been developed and used for the treatment of neuroendocrine tumours *in vivo* [5, 6]. Recent studies have shown that neuroblastoma cells may express SOM receptors with high-affinity binding, allowing biological activities *in vitro* [7–9]. Somatostatin receptors have also been identified in neuroblastoma tumour tissue, predominantly in samples from tumours of localised clinical stages without *MYCN* amplification [7, 10]. It has also been demonstrated that children with tumours expressing these receptors have a much better chance of survival [10]. Recently, techniques for the detection of somatostatin receptor-expressing tumour cells *in vivo* have been established [11]. Preliminary results indicate that somatostatin receptor scintigraphy (SRS) is positive at diagnosis or relapse in a majority of children with neuroblastoma, with a tendency that SRS detects tumours in children with a more favourable outcome [12, 13].

We have previously reported that high concentrations of SOM immunoreactivity (SOM-LI) may be detected in ganglioneuromas and a subset of neuroblastomas [14, 15]. Furthermore, we have shown that SOM-LI represents molecular forms (SOM-14 and SOM-28) with putative biological activity, indicating that SOM may play a functional role in neuroblastoma differentiation *in vivo* [16]. In the present study SOM-LI concentrations were analysed in a larger number of tumours and the results were compared to clinical and biological features. In a subset of children with neuroblastoma and ganglioneuroma, we analysed both SOM-LI in tumour tissue and SOM receptor expression *in vivo*, using SRS. Finally, SOM-LI concentrations and SOM receptors were analysed in human neuroblastoma SH-SY5Y xenografts in nude rats, and the therapeutic effects of an SOM analogue (octreotide), vasoactive intestinal peptide (VIP) and 13-*cis* retinoic acid were analysed with respect to the *in vivo* expression of SOM and VIP receptors.

MATERIALS AND METHODS

Patients and sample handling

Children with neuroblastoma ($n = 117$) and ganglioneuroma ($n = 13$) diagnosed and staged according to the International Neuroblastoma Staging System (INSS) [17], were included in the study. Seventy-nine of these children are alive and disease-free with a follow-up of 12–96 months from diagnosis (66 with neuroblastoma and all 13 with ganglioneuroma). Thirty-nine children with neuroblastoma died during follow-up (33%), whereas 12 are still under therapy (10%). As control tissues, 3 healthy adrenals from children over 1 year of age, 6 adult phaeochromocytomas, 5 other neuroendocrine tumours and 16 paediatric Wilms' tumours were analysed.

Primary tumour tissue was obtained at surgery, fresh frozen on solid CO_2 or liquid N_2 and kept frozen until analysis. Tumour samples were cut while still frozen, extracted and homogenised in 10 volumes of boiling acetic acid (1 mol/l) for 10 min.

Radioimmunoassay for somatostatin immunoreactivity (SOM-LI)

SOM-LI in acid tumour extracts was analysed using an antiserum raised against conjugated SOM-14 as described earlier [18]. This antiserum reacts with both SOM-14 and SOM-28 [16, 18]. The intra- and interassay coefficients of variation were 7% and 11%, respectively.

Animals and SH-SY5Y xenografts

Nude rats (WAG rnu/rnu) were injected with 20×10^6 cells (passage 28) of the adrenergic neuroblastoma cell line SH-SY5Y (kind gift from J Biedler) [19] s.c. on the lateral side of each hind leg. After establishment of significant tumour growth, animals were randomly selected for treatment with octreotide (1.5 or 7.5 μg, s.c. twice daily), VIP (10 or 40 μg, s.c., twice daily), 13-*cis*-retinoic acid (2 or 4 mg, oral, twice daily) or controls without therapy. Animals were anaesthetised with pentobarbital (50 mg/kg) during SRS and VIP receptor scintigraphy (VIP-RS). Tumour tissue from control animals was analysed for SOM-LI.

Somatostatin receptor scintigraphy

The somatostatin analogue pentetreotide (DTPA-D-Phe^1-octreotide) was labelled with ^{111}In and a mean dose of 34 MBq was injected at diagnosis into 15 children from whom tumour tissue was available for analysis of SOM-LI. Images were acquired at 4 and/or 24 h as previously described [12]. Rats were placed on the gamma-camera and injected with 20 MBq in the tail vein, and planar images were obtained as previously described after the injection and at 1, 4, 24 and 48 h [19].

Vasoactive intestinal peptide receptor scintigraphy (VIP-RS)

Iodination and purification of ^{131}I-VIP was performed using porcine VIP (similar amino acid sequence as rat and human) as previously described [19]. The rats were placed on the gamma-camera, 20 MBq ^{131}I-VIP was injected i.v. and images were obtained after the injection and at 1, 4, 24 and 48 h [19].

Statistical analysis

Statistical analysis was performed using Fisher's exact test for 2×2 tables, the Wilcoxon, Mann–Whitney test for 2 independent samples and the Kruskal–Wallis test with multiple comparisons for more than two groups. The median and interquartile range (median: lower quartile–upper quartile) were used as measures of central tendency and variation, respectively. Survival probability was calculated using the product limit method of Kaplan and Meier and compared using the Mantel–Haenszel log-rank test.

RESULTS

Somatostatin in tumour tissue

All 13 ganglioneuromas had very high SOM-LI concentrations (>16 pmol/g wet weight), significantly higher than

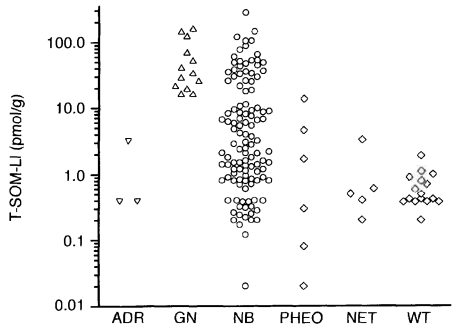

Figure 1. Somatostatin in tumour tissue extracts (SOM-LI pmol/g wet weight) of ganglioneuromas (GN, $n = 13$) and neuroblastomas (NB, $n = 117$) compared to healthy adrenals (ADR, $n = 3$) and control tumours (6 phaeochromocytomas, PHEO, 5 other neuroectodermal tumours, NET and 16 Wilms' tumours, WT). GN showed higher SOM-LI concentrations than all other tumours ($P < 0.001$) whereas NB had higher concentrations compared to control tumours ($P < 0.05$– 0.001).

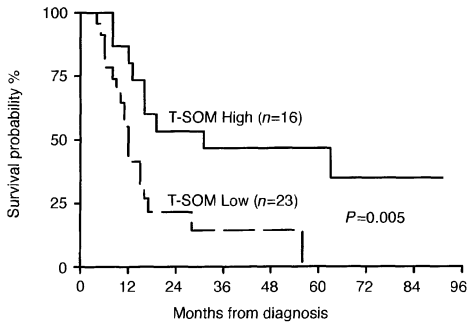

Figure 2. Survival from diagnosis for 39 children with advanced clinical stage (INSS 3 or 4) and > 12 months of age at diagnosis according to high (SOM-LI > 8 pmol/g, $n = 16$) or low somatostatin concentration in primary tumour tissue, respectively. Survival probability according to Kaplan–Meier was better for children with high SOM-LI (46.7 ± 12.9% and 35 ± 14% versus 14.3 ± 8.4% and 0% survival probability at 3 and 6 years, respectively) according to the Mantel–Haenszel log-rank test ($P = 0.005$).

neuroblastomas, healthy adrenals or control tumours ($P < 0.001$, Figure 1). Neuroblastomas contained higher SOM-LI concentrations (2.8: 0.84–20.05 pmol/g, median: lower quartile–upper quartile) than Wilms' tumours (0.45: 0.4–0.6 pmol/g, $P < 0.001$), phaeochromocytomas (0.75: 0.19–3.15 pmol/g, $P = 0.03$) and other neuroendocrine tumours (0.5: 0.3–1.95 pmol/g, $P = 0.018$). There was no significant difference between neuroblastomas of different stages, although there was a non-significant trend towards higher concentrations in stage 1, 2 and 4S tumours compared to tumours at unfavourable clinical stages 3 and 4. 18 neuroblastomas amplified for the *MYCN* oncogene had lower SOM-LI (1.2: 0.8–2.4 pmol/g) compared to 99 non-amplified tumours (4.0: 0.9–25.35 pmol/g, $P = 0.026$) *MYCN* amplified neuroblastomas from 10 children over 24 months at diagnosis had the lowest SOM-LI concentrations, significantly lower than those in 8 *MYCN* amplified tumours from younger children ($P < 0.05$).

In the whole neuroblastoma series, there was a non-significant tendency to higher SOM-LI in tumours from children with favourable clinical outcome ($P = 0.11$). This difference was significant in the most unfavourable subset of children, aged over 1 year with widespread tumours of stage 3 and 4 ($P = 0.03$). In this subset of 39 children, the 16 children with high SOM-LI content (> 8 pmol/g wet weight) had better survival probability than the 23 with low SOM-LI (46.7 ± 12.9% and 35 ± 14% versus 14.3 ± 8.4% and 0% survival probability at 3 and 6 years, respectively, $P = 0.005$, Figure 2).

Somatostatin receptor scintigraphy and somatostatin in tumour tissue

SRS was performed in 15 children and visualised significant tumour tissue in 10 of these, 9/14 neuroblastomas and 1/1 ganglioneuroma. Interestingly, there was no significant correlation between SOM-LI concentrations in tumour tissue and receptor expression as analysed with SRS (Table 1).

Somatostatin and somatostatin receptors in neuroblastoma xenografts

The SH-SY5Y xenografts grown in nude rats showed only a low level of SOM-LI concentration (0.08 pmol/g). However, SRS showed tumour tissue expressing somatostatin receptors (Figure 3).

Treatment with octreotide, VIP and 13-cis *retinoic acid* in vivo

Expression of somatostatin receptors but low levels of somatostatin peptide concentrations in the xenografts prompted us to try treatment with the somatostatin analogue octreotide, compared with VIP and 13-*cis*-retinoic acid. After four days of treatment, SRS and VIP-RS was performed as described. All treated rats showed positive scans for ^{111}In-pentetreotide, indicating the presence of high-affinity somatostatin receptors (Figure 4). Rats treated with octreotide or VIP showed higher uptake in the tumour tissue at ^{131}I-VIP scans compared to rats receiving treatment with retinoic acid or no treatment at all (Figure 5). From the scans, it was observed that rats receiving octreotide in the higher dose

Table 1. *Tumour somatostatin peptide content and receptor scintigraphy*

	Tumour concentration of somatostatin immunoreactivity				
	>16 pmol/g	8–16 pmol/g	4–8 pmol/g	1–4 pmol/g	<1 pmol/g
SRS					
Positive	1 + 1*	1	1	4	2
Negative	2		1		2

Somatostatin immunoreactivity in 14 neuroblastoma tumours and one ganglioneuroma (*), from children analysed at diagnosis for specific receptor expression using somatostatin receptor scintigraphy (SRS).

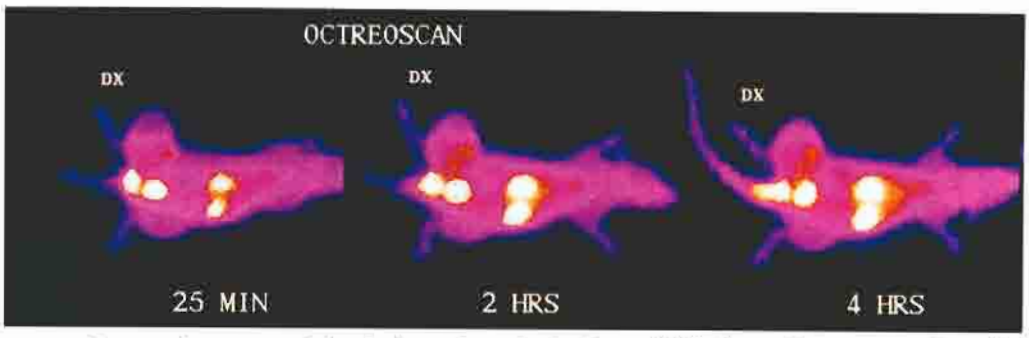

Figure 3. Somatostatin receptor scintigraphy in a nude rat bearing human SHSY-5Y neuroblastoma xenografts positively labelled for ^{111}In-pentetreotide (Octreoscan, Mallinckrodt). Scanning was performed at 25 min, 2 h and 4 h postinjection. The highest uptake is seen in the kidneys, bladder and at the injection site in the tail vein.

range showed more intense *in vivo* labelling of tumour tissue for both ^{111}In-pentetreotide and ^{125}I-VIP compared to control animals and rats receiving 13-*cis*-retinoic acid (Figures 4 and 5).

DISCUSSION

Somatostatin is known to inhibit growth and induce apoptosis in certain neuroblastoma cell lines *in vitro*. In the current study, we present data supporting a role of somatostatin in neuroblastoma biology *in vivo*. We found a higher somatostatin content in fully differentiated benign ganglioneuromas. In an unfavourable subset of advanced neuroblastomas, high somatostatin concentration was associated with favourable prognosis. Somatostatin receptor scintigraphy detected tumours expressing high-affinity receptors *in vivo*. This was found in tumours both with low and high concentrations of somatostatin immunoreactivity, respectively. Furthermore, SH-SY5Y xenografts with somatostatin binding but only very low peptide content were treated with a synthetic somatostatin analogue and showed an increase in scintigraphic detection of somatostatin and VIP receptors *in vivo*.

Using a specific radioimmunoassay for somatostatin, we found higher concentrations of immunoreactivity in ganglioneuroma and favourable neuroblastoma tumours in agreement with our previous findings [14, 15]. Furthermore, the analysed immunoreactivity represents the molecular forms SOM-14 and SOM-28 with biological activity *in vivo* [16]. In another study, higher tissue concentrations of SOM-LI were found in tumours with morphological differentiation and favourable clinical stage [21]. However, in that study comprising 16 neuroblastomas, no correlation with clinical outcome could be found for SOM-LI.

Plasma SOM-LI has only been studied in a limited series of children with neuroblastoma. Among 21 children, only 8 showed detectable plasma SOM-LI [16]. However, all these children showed increasing concentrations during surgical tumour manipulation. In all but one, postoperative concentrations were lower than those measured before surgical tumour removal, indicating tumour origin of increased systemic SOM-LI.

Somatostatin receptors have been shown both in cell lines and neuroblastoma tumour samples using binding studies and autoradiography, and *in vivo* in neuroblastoma patients using somatostatin receptor scintigraphy [7, 8, 10, 12, 13]. The presence of specific receptors is necessary for biological effects on neuroblastoma cells [7, 8]. In agreement with *in vitro* data, clinical effects of tumour treatment with somatostatin analogues in adult patients with carcinoid tumours are confined to those with tumours positive for SRS [22]. Hence, the described neuroblastoma xenograft model seemed to be a

Figure 4. ^{111}In-pentetreotide scintigraphy (Octreoscan) at 24 h postinjection in nude rats with SH5Y-5Y neuroblastoma xenografts treated for four days with octreotide (left, 7.5 μg×2, s.c.), VIP (middle, 40 μg×2, s.c.) and 13-*cis*-retinoic acid (right, 4 mg×2, p.o.) as described in *Materials and Methods*. Tumour sites are indicated by arrows.

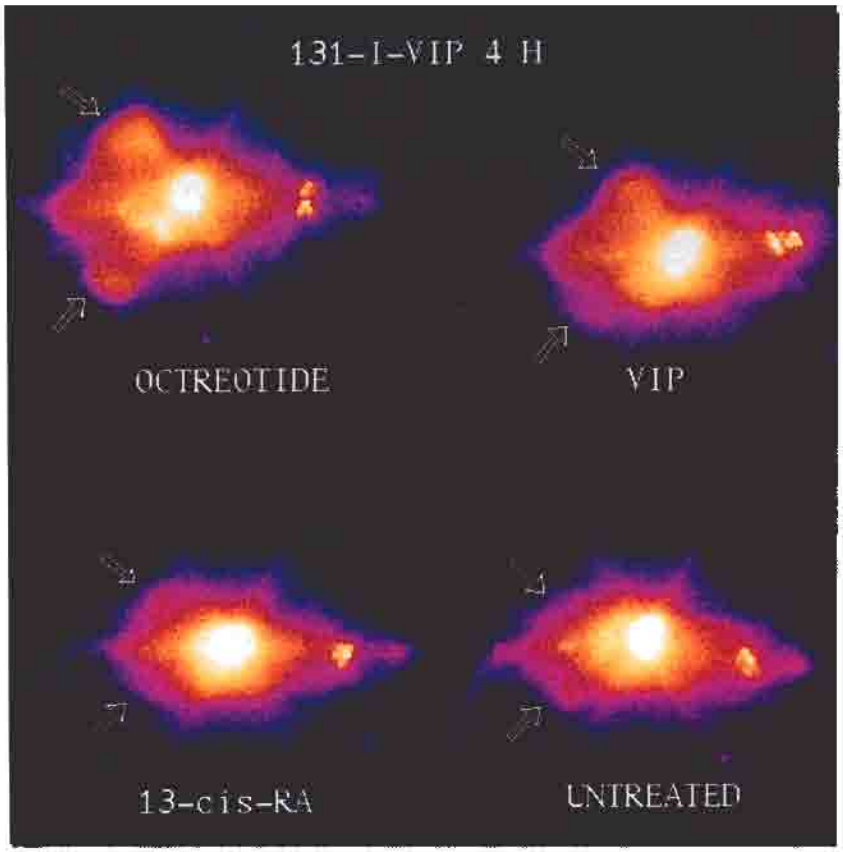

Figure 5. ^{131}I-VIP scintigraphy at 4 h postinjection in nude rats with SHSY-5Y neuroblastoma xenografts treated for 4 days with octreotide (upper left, 7.5 μg×2, s.c.), VIP (upper right, 40 μg×2, s.c.) and 13-*cis*-retinoic acid (lower left, 4 mg×2, p.o.) and an untreated rat (lower right). Tumour sites are indicated by arrows.

useful model to investigate the *in vivo* effects of a somatostatin analogue in neuroblastoma treatment. However, the detection of high-affinity somatostatin binding sites in the xenografts (Figure 3) was somewhat unexpected since Maggi and associates [8] reported SH-SY5Y cells to only bind SOM-14 with low affinity. We selected to analyse VIP receptors and compare the effects of octreotide to VIP and retinoic acid since the SH-SY5Y cell line has been reported to have an autocrine expression of VIP and VIP-R and also to respond to retinoic acid with upregulation of VIP-R [23, 24]. From our results in a limited series of *in vivo* experiments, it seems that octreotide was more effective than 13-*cis*-retinoic acid in upregulating the somatostatin and VIP binding sites (Figures 4 and 5). Previous data have indicated that VIP receptor expression in neuroblastoma is regulated by VIP in an autocrine manner [25, 26]. However, we are not aware of studies showing this effect from somatostatin on SOM or VIP receptors *in vitro* or *in vivo*. Downregulation of SOM binding in neuroblastoma tumour samples was observed in 5 children during disease progression [7]. VIP synthesis is increased in neuroblastoma cells by differentiation induced by retinoic acid as well as by VIP [26, 27]. We only found low concentrations of VIP immunoreactivity in the untreated xenografts (data not shown), and the effect of treatment has not yet been analysed in this regard. In conclusion, results obtained from clinical tumour samples support a correlation of somatostatin with neuroblastoma tumour differentiation and favourable prognosis. Using a xenograft model, treatment with the somatostatin analogue octreotide indicated the usefulness of this therapeutic option in human neuroblastoma. Somatostatin receptor scintigraphy seems to be useful not only to detect tumour tissue for diagnosis and staging, but also for the future selection of patients for specific targeted therapy using the growth inhibitory effects of somatostatin in neuroblastoma.

1. Kogner P. Neuropeptides in neuroblastomas and ganglioneuromas. In Nyberg F, Sharma HS, Wiesenfeld-Hallin Z, eds. *Progress in Brain Research, 104, Neuropeptides in the Spinal Cord*. Amsterdam, Elsevier, 1995, 325–338.
2. Reichlin S. Somatostatin. *New Engl J Med* 1984, **309**, 1495–1501, 1556–1563.
3. Shulkes A. Somatostatin: physiology and clinical applications. In Fuller P, Shulkes A, eds. *Baillière's Clinical Endocrinology and Metabolism*, 1994, **8**, 215–236.

4. Patel YC, Greenwood MT, Panetta R, *et al.* Mini review: the somatostatin receptor family. *Life Sci* 1995, **57**, 1249–1265.
5. Schally AV. Oncological applications of somatostatin analogues. *Cancer Res* 1988, **48**, 6977–6985.
6. Lambert SWJ, van der Lely AJ, de Herder WW, Hofland LJ. Octreotide. *New Engl J Med* 1996, **334**, 246–254.
7. O'Dorisio MS, Chen F, O'Dorisio TM, Wray D, Qualman SJ. Characterization of somatostatin receptors on human neuroblastoma tumours. *Cell Growth Diff* 1994, **5**, 1–8.
8. Maggi M, Baldi E, Finetti G, *et al.* Identification, characterization, and biological activity of somatostatin receptors in human neuroblastoma cell lines. *Cancer Res* 1994, **54**, 124–133.
9. Candi E, Melino G, De Laurenzi V, *et al.* Tamoxifen and somatostatin affect tumours by inducing apoptosis. *Cancer Lett* 1995, **96**, 141–145.
10. Moertel CL, Reubi JC, Scheithauer BS, Schaid DJ, Kvols LK. Expression of somatostatin receptors in childhood neuroblastoma. *Am J Clin Pathol* 1994, **102**, 752–756.
11. Krenning EP, Kwekkeboom DJ, Pauwels S, Kvols LK, Reubi JC. Somatostatin receptor scinitigraphy. *Nucl Med Ann* 1995, 1–50.
12. Sautter-Bihl ML, Dörr U, Schilling FH, *et al.* Somatostatin receptor imaging: a new horizon in the diagnostic management of neuroblastoma. *Semin Oncol* 1994, **21**(Suppl. 13), 38–41.
13. Schilling FH, Kogner P, Borgström, *et al.* Somatostatin receptor scintigraphy (SRS) in neuroblastoma (NB): preliminary results. *Med Ped Oncol* 1992, **27**, 332.
14. Kogner P, Björk O, Dominici C, Hedborg F, Theodorsson E. Vasoactive intestinal peptide (VIP) and somatostatin in childhood ganglioneuromas and neuroblastomas. *Proc Am Soc Clin Oncol* 1992, **11**, 371.
15. Kogner P, Theodorsson E, Björk O. Neuropeptides indicating growth, differentiation and outcome in childhood neuroblastoma and ganglioneuroma. *Clin Chem Enzyme Commun* 1993, **5**, 289–294.
16. Bjellerup P, Theodorsson E, Kogner P. Somatostatin and vasoactive intestinal peptide (VIP) in neuroblastoma and ganglioneuroma: chromatographic characterisation and release during surgery. *Eur J Cancer* 1995, **31A**, 481–485.
17. Brodeur GM, Pritchard J, Berthold F, *et al.* Revisions of the international criteria for neuroblastoma diagnosis, staging and response to treatment. *J Clin Oncol* 1993, **11**, 1466–1477.
18. Efendic S, Nylén A, Roovete A, Uvnäs-Wallenstein K. Effects of glucose and arginine on the release of immunoreactive somatostatin from the isolated perfused rat pancreas. *FEBS Lett* 1978, **92**, 33–35.
19. Hassan M, Refai E, Andersson M, Schnell PO, Jacobsson H. *In vivo* dynamical distribution of ^{131}I-VIP in the rat studied by gamma-camera. *Nucl Med Biol* 1994, **21**, 865–872.
20. Biedler J, Helson L, Spengler BA. Morphology and growth, tumorigenicity, and cytogenetics of human neuroblastoma cells in continous culture. *Cancer Res* 1973, **33**, 2643–2652.
21. Qualman SJ, O'Dorisio MS, Fleshman DJ, Shimada H, O'Dorisio TM. Neuroblastoma. Correlation of neuropeptide expression in tumour tissue with other prognostic factors. *Cancer* 1992, **70**, 2005–2012.
22. Jansson ET, Westlin JE, Eriksson B, *et al.* (^{111}In-DTPA-D-Phe^1) octreotide scintigraphy in patients with carcinoid tumours: the predictive value for somatostatin analogue treatment. *Eur J Endocrinol* 1994, **131**, 577–581.
23. Muller JM, Lolait SJ, Yu VC, Sadee W, Waschek JA. Functional vasoactive intestinal polypeptide (VIP) receptors in human neuroblastoma subclones that contain VIP precursor mRNA and release VIP-like substances. *J Biol Chem* 1989, **264**, 3647–3650.
24. Waschek JA, Muller JM, Duan DS, Sadee W. Retinoic acid enhances VIP receptor expression and responsiveness in human neuroblastoma cell SH-SY5Y. *FEBS Lett* 1989, **250**, 611–614.
25. Dorisio MS, Fleshman DJ, Qualman SJ, O'Dorisio TM. Vasoactive intestinal peptide: autocrine growth factor in neuroblastoma. *Regul Pept* 1992, **37**, 213–226.
26. Pence JC, Shorter NA. The autocrine function of vasoactive intestinal peptide on human neuroblastoma cell growth and differentiation. *Arch Surg* 1993, **128**, 591–595.
27. Agoston DV, Colburn S, Krajniak KG, Waschek JA. Distinct regulation of vasoactive intestinal peptide (VIP) expression at mRNA and peptide levels in human neuroblastoma cells. *Neurosci Lett* 1992, **139**, 213–216.

Acknowledgements—This work was in part supported by the Swedish Children's Cancer Foundation, Swedish Cancer Society and Research Funds of the Karolinska Institute. The authors wish to acknowledge Professor Suad Efendic for the kind gift of the SOM-14 specific antiserum, Professor Viktor Mutt for generously providing VIP, Teresia Svensson and Ingrid Vedin for expert technical assistance and Stig Larsson for generous support and valuable discussions.

IV

Apolipoprotein CIII promotes Ca^{2+} dependent β-cell death in type 1 diabetes

Lisa Juntti-Berggren[*†‡], Essam Refai[§†], Ioulia Appelskog[*], Mats Andersson[¶], Gabriela Imreh[*], Nancy Dekki[*], Sabine Uhles[*], Lina Yu[*], William J Griffiths[§], Sergei Zaitsev[*], Ingo Leibiger[*], Shao-Nian Yang[*], Gunilla Olivecrona[‖], Hans Jörnvall[§] & Per-Olof Berggren[*]

[*]The Rolf Luft Center for Diabetes Research, Dept. of Molecular Medicine, Karolinska Institutet, Stockholm, Sweden
[§]Dept. of Medical Biochemistry and Biophysics, Karolinska Institutet, Stockholm, Sweden
[¶]Microbiology and Tumor Biology Center, Karolinska Institutet, Stockholm, Sweden
[‖]Dept. of Medical Biosciences, Physiological Chemistry, Umeå University, Umeå, Sweden
[†]These authors contributed equally to this work
[‡]Correspondence should be addressed to L.J-B. (lisa.juntti-berggren@molmed.ki.se).

ABSTRACT. In type 1 diabetes (T1D) there is a specific destruction of the insulin secreting pancreatic β-cell. Although the exact molecular mechanisms underlying β-cell destruction are not known, sera from T1D patients have been shown to promote Ca^{2+}-induced apoptosis. We now demonstrate that apolipoprotein CIII (apoCIII) is increased in serum from T1D patients and that this serum factor both induces increased cytoplasmic free Ca^{2+} concentration ($[Ca^{2+}]_i$) and β-cell death. The apoCIII induced increase in $[Ca^{2+}]_i$ reflects an activation of the voltage-gated L-type Ca^{2+}-channel. Both the effects of T1D sera and apoCIII on the β-cell are abolished in the presence of antibody against apoCIII. Increased serum levels of apoCIII can thus account for the increase in -cell $[Ca^{2+}]_i$ and thereby β-cell apoptosis associated with T1D.

Abbreviations: ApoCIII, apolipoprotein CIII, T1D, type 1 diabetes

INTRODUCTION

Research over the last 30 years has established that type 1 diabetes (T1D) is an autoimmune disease, but the mechanisms/events that trigger the initiation and progression of the disease are still not identified. Genetic, immunological and environmental factors are involved in the pathogenesis of T1D and most likely the events involved differ between different patients. Voltage-gated L-type Ca^{2+}-channels have an important physiological role in pancreatic β-cell signal-transduction (1). These channels constitute an essential link between transient changes in membrane potential and insulin release. Changes in cytoplasmic free Ca^{2+} concentration ($[Ca^{2+}]_i$) in the β-cell are associated with the activation of a spectrum of intracellular signals and are strictly regulated as prolonged high $[Ca^{2+}]_i$ is harmful to the cells. Sera from newly

diagnosed T1D patients have been shown to increase the activity of voltage-gated L-type Ca^{2+}-channels in β-cells resulting in increased $[Ca^{2+}]_i$ upon depolarization and β-cell apoptosis, effects that can be prevented by Ca^{2+}-channel blockers (2). The key question has been what factor in T1D serum that is responsible for the changes in $[Ca^{2+}]_i$. In the present study, we have revealed the identity of a key factor in T1D sera that increases $[Ca^{2+}]_i$ as well as promotes apoptosis and found it to correspond to apolipoprotein CIII (apoCIII). The fact that not all sera from T1D patients affected $[Ca^{2+}]_i$ indicates that T1D is not caused by a single factor like apoCIII, which is in agreement with clinical observations suggesting that different factors can act in concert with the autoimmune abnormalities resulting in β-cell destruction.

Methods

Media The basal medium used both for isolation of cells and for experiments was a HEPES buffer (pH 7.4), containing (in mM): 125 NaCl, 5.9 KCl, 1.3 $CaCl_2$, 1.2 $MgCl_2$, 25 HEPES. Bovine serum albumin was added to the medium at a concentration of 1 mg/ml. For cell culture, RPMI 1640 medium was supplemented with 100 μg/ml streptomycin, 100 IU penicillin and 10% fetal calf-, normal human- or diabetic serum.

Preparation of cells Adult mice from a local colony(3) were starved overnight. Pancreatic islets were isolated by a collagenase technique and cell suspensions were prepared as previously described (4, 5). Cells were seeded onto glass coverslips and cultured at 37 ^{0}C in a humidified atmosphere of 5% CO_2 in air.

Preparation and purification of sera Sera from T1D patients and control subjects were collected, identically sterile-processed and stored frozen at –20 °C until used. The sera were heat-inactivated by incubation at 56 °C for 30 min. Thereafter β-cells were incubated overnight in RPMI 1640 culture medium with 10% of the sera and changes in $[Ca^{2+}]_i$ were recorded, subsequent to depolarization with 25 mM KCl. The five T1D sera that induced an enhanced $[Ca^{2+}]_i$ response were centrifuged and the supernatant was passed through a 0.45 mm sterile filter. Samples were loaded on Sep-Pak C_{18} (Waters, Ma) preconditioned with 0.1% TFA. After a wash with 0.1% TFA, proteins were eluted with 60% acetonitrile in 0.1% TFA and therafter lyophilized. Batches of one milligram of the lyophilized sample were dissolved in 500 μl 0.1% TFA, centrifuged and injected into a RP-HPLC with a Vydac C_{18}

(0.46 x 25 cm) column (Grace Vydac, Hesperia, Ca). The separation was made using a linear gradient of 20-60% acetonitrile in 0.1% TFA for 40 min at 1 ml/min. Fractions of 1 ml were collected and lyophilized.

Purification of isoforms of apolipoprotein CIII (apoCIII) ApoCIII was purified from human serum by adsorption to a lipid emulsion and delipidation, followed by chromatography of the lipid-associated proteins under denaturing conditions in guanidinium chloride and urea, respectively, as previously described (6). The apoCIII isoforms were dialyzed against ammonium bicarbonate and lyophilized before use.

Measurements of $[Ca^{2+}]_i$ Cells, attached to coverslips, were pretreated with the different compounds as described in the results and thereafter incubated in basal medium with 2 μM fura-2AM (Molecular Probes, Eugene, OR) for 30 min. The coverslips were mounted as the bottom of an open chamber and cells were perifused with medium. Fluorescence signals were recorded with a SPEX Fluorolog-2 system connected to an inverted Zeiss Axiovert epifluorescence microscope. The excitation and emission wavelengths were 340/380 and 510 nm, respectively. The results are presented as 340/380 excitation ratios, directly representative of $[Ca^{2+}]_i$ (7).

Patch clamp Whole-cell Ca^{2+} currents were recorded by using the perforated-patch variant of the whole-cell patch-clamp recording technique to eliminate the loss of soluble cytoplasmic components. Electrodes were filled with (in mM): 76 Cs_2SO_4, 1 $MgCl_2$, 10 KCl, 10 NaCl, and 5 HEPES (pH 7.35), as well as amphotericin B (0.24 mg/ml) to permeabilize the cell membrane and allow low-resistance electrical access without breaking the patch. Pancreatic β-cells were incubated in RPMI 1640 medium with apoCIII (10 μg/ml) or vehicle overnight. The cells were bathed in a solution containing (in mM): 138 NaCl, 10 tetraethylammonium chloride, 10 $CaCl_2$, 5.6 KCl, 1.2 $MgCl_2$, 5 HEPES and 3 D-glucose (pH 7.4). Whole-cell currents induced by voltage pulses (from a holding potential of -70 mV to several clamping potentials from -60 to 50 mV in 10 mV increments, 100 ms, 0.5 Hz) were filtered at 1 kHz and recorded. All recordings were made with an Axopatch 200 amplifier (Axon Instruments, Foster City, California) at room temperature (about 22 °C). Acquisition and analysis of data were done using the software program pCLAMP6 (Axon Instruments, Foster City, California).

Protein characterization Primary sequence was obtained in ABI 494C and cLC sequencers. Protein molecular weights were determined by electrospray mass spectrometry (AutoSpec hybrid tandem mass spectrometer, Micromass). For recording of positive-ion conventional-ES spectra, samples (16 pmol/ml) were introduced into the ES interface by infusion or loop injection at a flow rate of 3 ml/min. To determine the position of the glycosylation, the native protein was digested with trypsin 1:10 w/w (Promega, Madison, WI). The resulting fragments were separated by HPLC using a Vydac C_8 (2.1 x 150 mm) and a gradient of 0-50% B in 50 min (buffer A, 5% acetonitrile/0.1% TFA; B, 80% acetonitrile/0.1% TFA). The fragments separated were applied to mass analysis.

Quantification of apoCIII Sera were collected and prepared as described above. The relative amounts of apoCIII in T1D serum and control serum, respectively were evaluated by comparisons of the peak area corresponding to apoCIII in the second RP-HPLC.

Flow cytometric analysis of cell death RINm5F cells were cultured for 36 h in the presence of 10% control serum, control serum and 40 μg/ml apoCIII or T1D serum with or without 100 or 200 μg/ml anti-apoCIII. The whole cell population was collected and stained with EGFP-conjugated Annexin V and propidium iodide (PI) (BD PharMingen) and analyzed on a FACscan using CELLQuest acquisition software (Becton Dickinson, Immunocytometry System). FACS gating, based on forward and side scatter, was used to exclude cellular debris and autofluorescence and typically 10 000 cells were selected for analysis.

Statistical analysis Statistical significance was evaluated by Student´s t-test and *P* values <0.05 were considered significant. Data are expressed as means ± SEM.

Results and Discussion

We have previously shown that T1D serum can activate voltage-gated L-type Ca^{2+}-channels in the pancreatic β-cell, resulting in increased $[Ca^{2+}]_i$ and thereby β-cell apoptosis (2). In order to identify the factor in T1D serum responsible for these effects, we have now screened sera from seven newly diagnosed T1D patients (Table 1), using increases in $[Ca^{2+}]_i$ as a readout. Mouse pancreatic β-cells were cultured overnight with 10% sera from the actual patients or normal subjects. Sera from five of the patients induced a significantly higher increase in $[Ca^{2+}]_i$, when cells were depolarized with 25 mM KCl, leading to an opening of

voltage-gated L-type Ca^{2+}-channels, than sera from healthy blood donors (Fig. 1). Positive sera were pooled, concentrated and fractionated by reversed phase (RP)-HPLC. When fractions were tested on isolated mouse pancreatic β-cells, one fraction (No. 3, Fig. 2A) eluting between 52-60% acetonitrile, induced a more pronounced increase in $[Ca^{2+}]_i$ when cells were depolarized with high concentrations of K^+. After further purification of the component(s) in this fraction by repeated RP-HPLC runs (Fig. 2B,D), all fractions obtained were tested for effects on $[Ca^{2+}]_i$ by incubation with mouse β-cells overnight. The results from this second purification (Fig. 2B) showed a higher activity in fraction 2 (Fig. 2C). The protein that induced an increase in $[Ca^{2+}]_i$ indicated by the bar in Fig. 2D was determined. Sequence information was obtained both by C-terminal and N-terminal degradations. The sequences were identical to those of human apoCIII for 20 N-terminal and 5 C-terminal amino acid residues.

ApoCIII plays a key role in the regulation of the metabolism of triglyceride-rich lipoprotein (TRL) (8). It controls the catabolism of TRL by inhibiting the activity of lipoproteinlipase (LPL) (9,10), thereby inducing hypertriglyceridemia. ApoCIII also inhibits the binding of remnant lipoproteins to catabolic receptors like the LDL receptor related protein (LRP) (11). When the apoCIII gene was disrupted in mice, there was a 70% reduction in triglyceride levels (12). Overexpression of human apoCIII in transgenic mice results in hypertriglyceridemia (13). ApoCIII is a 79-residue, 8.8 kDa polypeptide (14) with three known isoforms that differ in terms of glycosylation, $CIII_0$ (no sialic acid), $CIII_1$ (one sialic acid residue) and $CIII_2$ (two sialic acid residues), contributing approximately 10%, 55% and 35%, respectively, of total plasma apoCIII (15). Mutagenesis of the glycosylation site and expression in stable cell lines suggest that intracellular glycosylation is not required for the transport and secretion functions (16). Lack of glycosylation does not affect the affinity of apoCIII for VLDL and HDL (16). Insulin is involved in the regulation of the apoCIII gene and induces a dose-dependent down-regulation at the transcriptional level. Overexpression of the apoCIII gene could contribute to the hypertriglyceridemia seen in T1D patients (17). Although surprising at first glance, mice transgenic for the human apoCIII gene, are neither insulin-resistant nor hyperinsulinemic (18). However it is important to keep in mind that in T1D we are dealing with a complex interplay between genetic predisposition, immunological changes and environmental factors that together promote the destruction of the β-cells.

The concentration of apoCIII has previously been found to be higher in diabetic patients than in normal subjects (19-27). In insulin deficient rats there was no significant change in apoCIII

in one study (28), while others have reported an increase in the proportions of the sialylated apoCIII (29, 30). We analyzed the apoCIII purified from T1D sera by mass spectrometry for subcomponent identification. The major components had apparent masses of 9423 and 9714 Da (Fig. 2E), corresponding to the mono- and di-glycosylated forms of apoCIII (theoretical, calculated values are: $CIII_0$ 8764 Da, $CIII_1$ 9420 Da, $CIII_2$ 9712 Da). To determine the positions of glycosylation, the protein was digested with trypsin and the fragments were separated by RP-HPLC. When the separated fragments were analyzed by mass spectrometry, seven of the eight fragments showed masses identical to the theoretical values. The mass difference was localized to the C-terminal fragment, previously shown to be glycosylated (31). The absence of a non-glycosylated C-terminal fragment indicated that the isolated apoCIII forms were glycosylated. The relative amounts of apoCIII in T1D and control sera were evaluated by comparisons of the peak area corresponding to apoCIII in the second RP-HPLC (Fig. 3A). In T1D sera the levels of the sialylated isoforms of apoCIII ($apoCIII_1$ and $apoCIII_2$) were four-fold higher than in non-diabetic sera. The non-sialylated isoform ($apoCIII_0$) could not be detected.

The concentration of apoCIII has been reported to be between 60-140 μg/ml in control subjects and 90-270 μg/ml in diabetics (9, 19, 20, 24-27). These variations may to a certain extent reflect the fact that various methods have been used for the determinations. In our experiments we have used 10% T1D serum in the culture medium instead of 10% fetal calf serum normally used. Based on the levels found in diabetic patients we have therefore chosen 10-50 μg/ml of apoCIII, a concentration range affecting intracellular Ca^{2+}-handling. We have also tested three lower concentrations (1, 3 and 6 μg/ml), but these did not affect $[Ca^{2+}]_i$ (data not shown).

Commercially available apoCIII (Sigma), which constitutes a mixture of $apoCIII_1$ and $apoCIII_2$, was tested at a concentration of 10 μg/ml and was shown to stimulate Ca^{2+} influx similar to the product isolated from T1D sera (Fig. 3B). Co-incubation of β-cells with 100 μg/ml of a polyclonal antibody against human apoCIII (Academy BioMedical Company, Houston, TX) blocked the activity of both the commercial apoCIII and the T1D serum (Fig. 3B,C). The polyclonal antibody had no activity by itself (data not shown). When testing the three isoforms of apoCIII by incubation of β-cells at a concentration of 10 μg/ml, both the glycosylated ($CIII_1$ and $CIII_2$) and the non-glycosylated isoform caused a significantly higher increase in $[Ca^{2+}]_i$ than cells that had been incubated with only the vehicle, 0.1% triflouroacetic acid (TFA) (Fig. 3D). To study the effect of possible binding of apoCIII to

serum lipoproteins in the culture medium, cells were incubated in basal buffer containing no serum and 10 μg/ml apoCIII$_1$ for 2 and 6 h. There was a significantly elevated increase in $[Ca^{2+}]_i$ upon depolarization in all the experiments where the cells had been exposed to apoCIII$_1$ for 6 h, but only in one out of three experiments where the incubation time was only 2 h (data not shown).

There was a higher percentage of dead cells in the cell population exposed to T1D serum. This effect was prevented by the addition of anti-apoCIII (Fig. 3E). Furthermore, the addition of pure apoCIII to culture medium with control serum resulted in an increased cell death (Fig. 3E).

To elucidate the molecular mechanism underlying the stimulatory effect of apoCIII on $[Ca^{2+}]_i$, the activity of voltage-gated Ca^{2+}-channels was analysed in β-cells incubated with 10 μg/ml apoCIII. ApoCIII-treated cells displayed larger Ca^{2+}-channel currents than control cells during depolarizations in the range -10 to 10 mV, from a holding potential of –70 mV (Fig. 4A,B). These data demonstrate that apoCIII modulated the activity of the voltage-gated L-type Ca^{2+}-channel and that the effect occurred in the range of physiological depolarizations. So far immunoblot experiments have not revealed a direct interaction of apoCIII with the Ca^{2+}-channel (data not shown). Future experiments will clarify to what extent this may reflect limitations set by the immunoprecipitation protocol or the actual situation.

In our previous study (2) we tested T1D sera on GH_3 cells, a pituitary cell line, and obtained the same effect as in primary β-cells and RINm5F cells. This suggests that the observed effects induced by apoCIII may not be exclusive for the β-cells, but rather associated with the presence of voltage-gated L-type Ca^{2+}-channels. The sensitivity of the pancreatic β-cell to the cytotoxic effect of apoCIII and resulting increase in $[Ca^{2+}]_i$ is likely to reflect an inherent overall low tolerance to stress (32).

Our study shows that the sialylated forms of apoCIII were on average four-fold higher in sera from newly diagnosed T1D patients than in sera from healthy subjects. ApoCIII induced both an increase in $[Ca^{2+}]_i$ and β-cell death. The molecular mechanism underlying the stimulatory effect of apoCIII on $[Ca^{2+}]_i$ reflected an activation of the voltage-gated L-type Ca^{2+}-channel. Addition of an antibody against apoCIII blocked the effects of both T1D serum and apoCIII on $[Ca^{2+}]_i$ as well as on β-cell death. This suggests that the Ca^{2+} dependent cytotoxic effect of T1D serum on the pancreatic β-cell is mediated by apoCIII.

Acknowledgments. This work was supported by grants from Barndiabetesfonden, the Swedish Diabetes Association, Karolinska Institutet, the Swedish Research Council, the

Swedish Society for Medical Research, Novo Nordisk Foundation, the Family Persson Foundation, Berth von Kantzow's Foundation, Juvenile Diabetes Research Foundation International and National Institutes of Health (DK58508).

References

1. Efendic, S., Kindmark, H. & Berggren, P. O. (1991) *J Intern Med Suppl* **735,** 9-22.
2. Juntti-Berggren, L., Larsson, O., Rorsman, P., Ammala, C., Bokvist, K., Wahlander, K., Nicotera, P., Dypbukt, J., Orrenius, S., Hallberg, A. & Berggren, P. O. (1993) *Science* **261,** 86-90.
3. Hellman, B. (1965) *Ann N Y Acad Sci* **131,** 541-58.
4. Nilsson, T., Arkhammar, P., Hallberg, A., Hellman, B. & Berggren, P. O. (1987) *Biochem J* **248,** 329-36.
5. Lernmark, A. (1974) *Diabetologia* **10,** 431-8.
6. Bengtsson-Olivecrona, G. & Olivecrona, T. (1991) *Methods Enzymol* **197,** 345-56.
7. Kindmark, H., Kohler, M., Efendic, S., Rorsman, P., Larsson, O. & Berggren, P. O. (1992) *FEBS Lett* **303,** 85-90.
8. Fredenrich, A. (1998) *Diabetes Metab* **24,** 490-5.
9. Krauss, R. M., Herbert, P. N., Levy, R. I. & Fredrickson, D. S. (1973) *Circ Res* **33,** 403-11.
10. Ginsberg, H. N., Le, N. A., Goldberg, I. J., Gibson, J. C., Rubinstein, A., Wang-Iverson, P., Norum, R. & Brown, W. V. (1986) *J Clin Invest* **78,** 1287-95.
11. Kowal, R. C., Herz, J., Weisgraber, K. H., Mahley, R. W., Brown, M. S. & Goldstein, J. L. (1990) *J Biol Chem* **265,** 10771-9.
12. Maeda, N., Li, H., Lee, D., Oliver, P., Quarfordt, S. H. & Osada, J. (1994) *J Biol Chem* **269,** 23610-6.
13. Ito, Y., Azrolan, N., O'Connell, A., Walsh, A. & Breslow, J. L. (1990) *Science* **249,** 790-3.
14. Brewer, H. B., Jr., Shulman, R., Herbert, P., Ronan, R. & Wehrly, K. (1974) *J Biol Chem* **249,** 4975-84.
15. Kashyap, M. L., Srivastava, L. S., Hynd, B. A., Gartside, P. S. & Perisutti, G. (1981) *J Lipid Res* **22,** 800-10.
16. Roghani, A. & Zannis, V. I. (1988) *J Biol Chem* **263,** 17925-32.
17. Chen, M., Breslow, J. L., Li, W. & Leff, T. (1994) *J Lipid Res* **35,** 1918-24.
18. Reaven, G. M., Mondon, C. E., Chen, Y. D. & Breslow, J. L. (1994) *J Lipid Res* **35,** 820-4.
19. Briones, E. R., Mao, S. J., Palumbo, P. J., O'Fallon, W. M., Chenoweth, W. & Kottke, B. A. (1984) *Metabolism* **33,** 42-9.
20. Joven, J., Vilella, E., Costa, B., Turner, P. R., Richart, C. & Masana, L. (1989) *Clin Chem* **35,** 813-6.
21. Stewart, M. W., Laker, M. F. & Alberti, K. G. (1994) *J Intern Med Suppl* **736,** 41-6.
22. Bren, N. D., Rastogi, A. & Kottke, B. A. (1993) *Mayo Clin Proc* **68,** 657-64.
23. Nestel, P. J. & Fidge, N. H. (1982) *Adv Lipid Res* **19,** 55-83.
24. Blackett, P., Sarale, D. C., Fesmire, J., Harmon, J., Weech, P. & Alaupovic, P. (1988) *South Med J* **81,** 469-73.
25. al Muhtaseb, N., al Yousuf, A. & Bajaj, J. S. (1992) *Pediatrics* **89,** 936-41.
26. Manzato, E., Zambon, A., Lapolla, A., Zambon, S., Braghetto, L., Crepaldi, G. & Fedele, D. (1993) *Diabetes Care* **16,** 469-75.
27. Reverter, J. L., Senti, M., Rubies-Prat, J., Lucas, A., Salinas, I., Pizarro, E., Pedro-Botet, J. & Sanmarti, A. (1993) *Clin Chim Acta* **223,** 113-20.
28. O'Looney, P., Irwin, D., Briscoe, P. & Vahouny, G. V. (1985) *J Biol Chem* **260,** 428-32.
29. Callow, M. J. & Redgrave, T. G. (1993) *Biochim Biophys Acta* **1168,** 271-9.
30. Bar-On, H., Roheim, P. S. & Eder, H. A. (1976) *J Clin Invest* **57,** 714-21.
31. Ito, Y., Breslow, J. L. & Chait, B. T. (1989) *J Lipid Res* **30,** 1781-7.
32. Lenzen, S., Drinkgern, J. & Tiedge, M. (1996) *Free Radic Biol Med* **20,** 463-6.

Table 1. **Characterization of the T1D patients**. Gender of the patients is designated as F, female, and M, male. The presence (Pos), absence (Neg) or no data available (ND) of antibodies to islet cells (ICA), GAD and tyrosin phosphatase IA2 (IA-2) are marked in the table. Healthy blood donors, all negative for ICA, GAD and IA-2, served as sources of control sera. *Insulin was the only medication administered.

Patient	Sex	Age (years)	Duration of T1D(weeks)	Medication	ICA	GAD	IA-2
1	M	32	<1	No*	Pos	Pos	Pos
2	F	32	12	No*	Neg	Pos	Neg
3	F	31	<1	No*	Pos	Pos	Pos
4	F	23	<1	No*	Pos	Neg	ND
5	M	19	<1	No*	Neg	Neg	Pos
6	F	35	<1	No*	Pos	Pos	Pos
7	F	33	28	No*	Pos	Pos	ND

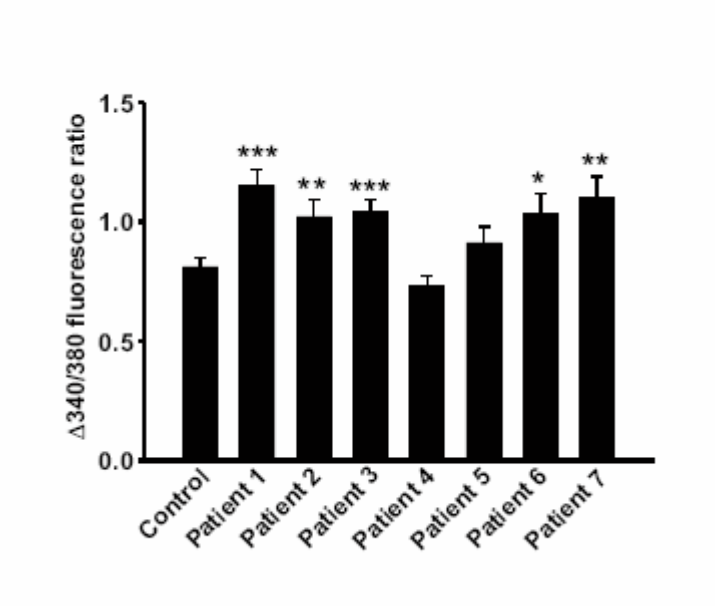

Figure 1 Changes in $[Ca^{2+}]_i$ in pancreatic β-cells from mice exposed to T1D or control sera. Five out of seven T1D sera induced an enhanced increase in $[Ca^{2+}]_i$, when the cells were depolarized with high concentrations of K^+ to open the voltage-gated Ca^{2+}-channel, compared to cells that had been exposed to normal serum (n = 29, 28, 32, 47, 21, 27, 31 and 18, respectively), *** $P < 0.001$, ** $P < 0.01$ and * $P < 0.05$ versus control.

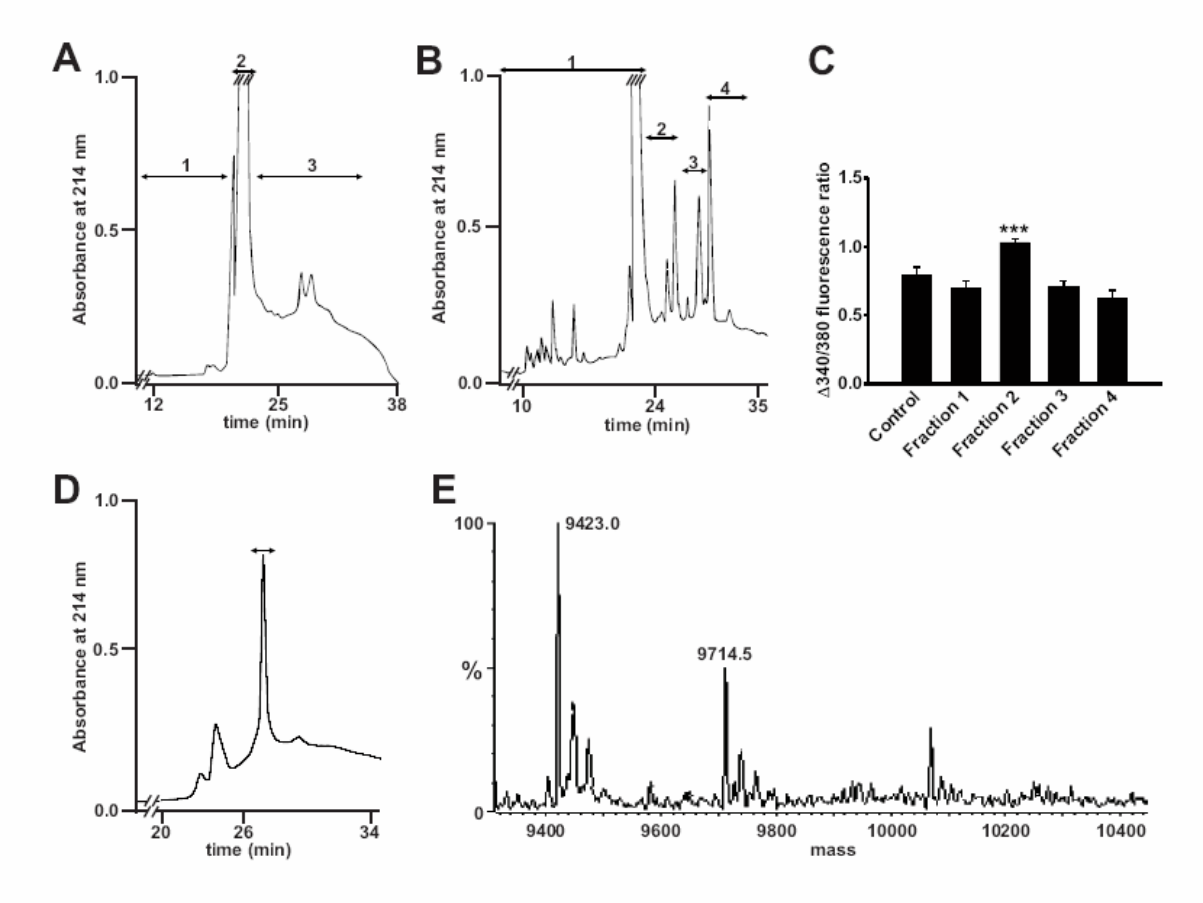

Figure 2 Stepwise separation and identification of the active fraction in T1D serum. **A,** After the first RP-HPLC separation the fraction marked 3 was found to give a higher increase in $[Ca^{2+}]_i$. **B,** Fraction 3 (Fig. 2A) was rerun on RP-HPLC under identical conditions. The fractions were again tested for $[Ca^{2+}]_i$ stimulating activity (Fig. 2C), and one positive fraction (No. 2) was identified. **D,** The active fraction (Fig. 2B) was rechromatographed. The fraction, inducing a higher increase in $[Ca^{2+}]_i$ when β-cells were depolarized with high concentrations of K^+, is marked with a bar. **C**, Pancreatic β-cells incubated with four fractions from RP-HPLC of diabetic sera from Fig. 2B (n = 6, 11, 12, 11 and 10, respectively), *** $P < 0.001$ versus control. **E**, The active fraction from Fig. 2C was analyzed by electrospray mass spectrometry.

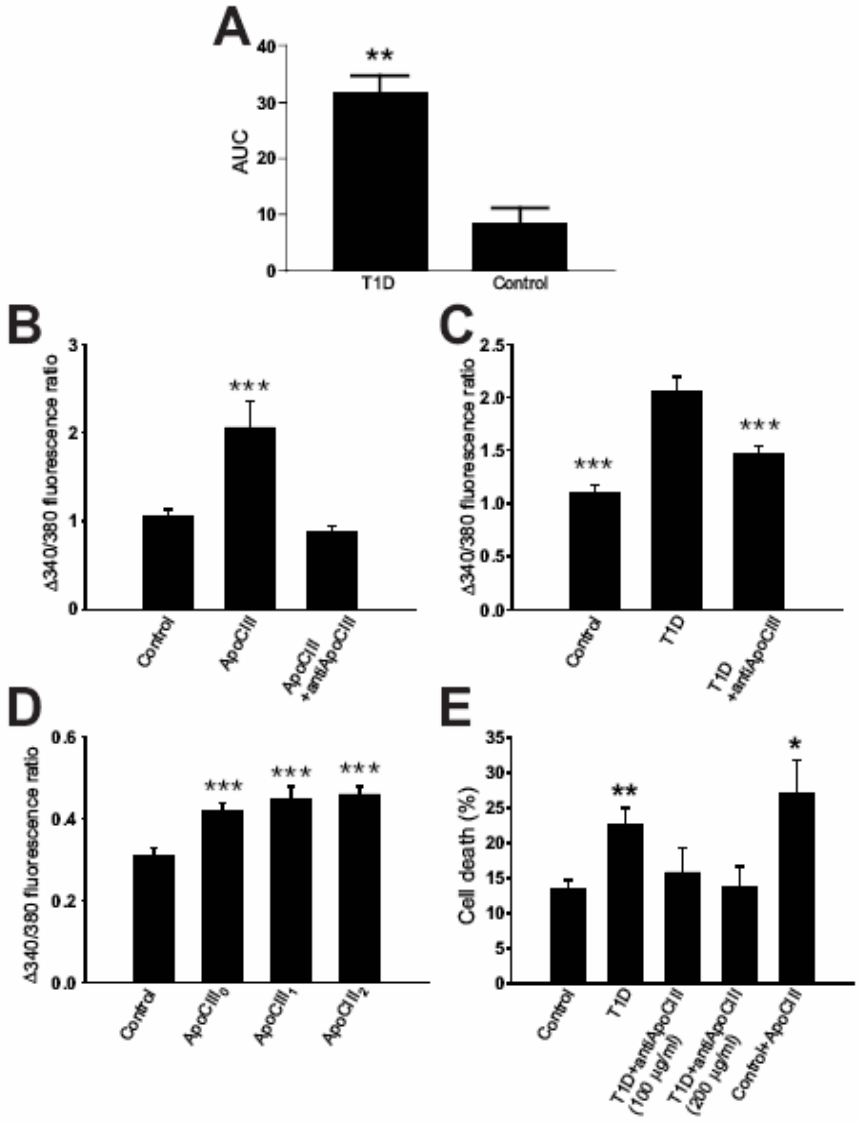

Figure 3 Amounts of apoCIII in T1D serum and effects on $[Ca^{2+}]_i$ and cell death. **A**, Relative levels of $apoCIII_{1+2}$ in T1D and control serum, given as area under the curve (AUC), $^{**}P < 0.01$ (n=5). **B,** Pancreatic β-cells were incubated with apoCIII or apoCIII + antibodies against human apoCIII (n= 63, 35 and 33), $^{***}P < 0.001$ versus control. **C,** β-cells were incubated with a control or a T1D serum and T1D serum + anti-apoCIII (n= 18, 17 and 20), $^{***}P < 0.001$ versus T1D serum. **D**, Mouse β-cells were incubated with $apoCIII_0$, $apoCIII_1$, $apoCIII_2$ or the vehicle (control) (n = 54, 40, 48, 37), *** $P < 0.001$ versus control. **E**,The insulin secreting cell line RINm5F was exposed to control and T1D sera and T1D serum with the addition of two concentrations of anti-apoCIII and finally control serum with apoCIII (n=5), $^{*}P < 0.05$ and $^{**}P < 0.01$, versus control.

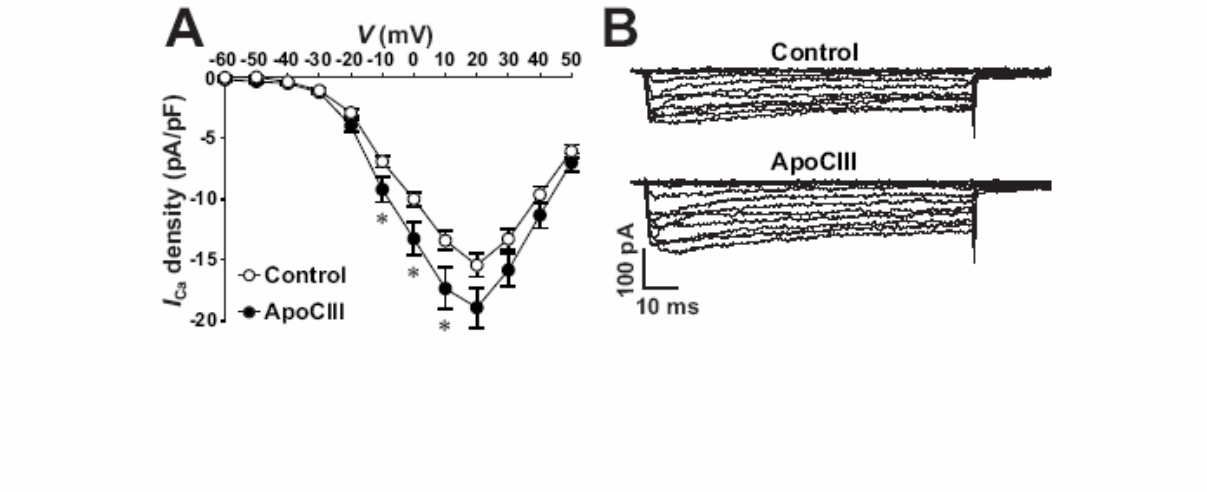

Figure 4 Interaction of apoCIII with the voltage-gated L-type Ca^{2+} channel. **A**, Summary graph of current density-voltage relationships. ApoCIII-treated cells (filled circles, n = 56) and control cells (open circles, n = 55) were depolarized to potentials between -60 and 50 mV, in 10 mV increments, from a holding potential of -70 mV, *P < 0.05. **B**, Sample whole-cell Ca^{2+} current traces from a control cell (cell capacitance: 4.3 pF) and a cell incubated with apoCIII (cell capacitance: 4.2 pF). Cells were depolarized by a set of voltage pulses (100 ms, 0.5 Hz) between -60 and 50 mV, in 10 mV increments, from a holding potential of -70 mV.

V

Transthyretin promotes Ca^{2+} increase and insulin release in pancreatic β-cells

Essam Refai[*†], Nancy Dekki[‡†], Shao-Nian Yang[‡], Lina Yu[‡], Svante Norgren[¶], Sophia M Rössner[¶], Mats Andersson[§], Hans Jörnvall[*], Per-Olof Berggren[‡] & Lisa Juntti-Berggren[‡]

[*]Department of Medical Biochemistry and Biophysics, Karolinska Institutet, Stockholm, Sweden

[‡] The Rolf Luft Center for Diabetes Research, Karolinska Institutet, Stockholm , Sweden

[¶] Department of Clinical Sciences, Division of Pediatrics, Huddinge Hospital, Stockholm, Sweden

[§] Microbiology and Tumor Biology Center, Karolinska Institutet, Stockholm, Sweden

[†] These authors contributed equally to this work

ABSTRACT. Transthyretin (TTR) mainly exists as a stable tetramer under physiological conditions, but a small amount of monomer has recently been found *in vivo* in normal individuals. We now demonstrate that total TTR enhances the activity of voltage-gated L-type Ca^{2+} channels, increases cytoplasmic free Ca^{2+} concentration ($[Ca^{2+}]_i$) and promotes insulin release. In addition we show that the concentration of total TTR is decreased in type 1 diabetes (T1D), while that of the monomeric form is increased. Also the monomeric form of TTR affects $[Ca^{2+}]_i$ and insulin release. Conversion of the tetrameric form of TTR to the monomeric form may constitute an important step associated with the development of β-cell dysfunction in TID.

Transthyretin (TTR) is a tetrameric protein of four identical subunits of 14 kDa that is synthesized primarily in the liver and in the choroid plexus of the brain (*1*). It is a transport protein for thyroxine and retinol in association with retinol-binding protein, for retinol. TTR has a complex equilibrium between different quartenary structures in serum (*2*), but exists mainly as a tetramer, with only a small amount of TTR monomer, *in vivo* in normal individuals (*3*,*4*). When the concentration of TTR is measured in serum

samples by conventional methods it is the tetrameric form that is detected. It is possible to estimate the amount of monomeric TTR both by SDS-PAGE, without reductive preboiling, and by reverse phase (RP)-HPLC. As shown in Fig 1, the monomer elutes before the tetramer on RP-HPLC (peak 2; peak 1 being non-TTR material). The monomeric form is verified by total mass determination, 14 kDa by MALDI mass spectrometry, and a monomer band on SDS-PAGE. A second fraction upon HPLC (peak 3) yields a mass value of 50 kDa and on SDS-PAGE shows a monomer plus several aggregates, including tetramer. It appears possible that lack of complete dissociation of the tetramer upon SDS-PAGE may be due to the presence of some cross-linked or else chemically modified forms of TTR. Cys-10 of TTR has previously been shown to be sensitive to modification (*2*) and we therefore tested both the monomer and tetramer fractions from the HPLC by sequencer degradation, which however showed identical results for 15 cycle in both cases, suggesting that Cys-10 is not likely to be involved in the relative stability of the tetramer now observed.

We have measured changes in cytoplasmic free Ca^{2+} concentration, $[Ca^{2+}]_i$, in β-cells pretreated with TTR and stimulated with glucose and KCl. TTR at a concentration of 100- and 150 mg/l induced a more pronounced increase in $[Ca^{2+}]_{i,}$ subsequent to stimulation with glucose and KCl (Fig 2 A,B), compared to control, while 50 mg/l was without effect. Basal $[Ca^{2+}]_i$ was not affected. In trying to elucidate the cellular mechanism underlying the increase in $[Ca^{2+}]_i$, the activity of voltage-gated Ca^{2+}-channels was analysed in cells incubated with 150 mg/l commercial TTR, which has both monomer and tetramer forms (Fig 1). Ca^{2+} currents registered from TTR-treated cells, depolarized to -20 mV, were significantly enhanced as compared to those from control cells (Fig 3). These data support that TTR acts on L-type Ca^{2+}-channels as the effect occurred in the range of physiological depolarisations (*5*) and it is known that mouse β-cells contain exclusively L-type Ca^{2+}-channels (*6*). The stimulus-secretion coupling in the pancreatic β-cell is a complex process where changes in $[Ca^{2+}]_i$ serve as a key regulator of insulin release (*7*). To clarify the extent to which the TTR-induced changes in $[Ca^{2+}]_i$ were paralleled by changes in insulin release, mouse β-cells were incubated overnight with commercial TTR, consisting of both tetra- and monomer, and thereafter stimulated with glucose and KCl (Fig 4 A-C) in a perifusion system. There was no difference in

insulin secretion, evaluated as area under the curve (AUC), in cells exposed to 50 mg/l total TTR**,** whereas 100 mg/l gave an increase in glucose stimulated insulin release ($p<0.05$) and 150 mg/l in both basal ($p<0.05$) and glucose stimulated insulin release ($p<0.05$) (Fig 4 D,E). None of the TTR concentrations influenced KCl stimulated insulin release.

We have previously shown that serum from adult patients with newly diagnosed type 1 diabetes (T1D) induces a higher activity in voltage-gated L-type Ca^{2+}-channels than serum from healthy subjects (*8*). We have now incubated pancreatic β–cells overnight in culture medium with 10 % sera from 21 children with newly diagnosed T1D or healthy controls. The changes in $[Ca^{2+}]_i$, upon depolarisation with KCl, were measured and in 11 of the diabetic sera the increase was higher (positive sera) and in 10 the increase was similar (negative sera) compared to cells exposed to normal sera. Searching for possible serum components responsible for the observed effects on $[Ca^{2+}]_i$, it is of interest to note that the serum concentration of total TTR is decreased in children with T1D (*9-11*). Due to limited amount of serum material we could only measure the concentration of TTR, with kinetic nephelometri, in nine positive, three negative and ten control sera (Table 1). The levels were 116±11 mg/l in diabetic sera and 220±18 mg/l in control sera ($p<0.001$). Of the three negative diabetic sera (No 10-12, Table 1) one had a TTR level comparable with control sera (196 mg/l) while the other two were in the same low range as the positive diabetic sera. Knowing the possibility to estimate the amount of monomer, we analysed sera from both T1D and controls for SDS-PAGE patterns. As shown in Fig 5, the band representing the TTR monomer has a higher intensity on silverstained SDS-PAGE in sera from both adults (Fig 5A) and children (Fig 5B) with T1D than in healthy controls. We find that in the group of ten tested children there was an up-regulation of the monomer in six of them.

Our observation that the band on SDS-PAGE, representing TTR monomer, was of a higher intensity in T1D patients, while the serum level of the tetramer was decreased, made us test the monomer on β-cell $[Ca^{2+}]_i$. The TTR monomer was purified from commercially available TTR by HPLC and $[Ca^{2+}]_i$ measurements were made on β-cells incubated with 1 and 2 μg/ml of the monomer. The concentrations were chosen based on the only study to our knowledge where the levels of monomer have been measured in

serum from patients with familial amyloid polyneuropathy (FAP) and normal subjects (*4*). In the latter group the concentration was 565± 231 ng/ml and as our diabetic patients had a stronger band than the controls, we decided to take one concentration in the upper normal range and in addition one higher concentration. In cells exposed to 1- and 2 μg/ml of the monomer, glucose and depolarization with high K^+ gave a more pronounced increase in $[Ca^{2+}]_i$ compared to controls (Fig 2 C,D). No difference in basal $[Ca^{2+}]_i$ was observed. Insulin secretion, stimulated by glucose and KCl, was not affected by the monomer in either of the chosen concentrations, although basal insulin secretion was significantly higher in cells treated with 2 μg/ml monomer. The increased basal secretion may reflect a negative effect on β-cell function. However, neither 150 mg/l of total TTR nor 2ug/ml of TTR monomer did induce cell death (Fig 6).

In parallel with overnight incubation of cells, samples with the three concentrations of the monomer were incubated overnight and thereafter run on SDS-PAGE. This revealed that parts of the added monomer had reaggregated to tetramer (data not shown). Taken into consideration the relative responses to total TTR versus monomer TTR, the monomeric form is the likely candidate responsible for the effects.

We now demonstrate that TTR promotes an increase in both $[Ca^{2+}]_i$ and insulin release, the former effect being explained by a direct activation of the voltage-gated L-type Ca^{2+} channel. Moreover, we demonstrate that the concentration of total TTR is decreased in T1D, while that of the monomeric form is increased. It is of interest to note that also the monomeric form of TTR interferes with the pancreatic β-cell stimulus-secretion coupling. Hence, it is likely that conversion of the tetrameric form of TTR to the monomeric form may constitute an important step associated with the development of β-cell dysfunction in TID. Nevertheless, such a possible interference of monomeric TTR with cell function will not lead to β-cell destruction per se.

Methods

Identification of TTR in sera from patients with T1D

Sera from T1D patients and control subjects were collected, identically sterile-processed, heat-inactivated by incubation at 56ºC for 30 min and stored frozen at -20ºC until used.

Changes in $[Ca^{2+}]_i$ were tested in β-cells when they were depolarized with 25 mM KCl. Those diabetic sera that induced a higher increase than sera from controls, were centrifuged and the supernatant was passed through a 0.45 mm sterile filter. Samples were loaded on Sep-Pak C18 pre-conditioned with 0.1% trifluoroacetic acid (TFA). After application of the sample, and a 5 ml wash with 0.1% TFA, proteins were eluted with 60% acetonitrile in 0.1% TFA. This procedure was repeated twice. The two fractions were pooled and the volume was reduced by lyophilization. The lyophilized material was submitted to SDS-PAGE, with a reference of control sera from healthy subjects. The gel was silver stained and bands of the diabetic and non-diabetic sera were compared. The band at 14 kDa showed an up-regulation in diabetic sera.

Two SDS-PAGEs were run at the same time. One gel was stained with Coomassie Brilliant Blue and one was blotted on PVDF membrane and stained lightly. The band at 14 kDa was cut and in-gel digested with trypsin. After digestion, the material was run on HPLC. Fractions were collected and mass fingerprinted by MALDI mass spectrometry, identifying TTR. This result was confirmed by amino acid sequencer analysis for 15 cycles.

Media

The medium used for isolation of pancreatic β-cells as well s in the experiments was a HEPES buffer (pH 7.4) containing (in mM) 125 NaCl, 5,9 KCl, 1,2 $MgCl_2$, 1,28 $CaCl_2$ and 3 glucose. Bovine serum albumin was added at a concentration of 1mg/ml. For cell culture RPMI 1640 culture medium supplemented with 10% fetal bovine serum was used.

Preparation of cells

Pancreatic islets from ob/ob mice were isolated by a collagenase technique and mechanically disrupted into cells (*12, 13*). Cells were either seeded onto plastic coverslips or used as cell suspensions.

Measurements of insulin release

Cells in suspension were incubated overnight with 50-, 100- or 150 mg/l TTR (Sigma) and 1or 2 ug/ml monomer. Control cells were incubated with the vehicle (water) of TTR. Dynamics of insulin release were studied by perifusing islet cell aggregates mixed with Bio-Gel P4 polyacrylamide beads (Bio-Rad) in a 0.5 ml column at 37°C (*14*). The flow rate was 0.2ml/min and 2 min fractions were collected and analyzed for insulin by radioimmunoassay using a rat insulin standard (Novo Nordisk).

Measurements of $[Ca^{2+}]_i$

Changes in $[Ca^{2+}]_i$ were recorded in cells preincubated with 50-, 100 or 150 mg/l TTR and 1-, 2- or 5 ug/ml TTR monomer. Cells were attached to coverslips, loaded with 2 μM fura-2/AM (Molecular Probes) and mounted on an inverted epifluorescence microscope (Zeiss, Axiovert 135) connected to a Spex fluorolog-2 system for dual-wavelength excitations fluorimetri. The emissions of the two excitation wavelengths of 340 and 380 nm were used to calculate the fluorescence ratio 340/380 reflecting changes in $[Ca^{2+}]_{i.}$ In order to compensate for possible variations in output of light intensity from the two monochromators, calibration was done where the two monochromators were set at 360 nm. Each experiment also included measurements of a 360/360 ratio. The calibration parameters as well as every experiment was normalized by dividing all fluorescence ratios with the corresponding 360/360 ratio.

Purification of the TTR monomer

TTR was run on a reverse phase (RP)-HPLC with an Everest 238 EV 54-C_{18} (0.46 x 25 cm) column**.** The separation was made using a linear gradient of 20-60 % acetonitrile in 0.1% TFA for 30 min at 1 ml/min. Fractions A1,A2 and A3 were collected and lyophilized**.** They were then run on a Novex Tricine gel 10-20%. Fraction A2 showed the mono form at a mass of 14 kDa (Fig.1).

Patch clamp

Whole-cell Ca^{2+} currents were recorded in β-cells, incubated overnight with 150 mg/l TTR or the vehicle, by using the perforated-patch variant of whole-cell patch-clamp recording technique. Electrodes were filled with (in mM): 76 Cs_2SO_4, 1 $MgCl_2$, 10 KCl, 10 NaCl, and 5 Hepes (pH 7.35), as well as amphotericin B (0.24 mg/ml). The cells were bathed in a solution containing (in mM): 138 NaCl, 10 tetraethylammonium chloride, 10 $CaCl_2$, 5.6 KCl, 1.2 $MgCl_2$, 5 HEPES and 3 D-glucose (pH 7.4). Whole-cell currents induced by voltage pulses (from a holding potential of -70 mV to several clamping potentials from -60 to 50 mV in 10 mV increments, 100 ms, 0.5 Hz) were filtered at 1 kHz and recorded. All recordings were made with an Axopatch 200 amplifier (Axon Instruments, Foster City, California) at room temperature (about 22 °C). Acquisition and analysis of data were done using the software program pCLAMP6 (Axon Instruments, Foster City, California).

Flow cytometric analysis of cell death

Cells from ob/ob mice were cultured for 48 h in the presence of 2 μg/ml TTR monomer, 150 mg/ml total TTR or the vehicle. The whole cell population was collected and stained with propidium iodide (PI) (BD PharMingen) and analysed on a FACscan using CELLQuest acquisition software (Becton Dickinson, Immunocytometry System). FACS gating, based on forward and side scatter, was used to exclude cellular debris and autofluorescence and typically 10 000 cells were selected for analysis.

Statistics

Statistical significance was evaluated by Student´s t-test and p values <0.05 were considered significant. Data are presented as means ± s.e.m.

References

1. **D. R. Soprano, J. Herbert, K. J. Soprano, E. A. Schon, D. S. Goodman, *J Biol Chem* 260, 11793-8 (Sep 25, 1985).**
2. **T. Pettersson, A. Carlstrom, H. Jornvall, *Biochemistry* 26, 4572-83 (Jul 14, 1987).**
3. **C. C. Blake, M. J. Geisow, S. J. Oatley, B. Rerat, C. Rerat, *J Mol Biol* 121, 339-56 (May 25, 1978).**
4. **Y. Sekijima *et al.*, *Amyloid* 8, 257-62 (Dec, 2001).**
5. **P. Rorsman, G. Trube, *J Physiol* 374, 531-50 (May, 1986).**
6. **F. M. Ashcroft, P. Rorsman, *Prog Biophys Mol Biol* 54, 87-143 (1989).**
7. **P. O. Berggren *et al.*, *Adv Exp Med Biol* 334, 25-45 (1993).**
8. **L. Juntti-Berggren *et al.*, *Science* 261, 86-90 (Jul 2, 1993).**
9. **M. Gebre-Medhin, U. Ewald, T. Tuvemo, *Acta Paediatr Scand* 74, 961-5 (Nov, 1985).**
10. **A. M. Kobbah, K. Hellsing, T. Tuvemo, *Acta Paediatr Scand* 77, 734-40 (Sep, 1988).**
11. **S. K. Jain, R. McVie, J. Duett, J. J. Herbst, *Horm Metab Res* 25, 102-4 (Feb, 1993).**
12. **A. Lernmark, *Diabetologia* 10, 431-8 (Oct, 1974).**
13. **P. Arkhammar, P. O. Berggren, P. Rorsman, *Biosci Rep* 6, 355-61 (Apr, 1986).**
14. **T. Kanatsuna, A. Lernmark, A. H. Rubenstein, D. F. Steiner, *Diabetes* 30, 231-4 (Mar, 1981).**

Acknowledgements We thank the Swedish Research Council, Novo Nordisk Foundation, Swedish Diabetes Association, Swedish Society for Diabetes Research, Barndiabetesfonden, Karolinska Institutet, the Family Persson Foundation, Bert von Kantzows Foundation, the Juvenile Diabetes Research Foundation International, and the National Institutes of Health

Competing interest statement The authors declare that they have no competing financial interest.

Correspondence and requests for material to L.J-B (e-mail: lisa.juntti-berggren@molmed.ki.se)

Table 1 **Concentration of TTR in sera from T1D patients and healthy controls**

	TTR (diabetic sera) (mg/l)	TTR (control sera) (mg/l)
1	103	227
2	112	248
3	90	169
4	76	203
5	134	205
6	151	172
7	70	178
8	130	318
9	151	317
10	196	165
11	78	
12	105	
Mean±s.e.m	116±11	220±18

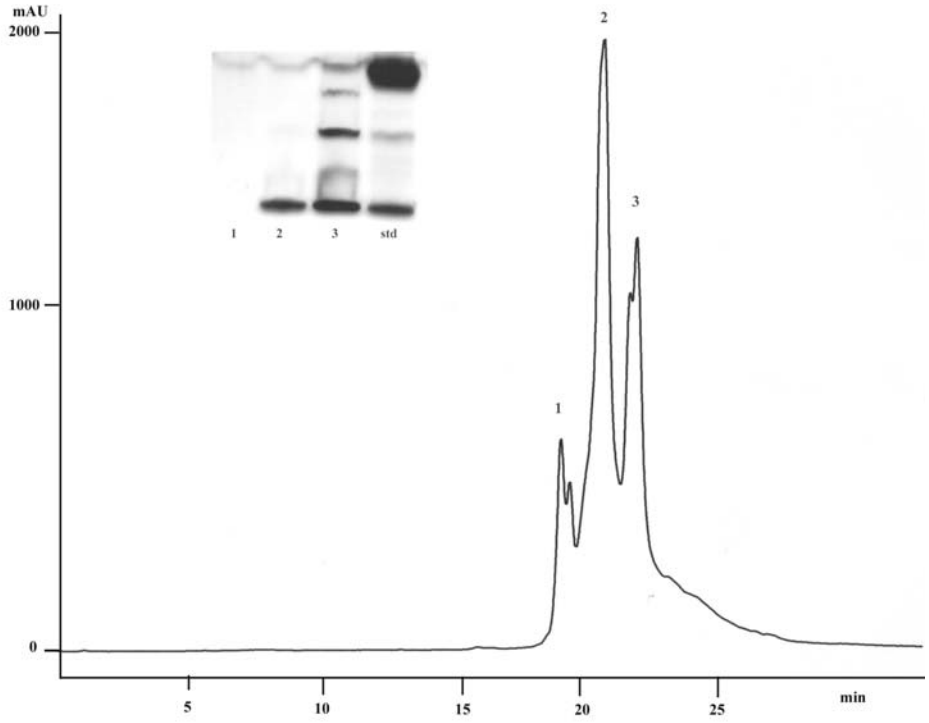

Figure 1 SDS-PAGE pattern of TTR. Commercial TTR run on HPLC with a Vydac C18 column, ACN in 0.1% TFA; gradient 20-60% in 40 min, fractions 1, 2, & 3 were collected and run on SDS-PAGE, STD refers to the commercial TTR before HPLC run.

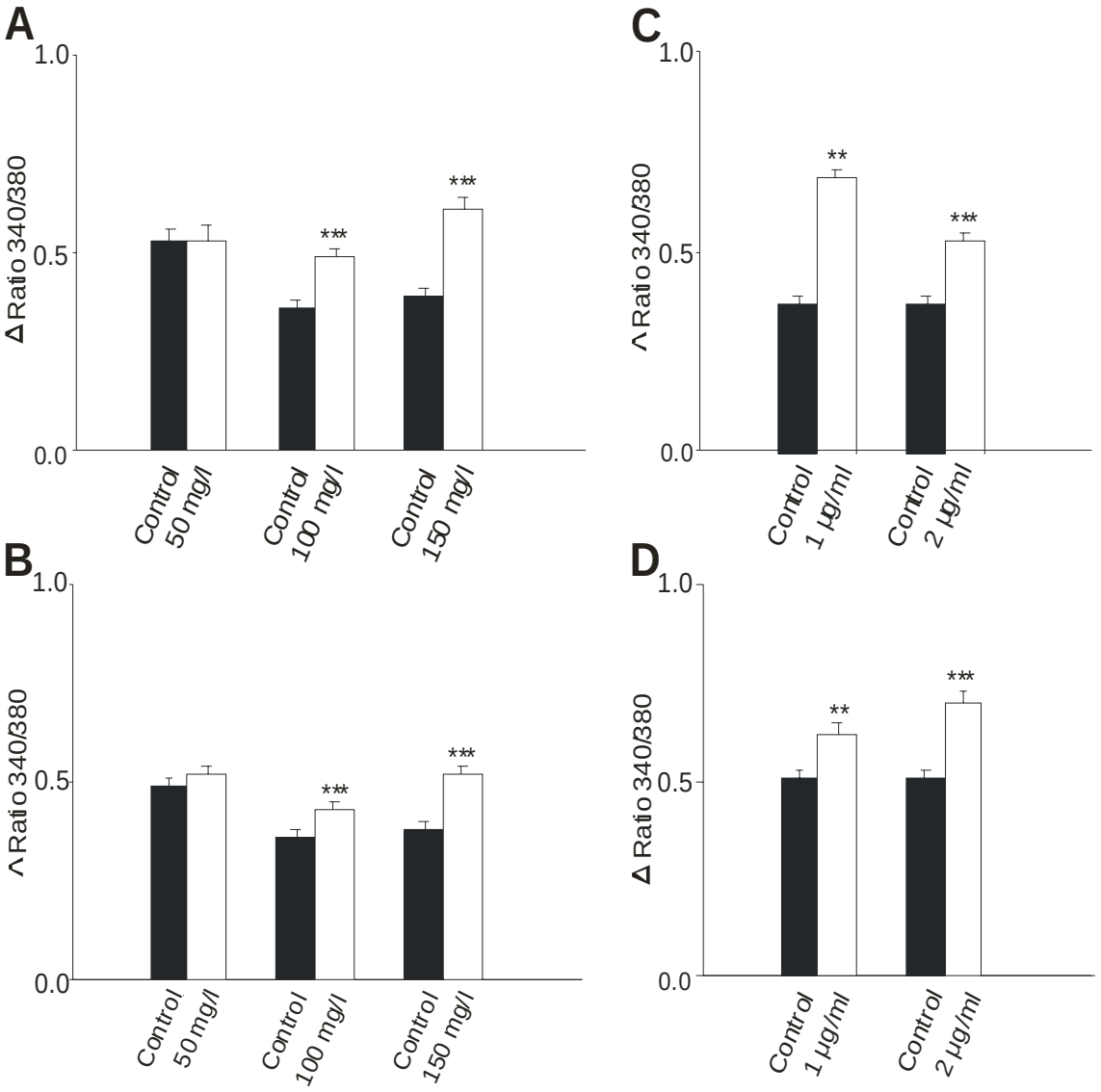

Figure 2 Effects of total TTR and TTR monomer on $[Ca^{2+}]_i$. a, b, Cells incubated with total TTR. **c, d,** Cells incubated with the monomer. In **a** and **c** the increase in $[Ca^{2+}]_i$ is shown when cells were stimulated with glucose (**a,** *n*= 48, 98, and 64, respectively for control cells and 46, 113, and 82 for TTR treated cells. **c,** *n*=50, 50 and 56, respectively for control cells and 73, 47, 74, respectively for TTR monomer treated cells) In **b** and **d,** the delta increase in $[Ca^{2+}]_i$ is shown when cells were depolarised with KCl.(**b,** *n*= 48, 97, and 71**,** respectively for control cells and 44, 111 and 90 for TTR treated cells. **d,** *n*=83, 83 and 65, respectively for control cells and 83, 60 and 83 for TTR monomer treated cells). (***p<0.001).

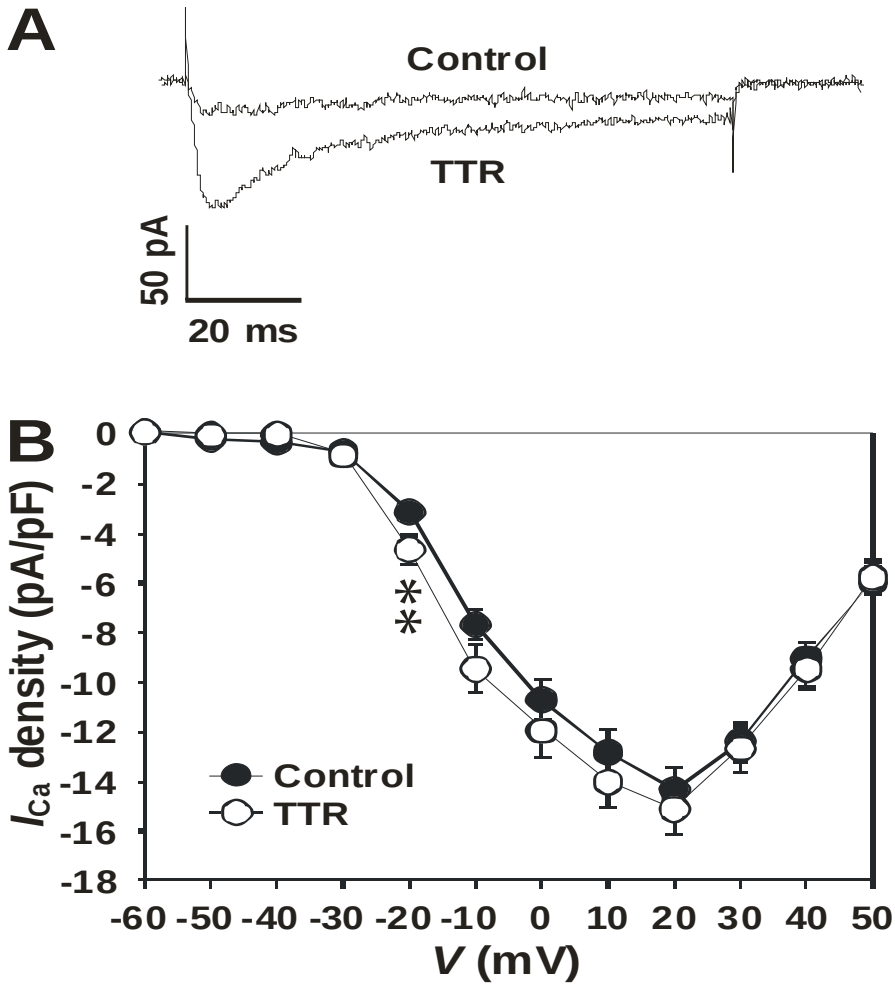

Figure 3 Effects of TTR on voltage-gated Ca^{2+} currents. **A**) Sample whole-cell Ca^{2+} current traces, generated by a depolarizing voltage pulse (100 ms) to -20 mV from a holding potential of -70 mV, from a control cell (upper trace) and a cell incubated with TTR (lower trace). **B**) Whole-cell Ca^{2+} current-voltage relationships in pancreatic β-cells in the presence and absence of TTR. The TTR-treated β-cells display larger Ca^{2+} currents than control cells when they were depolarized to -20 mV.(** $p < 0.01$).

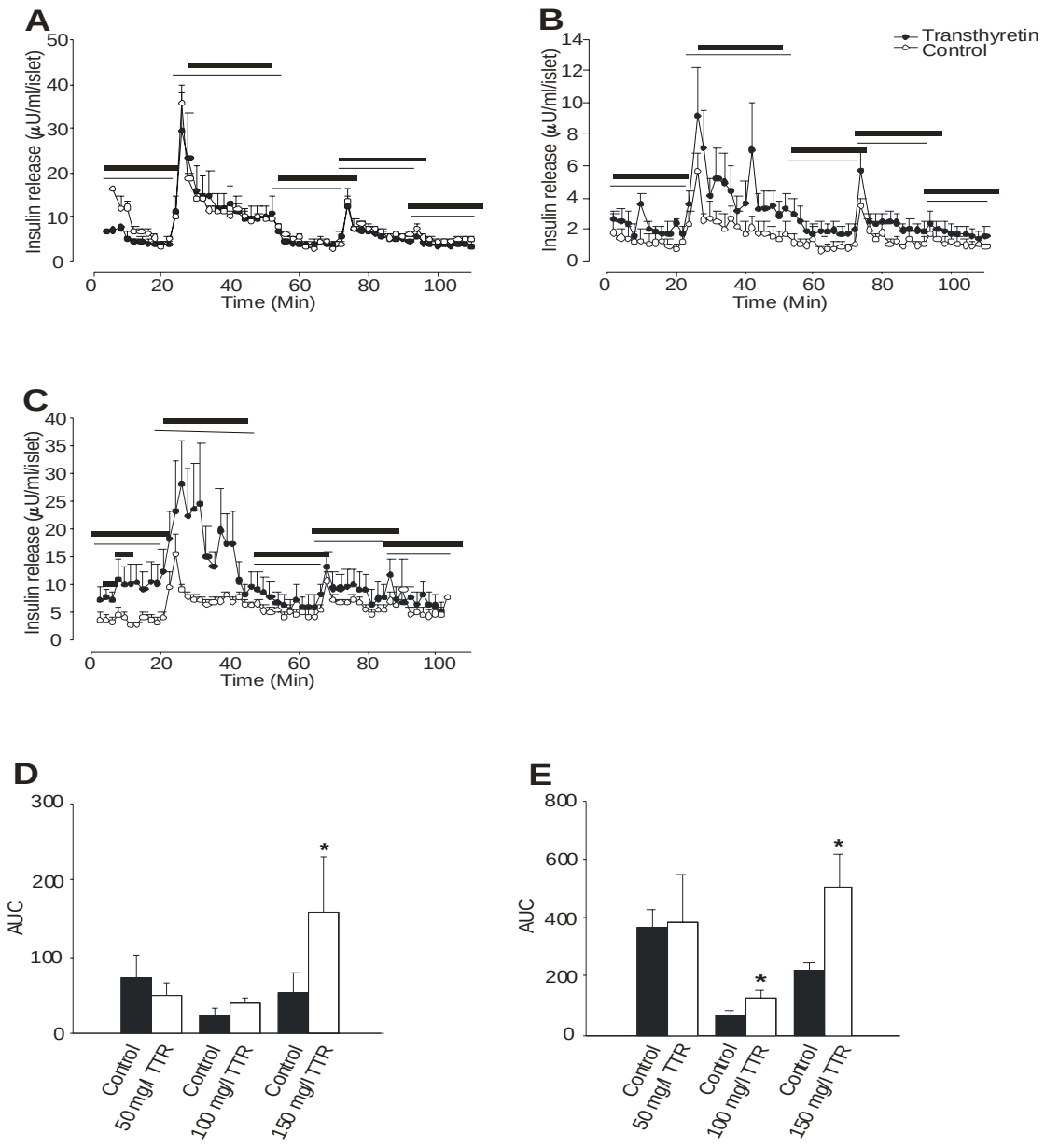

Figure 4 Effects of total TTR on insulin secretion. Insulin release was measured in β-cells pre-incubated with **A,** TTR at 50 mg/l (*n*=5); **B,** at 100 mg/l (*n*=3); **C,** at 150 mg/l (*n*=5);. The insulin release expressed as AUC for **D,** basal and **E,** glucose stimulated secretion. (*p<0.05, **p<0.01)

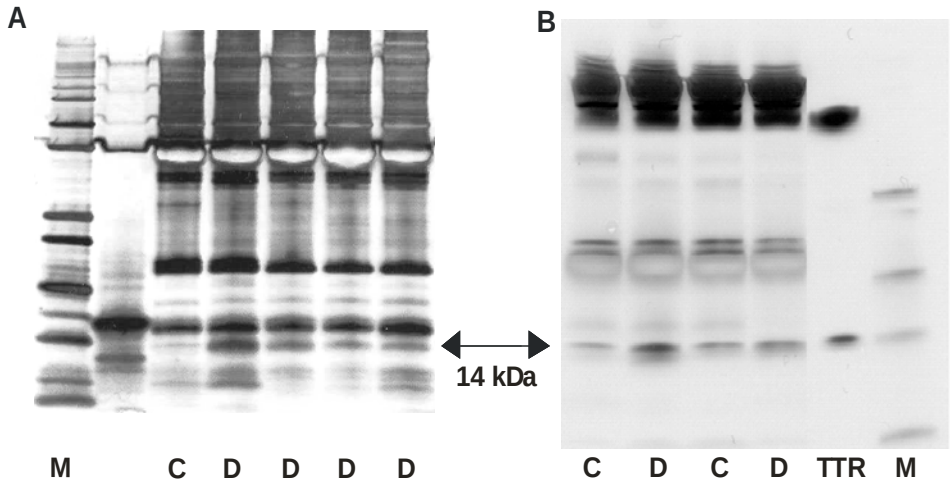

Figure 5 Sera on SDS-PAGE from adults and children with T1D and healthy controls. A. Five T1D sera (D) from adults and one control serum (C). **B.** Sera from two TID (D) and two control sera (C). The band for the monomeric form of TTR is marked with an arrow. In both **A** and **B**, lanes with commercial TTR and a broad range marker (M) were run.

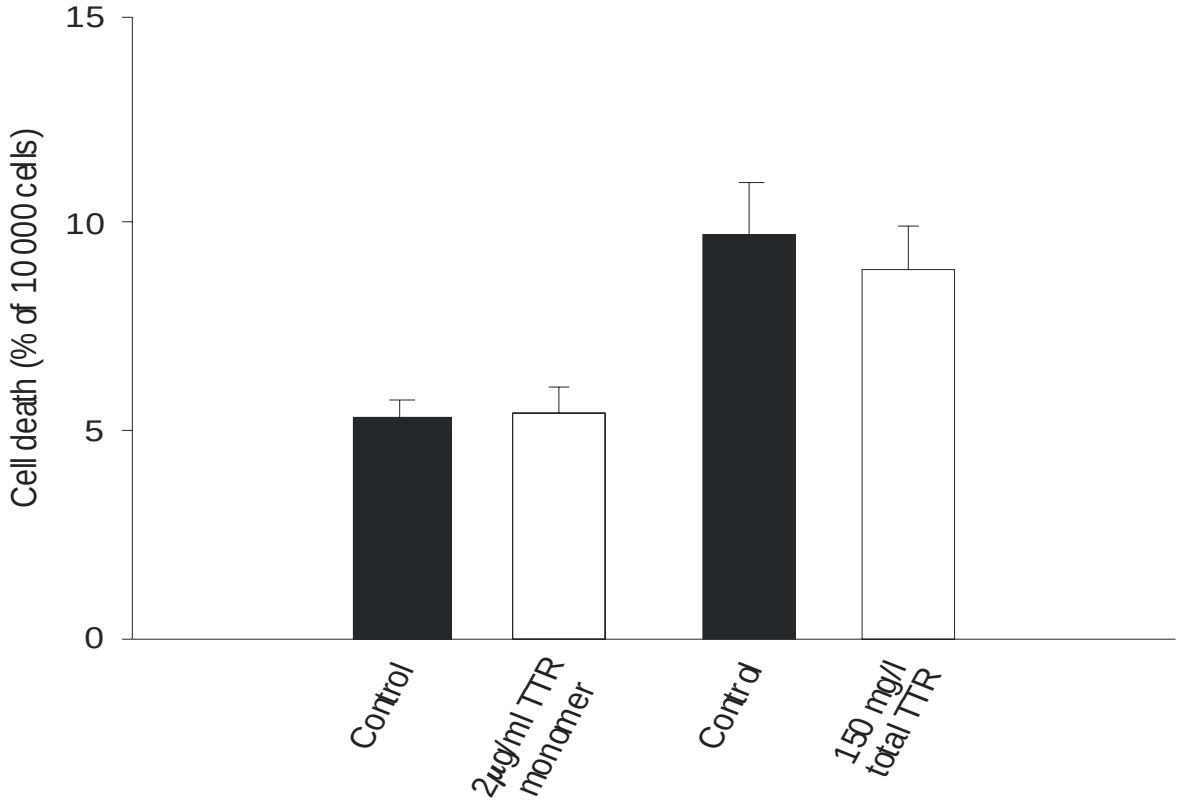

Figure 6 Effect of total TTR and TTR monomer on cell death. FACS analysis were done on pancreatic β-cells exposed to total TTR or TTR monomer (n=5). Cell death is expressed as the percentage of 10 000 counted cells.